Non-Deterministic Analysis of Slope Stability based on Numerical Simulation

By the Faculty of Geosciences, Geoengineering and Mining

of the Technische Universität Bergakademie Freiberg

approved

Thesis

to attain the academic degree

Doktor-Ingenieur

Dr.-Ing.

Submitted by

M. Sc. Hong Shen
born on the 10.09.1984 in Hunan, China

Referees:
Prof. Dr.-Ing. Herbert Klapperich
Prof. Dr. rer. nat. habil. Rafig Azzam
Prof. Dr.-Ing. Wei Wu

Conferment date: Freiberg, 29.06.2012

Contents

Figures

Tables

List of Abbreviations and Symbols

asl	Above Sea Level
c	Cohesion
CDF	Cumulative Density Function
COV	Coefficient of Variation
c_u	Undrained Shear Strength
CV	Coefficient of Variation
d	Minimum Distance Between the Original Point and Limit State Line
DEM	Digital Elevation Map
DEM	Distinct Element Method
E(x)	Expected Value of x
$f(x)$	Probability Density Function of x
FDM	Finite Difference Method
FEM	Finite Element Method
FFT	Fast Fourier Transform
FORM	First Order Reliability Method
FOSM	First Order Second Moment method
FS	Factor of Safety
F_x	Cumulative Density Function of x
$g(X)$	Performance Function of Slope Stability
GIS	Geographic Information System
ierfc	First Integral of the Complementary Error Function
jc	Joint Cohesion
$j\varphi$	Joint Friction Angle
kn	Normal Stiffness of Joints
ks	Shear Stiffness of Joints
L	Load
L	Lower Limit of a Random Set Variable
LAS	Local Average Subdivision
LEM	Limit Equilibrium Method
m	Probability Assignment
MAP	Mean Annual Precipitation
MCS	Monte Carlo Simulation

NSFEM	Neumann Monte-Carlo Stochastic Finite Element Method
OGC	Open Geospatial Consortium
$p(x_i)$	Probability of the Value x_i
PDF	Probability Density Function
PEM	Point Estimate Method
P_f	Probability of Failure
Ps	Probability of Safety
PSFEM	Perturbation Stochastic Finite Element Method
R	Resistance Force
RFEM	Random Finite Element Method
RS	Random Set Theory
RSM	Response Surface Method
SDI	Spatial Data Infrastructure
SFEM	Stochastic Finite Element Method
SLEWS	Sensor based Landslide Early Warning System
SORM	Second Order Reliability Method
SOSM	Second Order Second Moment method
SRM	Strength Reduction Method
SSA	Slip Surface Stress Analysis
T	Averaging Domain
TBM	Turning Bands Method
TSFEM	Taylor Stochastic Finite Element Method
U	Upper Limit of a Random Set Variable
v	Skewness
V	Space
Var(x)	Variance of x
z	Slope-Normal Coordinate
α	Slope Angle
α	Relative Sensitivity
β	Reliability Index
γ	Unit Weight of Soil
$\Gamma(T)$	Variance Reduction Function
ε	Tolerance Error
η_{SR}	Sensitivity Ratio of Variable x

η_{SS}	Sensitivity Score of Variable x
θ	Autocorrelation Length
μ_{FS}	Mean of Safety Factor
μ_x	Mean of x
ξX	Standard Deviation Unit
ρ_s	Soil Density
$\rho_{X,Y}$	Correlation Coefficient of X and Y
σ	Total Stress
σ_{FS}	Standard Deviation of Safety Factor
σ_x	Standard Deviation of x
τ_d	Driving Stress
τ_f	Ultimate Shear Strength
τ_m	Shear Strength
φ	Friction Angle

Abstract

In geotechnical engineering, the uncertainties such as the variability and uncertainty inherent in the geotechnical properties have caught more and more attentions from researchers and engineers. They have found that a single "Factor of Safety" calculated by traditional deterministic analyses methods can not represent the slope stability exactly. Recently in order to provide a more rational mathematical framework to incorporate different types of uncertainties in the slope stability estimation, reliability analyses and non-deterministic methods, which include probabilistic and non probabilistic (imprecise methods) methods, have been applied widely. In short, the slope non-deterministic analysis is to combine the probabilistic analysis or non probabilistic analysis with the deterministic slope stability analysis. It cannot be regarded as a completely new slope stability analysis method, but just an extension of the slope deterministic analysis. The slope failure probability calculated by slope non-deterministic analysis is a kind of complement of safety factor. Therefore, the accuracy of non deterministic analysis is not only depended on a suitable probabilistic or non probabilistic analysis method selected, but also on a more rigorous deterministic analysis method or geological model adopted.

In this thesis, reliability concepts have been reviewed first, and some typical non-deterministic methods, including Monte Carlo Simulation (MCS), First Order Reliability Method (FORM), Point Estimate Method (PEM) and Random Set Theory (RSM), have been described and successfully applied to the slope stability analysis based on a numerical simulation method-Strength Reduction Method (SRM). All of the processes have been performed in a commercial finite difference code FLAC and a distinct element code UDEC.

First of all, as the fundamental of slope reliability analysis, the deterministic numerical simulation method has been improved. This method has a higher accuracy than the conventional limit equilibrium methods, because of the reason that the constitutive relationship of soil is considered, and fewer assumptions on boundary conditions of slope model are necessary. However, the construction of slope numerical models, particularly for the large and complicated models has always been very difficult and it has become an obstacle for application of numerical simulation method. In this study, the excellent spatial analysis function of Geographic Information System (GIS) technique has been introduced to help numerical modeling of the slope. In the process of modeling, the topographic map of

slope has been gridded using GIS software, and then the GIS data was transformed into FLAC smoothly through the program built-in language FISH. At last, the feasibility and high efficiency of this technique has been illustrated through a case study-Xuecheng slope, and both 2D and 3D models have been investigated.

Subsequently, three most widely used probabilistic analyses methods, Monte Carlo Simulation, First Order Reliability Method and Point Estimate Method applied with Strength Reduction Method have been studied. Monte Carlo Simulation which needs to repeat thousands of deterministic analysis is the most accurate probabilistic method. However it is too time consuming for practical applications, especially when it is combined with numerical simulation method. For reducing the computation effort, a simplified Monte Carlo Simulation-Strength Reduction Method (MCS-SRM) has been developed in this study. This method has estimated the probable failure of slope and calculated the mean value of safety factor by means of soil parameters first, and then calculated the variance of safety factor and reliability of slope according to the assumed probability density function of safety factor. Case studies have confirmed that this method can reduce about 4/5 of time compared with traditional MCS-SRM, and maintain almost the same accuracy.

First Order Reliability Method is an approximate method which is based on the Taylor's series expansion of performance function. The closed form solution of the partial derivatives of the performance function is necessary to calculate the mean and standard deviation of safety factor. However, there is no explicit performance function in numerical simulation method, so the derivative expressions have been replaced with equivalent difference quotients to solve the differential quotients approximately in this study. Point Estimate Method is also an approximate method involved even fewer calculations than FORM. In the present study, it has been integrated with Strength Reduction Method directly.

Another important observation referred to the correlation between the soil parameters cohesion and friction angle. Some authors have found a negative correlation between cohesion and friction angle of soil on the basis of experimental data. However, few slope probabilistic studies are found to consider this negative correlation between soil parameters in literatures. In this thesis, the influence of this correlation on slope probability of failure has been investigated based on numerical simulation method. It was found that a negative correlation considered in the cohesion and friction angle of soil can reduce the variability of safety factor and failure probability of slope, thus increasing the reliability of results.

Besides inter-correlation of soil parameters, these are always auto-correlated in space, which is described as spatial variability. For the reason that knowledge on this character is rather limited in literature, it is ignored in geotechnical engineering by most researchers and engineers. In this thesis, the random field method has been introduced in slope numerical simulation to simulate the spatial variability structure, and a numerical procedure for a probabilistic slope stability analysis based on Monte Carlo simulation was presented. The soil properties such as cohesion and friction angle were discretized to continuous random fields based on local averaging method. In the case study, both stationary and non-stationary random fields have been investigated, and the influence of spatial variability and averaging domain on the convergence of numerical simulation and probability of failure was studied.

In rock medium, the structure faces have very important influence on the slope stability, and the rock material can be modeled as the combination of rigid or deformable blocks with joints in distinct element method. Therefore, much more input parameters like strength of joints are required to input the rock slope model, which increase the uncertainty of the results of numerical model. Furthermore, because of the limitations of the current laboratory and in-site testes, there is always lack of exact values of geotechnical parameters from rock material, even the probability distribution of these variables. Most of time, engineers can only estimate the interval of these variables from the limit testes or the expertise's experience. In this study, to assess the reliability of the rock slope, a Random Set Distinct Element Method (RS-DEM) has been developed through coupling of Random Set Theory and Distinct Element Method, and applied in a rock slope in Sichuan province China.

Keywords: slope stability; Strength Reduction Method; reliability analyses; random field model; random set theory; distinct element method

1. Introduction

1.1 Background

A "slope failure" is the movement of a mass of rock, debris, or earth down a slope, under the influence of gravity (Nemcok et al., 1972; Varnes, 1978 ; Hutchinson, 1988; WP/WLI, 1990; Cruden, 1991; Cruden and Varnes, 1996) with many different forms, for example, landslide, debris flow, rock fall and so on. Many different phenomena can cause slope failures, including intense or prolonged rainfall, earthquakes, rapid snow melting, and a variety of human activities.

Slope failure is the second most destructive natural hazard after earthquake (Li et al., 1999; U.S. geological survey, 2000), but it is the most frequent geohazard. With climate change and urbanization, the frequency of slope failures increased sharply in last century. Most of the slope failures resulted from global climate change such as El Niño and unscientific human activities (Au, 1998; Yin et al., 2000; Schuster and Highland, 2001). Most slope failures concentrated in young tectonic mountains such as Rocky and Andes mountain chain of American continent (Radbruch-Hall et al., 1983; Parise and Wasowski, 1999; Collison et al., 2000; Mauritsch et al., 2000), hills of Japan and Taiwan, and the Himalayas of South Asia (Yamagishi et al., 2000; Lin et al., 2002; Bhasin et al., 2002).

Slope failures are always catastrophic due to their large affected areas and great energy, generated by the collapsed soil or rocks with rapid and long runout movement. Until now, a lot of studies have been performed on the large landslides (Schuster, 1996; Voight and Faust, 1992; Wu and Wang, 1989; Zhong, 1999; Sun, 2000; Yin, 2000; Huang et al., 2005), and some catastrophic landslides have been widely known. For example, the loess landslides triggered by the 1920 Haiyuan earthquake resulted in more than 100,000 fatalities (Close and McCormick, 1922). In 1963, a catastrophic landslide (called Vaiont Landslide) suddenly occurred on the southern slope of the Vajont reservoir dam in Italy, and more than 2,500 people lost their lives due to the overtopped flood caused by the landsliding (Voight and Faust, 1992). This is the most deadly landslide ever recorded in Europe. Further, on 18 May 1980, a giant landslide occurred on the slope of Mount St. Helens (a volcano located in Washington State of United States) triggered by melting snow and ice, causing a major lahar which traveled rapidly down the valley of the north Fork of the Toutle River, and 57 people were killed. More recently, triggered by earthquake, the 1999 Chiufengershan in Taiwan (Fig. 1.1) (Shou et al., 2003) and 2001 Las Colinas landslide in El Salvador (Fig. 1.2) (Baum

et al., 2001) also resulted in a huge number of fatalities (Catane et al., 2007).
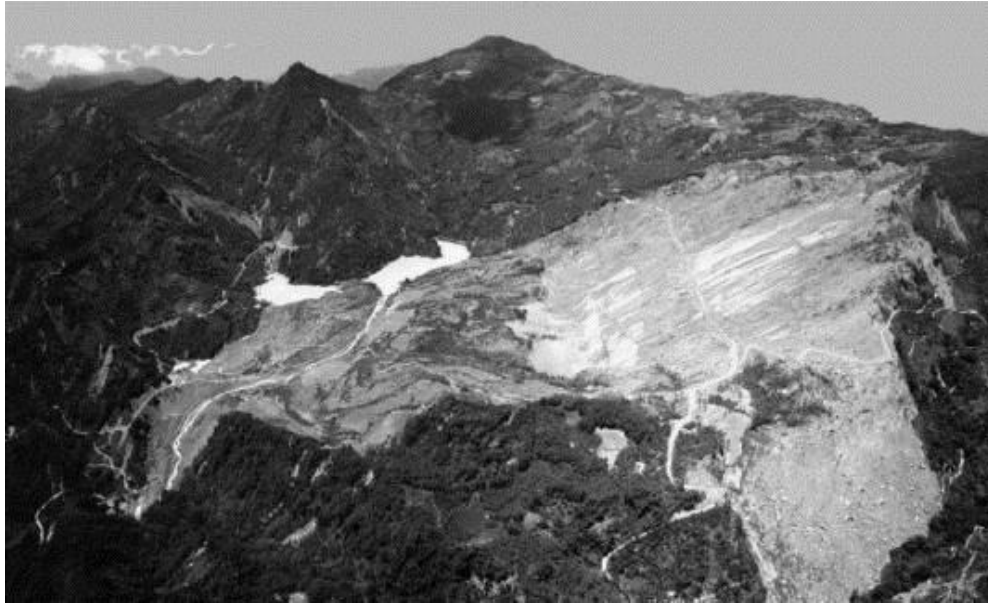
Fig. 1.1 Overview of the Chuifengershan Landslide (after Shou, 2003)

Fig. 1.2 Las Colinas Landslide triggered by M 7.6 earthquake in Central America in 2001

China is one of the countries which suffer slope failure disasters the most seriously in the world. Since 1980, due to increase in construction activities and change in climatic conditions, the number of slope failure hazards boosted in China. At present, serious slope failures occur in almost all areas of China, and the most severe areas are the provinces situated in west of China, which is a mountainous area. In temporal, most of the landslide

hazards, which are about 90% of the whole year, concentrate in the rain season, from June to September every year.

In China, the slope failures resulted in about 1,000 fatalities and great damage to infrastructures per year in the last 20 years (Li, 1992; Wang, 1999; Duan, 1999; Yin, 2000, 2001; Jiang, 2000). According to China Ministry of Land and Resources, in the first half of 2010, the number of geo-hazards was 14,614 in China, where the slope failures made up more than 98%, including landslides, slope collapses and debris flows (Fig. 1.3). The slope failure hazards in those six months induced 464 deaths as well as about 18 billion RMB loss.
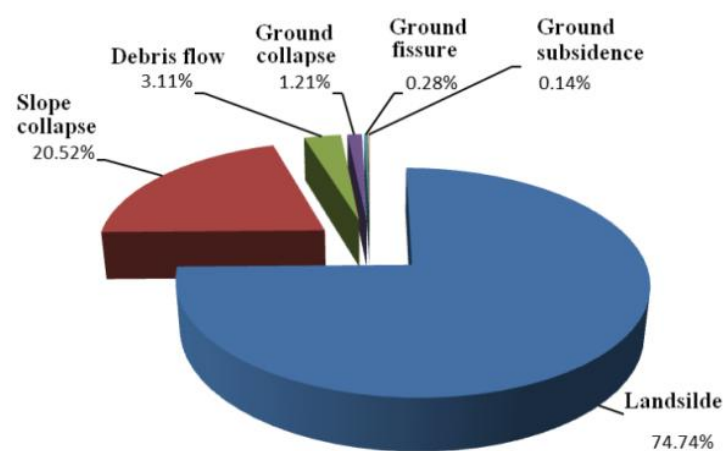
Fig. 1.3 Geo-hazards Statistics in China 1~6, 2010 (from China Ministry of Land and Resources)

Obviously, how to prevent and to mitigate the disaster of slope failure is an urgent mission for researchers and engineers in the world.

1.2 Thesis purpose significance and outline

Slope engineering is one of the three kinds of geotechnical engineering, besides earth pressure and bearing capacity of foundation. Many researchers and scholars have studied different aspects of slope stability, including slope deterministic analysis, slope probabilistic analysis, landslide risk analysis, the prediction, prevention and protection against risk of slope failure, and lots of significant achievements have been obtained (Morgenstern and Price, 1965; Spencer, 1967; Janbu, 1973; Brown and King, 1966; Griffiths and Lane, 1999; Matsui and San, 1992; Madsen and Larsen, 1987; Jiang, 1990; Tamaskovics, 2001; Azzam, 2011). However slope failure is still one of the most frequent and dangerous geological hazards in the world, and there are many difficulties in relative reasonable slope stability analyses and the timely forecast of slope failure hazard. In the future, with progressive

urbanization and global climate change, large scale single slope failure or slope failure hazard in a region will be more and more severe. Therefore many aspects of slope stability analysis require further studies, for instance: the geological background, failure mechanism, geotechnical mechanics, stability analyses methods, reinforcement methods of slope, landslide hazard mapping, risk prediction, triggers of landslides etc. The content of this thesis focuses on the study of slope reliability analyses based on numerical simulation.

1.2.1 Thesis objective

The slope stability analyses method have been studied for hundreds of years. However, with the development of modern computation techniques and new demands of engineering construction, the slope stability analysis methods need to be further improved. The purpose of this thesis is to study slope stability analysis considering the uncertainty of soil properties, and develop an efficient user-friendly framework combing the non-deterministic analyses methods with numerical simulations.

For estimating stability of slope more rigorously, slope non-deterministic analysis methods should consider all of the nonlinear properties of geological material, the large deformation of slope and the uncertainty of geomechanical parameters. The output of these methods should obtain the probability of failure and location of the corresponding slide of slope. It can provide the scientific foundation for the subsequent risk analyses, risk management, hazard forecast and reinforcement design of slopes.

1.2.2 Significance of study

This study has very important scientific significance and practical worth. The scientific significance: the slope reliability analysis is a front topic in slope engineering. It is an interdisciplinary topic which synthesizes engineering geology, geotechnical mechanics, elastic-plastic mechanics, nonlinear numerical simulation method, reliability theory and mathematic statistics, and computer. The achievement of this study can promote the development of these disciplines.

The practical worth: the slope probabilistic analysis methods combined with numerical simulation reflect the property of slope engineering more realistically, overcome the restrictions of many unreasonable postulates in existing slope stability analyses methods, and evaluate the failure probability or reliability of the slope more correctly and efficiently. Applying this study will enable people to consider the effects of soil or rock property

uncertainties and complex boundary condition of slope stability better. And based on the results of these non-deterministic analysis methods, engineers can carry out risk analyses, risk management, hazard forecast and reinforcement design of landslide more scientifically in subsequent work.

1.2.3 Thesis outline

The present thesis focuses on the non-deterministic method study of slope stability analysis based on numerical simulation. The main contents are:

Chapter 2: this chapter reviews the development of slope stability analysis. First, two kinds of most popular slope deterministic methods: Limit Equilibrium Methods (LEM) and Numerical Simulations are reviewed. The methodologies are extensively illustrated and their corresponding advantages and limitations are discussed. Next, the development of reliability theory and its application in slope stability analysis is reviewed, and the shortness of the present slope probabilistic methods is presented.

Chapter 3: this chapter starts by considering the primary sources and types of uncertainties in slope engineering, and underlying the importance of using probabilistic methods as alternative to the deterministic analysis to quantify uncertainties. And then a description of the most important statistical and probabilistic concepts of continuous random variables is provided based on some useful continuous probability distributions and their main characteristics. The chapter introduces the basic theory of reliability analysis, it is shown how the traditional safety factor relates to the probability of failure, which represents a more realistic measure of a system reliability. At last, the determination of geotechnical parameters based on real time monitoring data is discussed.

Chapter 4: With the development of computer, the numerical simulations, such as finite element or finite difference method are applied more and more frequently in slope stability analyses. However, the numerical modeling, especially for 3D, developed very slowly. This chapter investigates the integration of Geographic Information System (GIS) and the numerical simulation method-Strength Reduction Method in slope stability analysis. The functions such as profile automatic generation and gridding of Digital Elevation Map (DEM) features of GIS are used in the preliminary treatment of numerical modeling, and a program for transforming GIS data to commercial finite difference code FLAC is developed using FISH programming language. At last, the stability analysis of Xuecheng slope in 2D and 3D are studied to demonstrate the reliability of this technique.

Chapter 5: the mechanical properties of sediments, especially the soil shear strength, play an important role in slope stability. However, the mechanical properties of natural sediments are variable and depend on the way the sediments formed. Probability theory and reliability analysis can provide a rational framework for dealing with these uncertainties. In this chapter, three most widely used probabilistic methods Monte Carlo Simulation (MCS), First Order Reliability Method (FORM) and Point Estimation Method (PEM) for slope reliability analysis are discussed and applied based on Strength Reduction Method. The accuracy and feasibility of these methods are illustrated using two examples; a homogenous slope and a non-homogenous slope. The cohesion c and friction angle φ of soil which have the strongest influence on slope stability are considered as random variables with three kinds of distribution: independent normal random variables, independent log-normal random variables and negative correlated normal random variables.

Chapter 6: the spatial variability of soil properties is a critical factor that affects the probabilistic slope stability analysis. In this chapter, a practical method for probabilistic slope stability analysis based on the Monte Carlo simulation is presented. The proposed method considers the spatial variability of soil properties, adopts local average subdivision to build the random field model of soil properties, and applies Strength Reduction Method to estimate the safety factor of a slope. In the case study, the probability analysis of a two-layer slope with random field soil properties is carried out, and both the stationary and non-stationary random fields are considered. At last, the influence of local averaging on the convergence of analysis and probability of failure is investigated.

Chapter 7: the Random Set Distinct Element Method (RS-DEM) has been developed and applied in the stability analysis of a rock slope from China in this study. The influence of the discontinuity joints of rock material on the slope stability is considered, and the sensitivity analyses of different input parameters have been conducted. At last the uncertainties of the strength parameters of both, rock blocks and discontinuity joints are included in the reliability analysis model. In this study, the distinct element code UDEC has been used to model the rock material, and the Strength Reduction Method is used to calculate the safety factor of slope.

Chapter 8: a summary of the most relevant findings of this research is presented in the final chapter, along with the conclusions and recommendations for further research.

2. Literatures Review of Slope Stability Analysis

2.1 Deterministic slope stability analyses methods

Tons of research articles about slope stability analysis methods have been published since the first method developed by Fellenius in 1936. Nowadays among the available deterministic analysis methods, the most widely used are the Limit Equilibrium Slice Methods (LEM) and numerical simulation methods.

2.1.1 Limit equilibrium slice methods

For slope stability analysis, the Limit Equilibrium Slice Methods are the most popular among engineers and researchers, because these are traditional and well established. After the first slice technique (Fellenius, 1936) which based more on engineering intuition than on a rigorous mechanics principle appeared, there was a rapid development of the slice methods in the 1950s and 1960s by Bishop (1955); Janbu et al. (1956); Lowe and Karafiath (1960); Morgenstern and Price (1965); and Spencer (1967). The various slice methods of limit equilibrium analysis have been well surveyed and summarized in 1980s and 1990s (Fredlund and Krahn, 1984; Nash, 1987; Morgenstern, 1992; Duncan, 1996).

Most of the limit equilibrium methods are based on the technique of slices. The general formulation of these methods is shown in Figure 2.1.
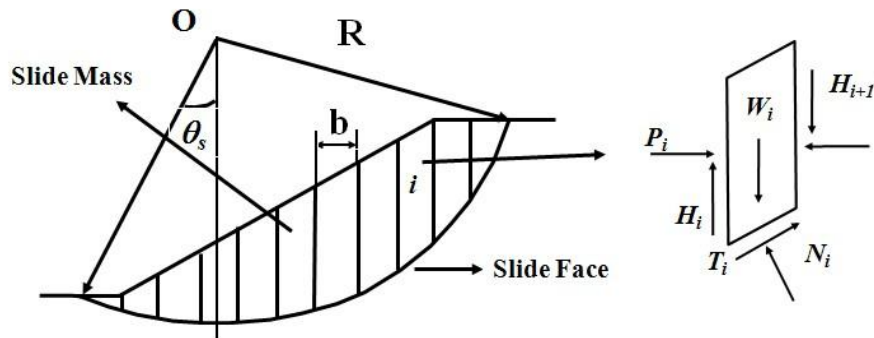
Fig. 2.1 Slices of slope and forces acting on them

These slice methods have some common features, and Zhu et al. (2003) have summarized them as follows:

1). The sliding body over the failure surface is divided into a finite number of slices. The slices are usually cut vertically, but horizontal as well as inclined cuts have also been used by various researchers. In general, the differences between different methods of

cutting are not common, and the vertical cut is preferred by most engineers at present.

2). The strength of the slip surface is mobilized to the same degree to bring the sliding body into a limit state. It means there is only a single factor of safety which is applied throughout the whole failure mass.

3). Assumptions regarding inter-slice forces are employed to render the problem determined.

4). The factor of safety is computed from force and/or moment equilibrium equations.

There is much common ground for the limit equilibrium methods, and there are also many differences among them about the slip surface or assumptions in force. For example, based on the shapes of slip surface assumed, the LEMs can be grouped as:

1). Methods of analysis which employ circular slip surfaces include: Fellenius (1936); Taylor (1949); and Bishop (1955).

2). Methods of analysis which employ non-circular slip surfaces include: Morgenstern and Price (1965); Spencer (1967); and Sarma (1973); Janbu (1973).

In the conventional limit equilibrium methods, no matter circular or non-circular slip surface, the shear strength τ_m which can be mobilized along the failure surface is given by:

$$\tau_m = \tau_f/FS \tag{2.1}$$

where *FS* is the factor of safety (based on force or moment equilibrium in the final form) with respect to the ultimate shear strength τ_f which is given by the Mohr-Coulomb relation as

$$\tau_f = c' + \sigma' \tan \varphi' \text{ or } c_u \tag{2.2}$$

where c' is the effective cohesion, σ' is the effective normal stress, φ' is the effective angle of internal friction and c_u is the undrained shear strength.

According to Eq. 2.2, except the soil properties i.e. cohesion and friction angle, the ultimate shear strength along a slip surface also depends on the effective normal stress σ' acting on the failure surface. However, the effective normal stress is not constant, but varies based on the topography of slope, density and saturation of soil and so on. Fröhlich (1953) analyzed the influence of σ' distribution on the slip surface on the calculated *FS*. He suggested an

upper and lower bound for the possible *FS* values. The lower bound theorem in plasticity adopts the following criteria: equilibrium equations, failure criterion and boundary conditions in terms of stresses. On the other hand, the upper bound theorem in plasticity adopts the following alternative criteria: compatibility equations and displacement boundary conditions, in which the external work equals the internal energy dissipations.

Hoek and Bray (1977) suggested that the lower bound assumption gives relative accurate values of the factor of safety. Based on the friction method, Taylor (1948) also concluded that a solution using the lower bound assumptions leads to a relative accurate safety factor for a homogeneous slope with circular failures. However the use of the lower bound method is difficult in most cases. Cheng et al. (2007c, d) have developed a numerical procedure, which is effectively the lower bound method but applicable to a general type of slope problem.

In the classical stability analysis, an average value of *FS* is obtained along the slip surface instead of the actual factor of safety which varies along the failure surface. However constant *FS* can not reflect the progressive failure of slope. There are some formulations where the factors of safety can vary along the failure surface. Chugh (1986) presented a procedure for determining a variable factor of safety along the failure surface within the framework of the LEM. He predefined a characteristic shape for the variation of the factor of safety along a failure surface, and this idea actually follows the variable inter-slice shear force function in the Morgenstern-Price method. The suitability of this variable factor of safety distribution is however questionable, as the actual local factor of safety should be mainly controlled by the local soil properties. Law and Lumb (1978) and Sarma and Tan (2006) have also proposed different methods with varying factors of safety along the failure surface. These methods however also suffer from the use of assumptions with no strong theoretical background. Cheng et al. (2007c) has developed another stability method based on the extremum principle which can allow for different factors of safety at different locations. All of these formulations attempt to model the progressive failure in a simplified way, but the introduction of additional assumptions is not favored by many engineers. In view of these limitations, most engineers still prefer the concept of a single factor of safety for a slope.

In the process of the LEMs in the slope stability analyses, there are basically two steps. The first is to calculate the safety factor based on a certain slip surface; the second is to repeat the

first step based on different potential slip surfaces, and search the critical slide face corresponding to the minimum safety factor. In recent years, many optimization methods are applied in searching vulnerable failure face, including the enumeration method, numerical analyses method and non numerical analyses methods (e.g. Simulated Annealing, Genetic Algorithm, Neural Network Method, Ants Algorithm and Bionic Algorithm) (Baker, 1980; Cellestino and Duncan, 1981; Li and White, 1987; Chen, 1988; Greco, 1997).

Duncan (1996) and Chen (2003) analyzed and observed the accuracy and feasibility of every LEM. They indicated that:

1). the safety factor of slope calculated by the Fellenius Method is the smallest, the result of Simplified Bishop Method is greater than the Fellenius Method by 6%~7%, and the result of Spencer Method is greater than the Simplified Bishop Method by 2%~3%;

2). the rigorous methods which satisfied both equilibrium conditions of force and moment, such as Morgenstern Price method, are more accurate (except for the numerical analyses problem);

3). for the circular slide face, the results of the Simplified Bishop and Morgensten-Price Methods are very close, which means that the Simplified Bishop Method has relatively high accuracy, so it is applied most extensively in practical engineering.

2.1.2 Numerical simulation methods

The classical limit equilibrium analysis only considers the ultimate limit state of the system, and provides no information on the development of strain which actually occurs. The design of a slope using a limit equilibrium analysis alone may be completely inadequate if the slope fails by complex mechanisms (e.g. progressive creep, internal deformation and brittle fracture, liquefaction of weaker soil layer, etc.) (Stead, 2001). For a natural slope, it is possible that part of the failure mass is heavily stressed so that the residual strength will be mobilized at some locations, while the ultimate shear strength may be applied to another part of the failure mass. This type of progressive failure may occur in over consolidated or fissured clays or materials with a brittle behavior. The use of the numerical simulation methods can provide an estimation of this progressive failure.

The numerical simulation methods are currently adopted in several well-known geotechnical finite element (Matsui and San, 1992, Griffiths and Lane, 1999), finite difference, distinct element or boundary element (Jiang, 1990) programs. Compared with

conventional slope stability analysis methods, the numerical simulation methods consider the relationship of stress and strain of slope material (i.e., constitutive relationship), and they aren't restricted by the geometry shape and material inhomogeneity. There are basically two kinds of numerical simulation technique: one is the Slip Surface Stress Analysis (SSA) (Zou, 1995; Duncan, 1996); and the other is the Strength Reduction Method (SRM), which developed in 1990s (Matsui, 1992; Swan, 1999; Dawson, 1999; Griffiths, 1999).

Same as the process of limit equilibrium methods, the Slip Surface Stress Analysis Method (Wright, 1973; Yamagami, 1988) defines the potential slip surface in advance, and then analyzes the stress distribution on this surface after numerical simulation converged, ultimately calculates the safety factor based on the principle of weighted average. Many researchers further studied the method of searching the critical slip surface in plenty of potential slip surfaces. Zou (1995) determined the initial and potential range of slide face through the stress distribution, and then searched the most vulnerable slide face and its corresponding safety factor. Kim and Li (1997) calculated the Gauss points stress through the finite element stress field, and then carried out the advanced search of noncircular slide face. Giam and Donald (1988) proposed the pattern search method to get the critical slide face and the minimum safety factor based on stress field.

The second numerical simulation slope stability approach is the Strength Reduction Method. This method is studied more actively (Woodward, 1999; Hamdy Faheem, 2004) than SSA, because it is very simple and can be conducted in the existing commercial numerical analyses programs, such as FLAC, Ansys, UDEC etc. In the strength reduction technique, the original shear strength parameters are reduced in order to bring the slope to fail. The domain under consideration is discretized and the equivalent body forces are applied to the system. The yield criterion adopted is usually the Mohr-Coulomb criterion, but the use of other yield criteria is also possible, such as Drucker-Prager criterion (Zheng et al., 2005). The numerical simulation methods can analysis the slope stability under different conditions. For example, Wu (2008) analyzed the slope stability in central Asia under severe seismic event using finite difference program FLAC3D and Finite Element program QUAKE/W.

In numerical simulation methods, there are mainly three kinds of slope failure criterion:

1). the non-linear equation solver cannot achieve convergence after a pre-set maximum number of iteration, and this is the most commonly used criterion (e.g. Dawson and Roth, 1999; Griffith and Lane, 1999; Lechman, 2000; Zhao and Zhen, 2002);

2). there is a sudden increase in the rate of change of displacement in the system (Song, 1997; Ge, 2003);

3). a failure mechanism has developed (Matsui, 1990; Zhen, 2002).

To define the critical failure surface from the SRM, both the maximum shear strain and the maximum shear strain increment definition can be used. Cheng et al. (2007e) have found that these two definitions give similar results in most cases.

Compared with the conventional limit equilibrium method, the main advantages of the SRM are as follows:

   1). the critical failure surface is found automatically from the localized shear strain arising from the application of gravity loads and the reduction of shear strength;

   2). it requires no assumption on the inter-slice shear force distribution;

   3). it is applicable to many complex conditions and can give information such as stresses, movements and pore water pressures;

   4). it can simulate the interaction of the soil and the structure inside, like piles, walls, and geotextile.

Griffiths and Lane (1999) pointed out that the widespread use of the SRM should be seriously considered by geotechnical practitioners as a powerful alternative to the traditional limit equilibrium methods.

2.2 Slope probabilistic analysis review

2.2.1 Probabilistic analyses methods review

In every deterministic slope stability analyses, the uncertainties in slope engineering are not considered. This common shortcoming sometimes causes collapse of slope even though the safety factor is greater than 1.0.

The probabilistic analysis, also called reliability analysis was first studied in airplane failure in 1930s. Since 1946 Freudenthal published "*Degree of Safety in Structure*" and lead the probability analyses in practical engineering design, people began to recognize the importance of uncertainties in structure engineering. In 1974 Hasofer and Lind defined that the reliability index is the minimum distance between the original point and the limit state surface in the Gauss space.

As the development of reliability theory and increased concentration on the uncertainties of the slope engineering, the slope probabilistic analysis got more and more attention by engineers and researchers. It was first used in slope engineering during 1970s (Matsuo et al., 1974, 1976; Ang et al., 1975; Alonso, 1976; Tang et al., 1976; Harr, 1977; Vanmarcke, 1977; Chowdhury, 1978). Thereafter many people conducted further studies and developed many probabilistic analysis methods (Ang et al., 1984; Chowdhury et al., 1984, 1987, 1933; Wolff, 1985; Nguyen, 1985; Li, Lumb, 1987; Oka, Wu, 1990; Christian, 1994, 1996, 1998; Low, 1997, 1998, 2005; Hassan, 1999; Liang, 1999; Malkawi, 2000; Auvinet, 2000; Bhattacharya, 2003).

The primitive probabilistic analysis method was "Second Moment Pattern" (Cornell, 1969, 1971). These methods produce a linearization of performance function about the mean value of the input random variables. These concern the first or second order of the performance function based on first and second moments of random variables, so is called the First Order Second Moment (FOSM) method or the Second Order Second Moment (SOSM) method (Griffiths, Fenton and Tveten, 2002; Christian and Bächer, 1992, 1994; Mostyn and Li 1993; Wolff, 1994; Duncan, 2000).

The drawback of the FOSM and SOSM methods is that the results depend on the mean value of the input variables at which the partial derivatives of the safety margin are evaluated (invariance problem). Therefore these methods are accurate only for linear functions, and the error will be quite large when the degree of non-linearity of performance function is higher. Hence the scholars proposed the First Order Reliability Method (FORM) and Second Order Reliability Method (SORM) where the performance function is linearized about the critical points, also called design point (Fiessler, 1979; Breitung, 1984; Tvedt, 1990; Koyluoglu and Nielsen, 1994; Yang-gang Zhao, 1999; Der Kiureghian, 1987; 1991). After Rackwitz and Fiessler (1978) proposed a method to transform the non normal variables to equivalent normal variables, the moment's methods can be applied for non normal random variables. Since recommended by International Joint Committee on Structural Safety (JCSS), this method is also called JC method.

The above mentioned moment's methods need to calculate the gradient of performance function. Therefore, the performance function is very important for these methods. For building the explicit performance function for complicate geotechnical problem, the Response Surface Method (RSM) was developed. The RSM was first proposed by Box and

Wilson (1954), and an explicit expression close to the implicit performance function is obtained by a statistic method in this technique. It can be considered as an uncertainty analysis methodology in which the impact of the input parameters and their interactions on the system response are evaluated, ending up with a relationship between the significant factors and the desirable system response in order to reduce the analysis complexity of the mechanical system (Cornel, 1990). The function obtained by this method can be used as an approximate model in an uncertainty analysis. Then one of the probabilistic analysis methods is employed. The RSM was applied in engineering reliability analyses since 1980s (Wong, 1984; 1985; Faravelli, 1989; 1992), subsequently, Bächer and Bourgund (1990), Rajashekhar and Ellingwood (1993), Liu and Moses (1994), Kim and Na (1997), Zheng and Das (2000) and Adhikari (2004) have improved this method for practical applications. Zangeneh et al. (2002) have employed this method to analyze the displacement of slopes in the earthquake environment. From practical point of view, this method has some shortcomings because first, it is necessary to estimate the response function using regression methods for each individual response, and the influence input parameters should be determined in advance. Second the slope probabilistic analysis is always based on safety factor function, but in practice, only the system responses like displacement, deformation can be monitored. Therefore, the performance function obtained from response surface method cannot be compatible with probabilistic analysis very well.

No matter the FORM, SORM or RSM, essentially they calculate the reliability index based on the moments of performance function, so all of them are approximate methods. It is necessary to look for a more effective and accurate reliability calculation method. Therefore, Monte Carlo Simulation (MCS) is appreciated by people.

The MCS method calculates the probability failure of slope based on the assumption of the probability density function of input random variables (Ang and Tang, 1984; Ross, 1995). The advantages of this method are: (1) the convergence velocity of simulation is unconcerned with the dimension of random variables; (2) the complexity of the performance function is not related to the simulation procedure; (3) the error of the results is very easy to be determined. So it is usually applied as a reference to check the accuracy of other methods. The disadvantage of MCS is that the number of simulations increases substantially with the reduction of failure probability, and the calculation time will be prolonged immensely.

Another alternative method to evaluate statistical moments of a performance function is the

Point Estimate Method, or shortly PEM. The Point Estimate Method was first developed by Rosenblueth (1975, 1981) and then further developed by other authors such as Lind (1983), Zhou and Nowak (1988), Harr (1989), Li (1992), Evans et al. (1993), Hong (1998), Christian and Baecher (1999). The basic idea of this method is to replace the probability distributions of continuous random variables by discrete equivalent distributions having the same first three central moments, to calculate the mean value, standard deviation and skewness of a performance function, which depends on the input variables.

While the PEM does not provide a full distribution of the output variable, as Monte Carlo does, it requires little knowledge of probability concepts and could be applied for any probability distribution. In future it might be widely used for reliability analysis and for the evaluation of failure probability of engineering systems.

The common ground of above studies is that, the reliability index or failure probability of slope is solved by the combination of the limit equilibrium slice method and some probabilistic methods (mainly FORM and MCS) (Ramly et al., 2002; Malkawi et al., 2000; Low 2007).

2.2.2 Finite element reliability analysis methods review

Because of the high accuracy of numerical simulation deterministic methods and increase of the calculation capability of computers, people began to combine numerical simulation with reliability theory to analyze the failure probability of slopes. In the beginning, the idea was to combine the Monte Carlo Simulation with finite element method directly (Shinozuka, 1976). However, the calculation work of this method is very huge, because MCS is based on a large number of repeating deterministic FEM. Precisely speaking, this is not a real random finite element method.

Currently years, research is focused on the establishment and solution of the performance function of the Stochastic Finite Element Method (SFEM). In 1970s, Cambou (1971) first applied the FORM to study the linear elastic problem, and then, Dendrou and Houstis (1987), B ächer and Ingra (1981) applied this method to solve the uncertainty problem in geotechnical engineering. Because this method is based on the Taylor's series expansion about the input random variables, it is called Taylor Stochastic Finite Element Method (TSFEM). After that, Hisada (1981, 1985) and Handa (1981) adopted first order and second order perturbation technique considering random variables fluctuation, and proposed Perturbation Stochastic Finite Element Method (PSFEM). In 1980's, Shinozuka and Yamazaki (1988) combined the

Neumann expansion with Monte Carlo finite element method, and developed Neumann Monte-Carlo Stochastic Finite Element Method (NSFEM) which is more accurate and effective. Liu et al (1988) applied partial difference method in stochastic finite element analysis, and introduced the 2D non linear stochastic finite element function. Kiureghian (1988) combined the reliability index calculation method FORM with Random Finite Element Method (RFEM) to calculate the reliability of frame structure. Wu et al. (1989, 1990 and 1992) extended this method to 2D and 3D, and calculated the reliability of gravity dam and arch dam.

The calculation work of aforementioned stochastic finite element methods is small, but it is difficult to develop the programs. Furthermore, a common point of these methods is to study the slope stability analysis based on the reliability of every Gauss point or element. However, in practical engineering, the reliability index of whole slope and the location of slide face are expected. Combined with the existing deterministic numerical simulation programs, there appeared many other methods as well. For instance, Marinilli et al. (1999) and Nour et al. (2002) combined the deterministic numerical simulation program with MCS to conduct the reliability analyses of foundation sedimentation. Fenton and Griffiths also combined the finite element program with MCS to carry out the reliability analyses of slope engineering considering the autocorrelation of random variables.

In slope stability analysis, there are many input parameters which increase the calculation work significantly. Therefore, the parameters sensibility analysis should be carried out first for specific slope. The parameters which have the strongest influence on the slope reliability should be considered, and the others may be ignored. Low (1998) and Madsen (1986) developed the sensibility calculation function about random variables distribution parameters when the basic random variables are independent. Imai (2000) and Liu (2003) analyzed the sensibility calculation method of reliability index to the random variables distribution parameters and critical state function parameters in Gauss space when the basic variables are correlated. Sudret (2002) discussed the sensibility calculation of displacement and stress to basic variables in finite element reliability analysis.

2.3 Slope non probabilistic analysis methods review

There are some limitations of probabilistic analysis methods, for example tail problem in which the failure of probability may vary by orders of magnitude when fitting different distributions to the same input data obtained from laboratory tests (Oberguggenberger and

Fellin, 2002). In many cases, the input data are insufficient, for example the probability distributions of variables are difficult to determine. Therefore, people proposed many imprecise methods during recent years to deal with these problems, such as Interval Approach (Moore, 1966; Goodman and Nguyen, 1985), Evidence Theory (Dempster, 1967; Shafer, 1976), Fuzzy Set Theory (Zadeh, 1965), Possibility Theory (Zadeh, 1978), Imprecise Probabilities (walley, 1991), Random Set Theory (Kendall, 1974), and Convex Model (Ben-Haim and Elishakoff, 1990).

Interval analysis introduced by Moore in 1966 is used to describe the parameter uncertainties either in geometry and loadings or in soil model parameters as interval quantities (Nasekhian, 2011). An interval number is interpretation as a random variable whose probability density function is unknown but non-zero in the range of the interval. It also can be interpreted as the intervals of confidence for α-cuts of fuzzy sets. In general, the interval concept serves as a basis of other non-probabilistic uncertainty models (Muhanna et al., 2007). For example, in the fuzzy set approach a continuous membership function of input parameters can be split into several α levels with corresponding intervals and the fuzzy set approach turns into several analyses on different α-cuts (Kaufmann and Gupta, 1991; Peschl and Schweiger, 2003). In the procedure of random set approach, the worst and the best cases of the system are obtained through a series of interval analyses based on the Cartesian product of focal elements of the input parameters (Nasekhian, 2011).

In 1965, Zadeh proposed the fuzzy set approach. The model parameters of geotechnical engineering, like geometrical, loading and soil model parameters are considered as fuzzy quantities in this method. Recent years the fuzzy set approach is applied in reliability analysis with different terminology and interpretations concerning the resulting reliability. For instance, Shrestha and Duckstein (1998) calculated the probability of a fuzzy failure based on the fuzzy reliability measure which satisfies the necessary properties of the probabilistic reliability measures, and they developed a kind of fuzzy reliability index. Dodagoudae and Venkatachalam (2000) computed the reliability of slopes using the term "fuzzy probability of failure". Peschl and Schweiger (2003) assessed the safety level of a geotechnical structure using the probability of failure in the framework of fuzzy set theory.

The random set theory was first proposed by Kendall in 1974, and then developed by several authors (e.g. Matheron, 1975; Goodman, 1995; and Dubois, 1991). It is a mathematical model which can cope with uncertainty of the system, while the exact values

of input parameters are not available and only the interval of these values can be obtained. In the beginning of the 21th century, random set field has been applied extensively in geotechnical engineering, but most of these are focused on the tunnelling. In 2000, Tonon et al. used random set theory to deal with the uncertainty in geomechanical classification of jointed rock masses and reliability analysis of tunnel lining. Peschl (2004) and Schweiger et al. (2007) have developed random set finite element method (RS-FEM) and have investigated the feasibility of this method in tunneling design.

In summary, the research about slope non-deterministic analyses methods have made much progress, but there are still many problems which need to be solved for practical application, especially the combination of existing numerical simulation programs with non deterministic methods.

3. Uncertainty Concepts for Slope Stability and Determination of Geotechnical Parameters

Introduction

The purpose of this chapter is to provide the most important uncertainty concepts of slope stability, which are fundamental for this study, such as the types of uncertainties, the reliability theory in slope engineering and the characteristic parameters of soil properties. At last, the determination of geotechnical parameters based on real time monitoring data is discussed.

3.1 Uncertainty in slope engineering

In the estimation and design of slope engineering, there are many kinds of uncertainties involved, like soil property uncertainty and models uncertainty. Generally they can be divided into the following three aspects:

1). Physic uncertainty

This type of uncertainty is an innate property of nature. In slope stability it is attributed to the natural variability or randomness of some property, such as the spatial variation of the soil properties, the randomness of boundary conditions, and the irregularity of topography. This kind of uncertainty can be quantified by measurements and statistical estimations, but it is unpredictable and therefore irreducible via collection of more experimental data or using more refined models.

2). Statistical uncertainty

Statistical uncertainty is attributed to lack of data and information about slope situations. In slope probabilistic analysis, the establishment of the probability distribution of every random variable is a fitting process based on the limited data from measurements or tests. Therefore there are three major sub-categories introduced: site characterization uncertainty, model uncertainty, and parameter uncertainty.

Site characterization uncertainty has to do with the adequacy of interpretations we make about the subsurface geology. It results from data and exploration uncertainties, including (i) measurement errors, (ii) inconsistency or inhomogeneity of data, (iii) data handling and transcription errors, and (iv) inadequate representativeness of data samples due to time and space limitations.

Model uncertainty reflects the error between the probability distribution determined by people and the real distribution of soil properties. The soil properties are stochastic in every space and every time. Every probability density function, no matter normal distribution or log normal distribution can not exactly describe them, but can just approximately describe.

Parameter uncertainty means that the parameters of probability distribution of random variables will be different when the samples and sample size are different. We can only deduce the true values through the statistic. Therefore, for a set of data, the parameters of their distribution also are considered as random variables, and their uncertainties depend on two things: the sample data and the knowledge we have.

3). Simulation uncertainty

Simulation uncertainty is attributed to lack of the understanding of physical laws that limits our ability to model the real world. Slope stability analysis and design is a process which simulates the relationship of a set of input random variables (e.g. slope geometric parameters, strength parameters etc.) and the output data (e.g. safety factor, reliability index, failure probability and etc.) through some mathematical models (e.g. equations, functions, algorithms, calculation simulation programs etc.), and these models are constructed based on mathematical mechanical abstract about the real process. The simulation uncertainty results to simplification postulates and unknown boundary conditions, also by other variables which are not contained in the models for their unknown effects. In reliability analysis, people always pay attention to the improvement of probabilistic methods, but ignore the hypothetical conditions of these simulation models. Consequently the idealized theoretic equations with many postulates and the input data produced by sampling are considered as the models and values.

In slope probabilistic analyses, these uncertainties need to be quantified, and brought into the reliability analyses to estimate the probability of slope failure. For getting the types and the numerical characteristics of the random variables distribution, the relative data must be collected through plenty of tests and measurements, and determined as standard probability distribution, discrete distribution or empirical distribution through statistical analysis. The engineering discrimination and geological deduction must lead in the uncertainty estimation in the whole analysis process, so that the probability models of uncertainties have more practical significance.

3.2 Random variables

In a probabilistic analysis, the parameters which affect the results of analysis significantly and have some uncertainties are considered as random variables. In slope probabilistic analysis, the soil parameters, which represent the major sources of uncertainties, are treated as random variables. Instead of a single value, random variables are considered as a range of values in accordance with a probability density function or probability distribution. The probability distribution quantifies the frequency of values in any given interval. Two commonly used distributions, the normal and the lognormal, are described later in this section.

3.2.1 Characteristics of random variables

The most important statistical parameters related to the soil parameters are the mean value, the standard deviation, the skewness, the autocorrelation length and the correlation coefficients between the soil properties. These are explained as follows.

1). Mean value: The mean value μ_x of a set of n measured values for random variable X is obtained by:

$$\mu_x = \sum_{i=1}^{N} x_i / n \tag{3.1}$$

2). Expected value: The expected value E(x) of a random variable is the mean value one with obtain if all possible values of the random variable were multiplied by their likelihood of occurrence and then summed. The expected value is defined as:

$$E(x) = \int x \cdot f(x)dx \approx \sum x \cdot p(x_i) \tag{3.2}$$

where

$f(x)$ = Probability density function of x (for continuous random variables)

$p(x_i)$ = Probability of the value x_i (for discrete random variables)

The mean value can be calculated from representative data, it provides an unbiased estimate of the expected value of a parameter; hence, the mean and expected value are numerically the same.

3). Variance: The variance Var(x) of a random variable X is the expected value of the squared difference between the random variable and its mean value. Where actual data are available, the variance of the data can be calculated by:

$$Var(x) = E[(x - \mu_x)^2] = \int (x - \mu_x)^2 f(x)dx = [(x_i - \mu_x)^2]/n \qquad (3.3)$$

The summation form above involving the x_i term provides the variance of a population containing exactly *n* elements. Usually, a sample of size *n* is used to obtain an estimate of the variance of the associated random variable which represents an entire population of items or continuum of material. To obtain an unbiased estimate of the population working from finite samples, the *n* is replaced by *n* - 1:

$$Var(x) = [(x_i - \mu_x)^2]/(n - 1) \qquad (3.4)$$

4). Standard deviation: To express the scatter or dispersion of a random variable about its expected value in the same units as the random variable itself, the standard deviation σ_x is taken as the square root of the variance; thus:

$$\sigma_x = \sqrt{Var(x)} \qquad (3.5)$$

5). Coefficient of variation: To provide a convenient dimensionless expression of the uncertainty inherent in a random variable, the standard deviation is divided by the expected value to obtain the coefficient of variation COV which is usually expressed as a percent:

$$COV(X) = \frac{\sigma_x}{E(x)} \times 100\% \qquad (3.6)$$

Summarized from literatures, the values of COV for various soil properties and in situ tests are shown in Table 3.1.

6). Skewness: In probability theory and statistics, skewness is a measure of the asymmetry of probability distribution of a real-valued random variable. The skewness value can be positive or negative, or even undefined. Qualitatively, a negative skew indicates that the tail on the left side of the probability density function is longer than the right side and the bulk of the values (possibly including the median) lie to the right of the mean. A positive skew indicates that the tail on the right side is longer than the left side and the bulk of the values lie to the left of the mean. A zero value indicates that the values are relatively evenly distributed on both sides of the mean, typically but not necessarily implying a symmetric distribution.

Table 3.1 Coefficients of Variation for geotechnical properties and in situ tests

Property or situ test	COV (%)	References
Unit weight (γ)	3~7	Harr (1987), Kulhawy (1992)
Buoyant unit weight (γb)	0~10	Lacasse and Nadim (1997), Duncan (2000)
Effective stress friction angle (φ')	2~13	Harr (1987), Kulhawy (1992), Duncan (2000)
Undrained shear strength (S_u)	13~40	Kulhawy (1992), Harr (1987), Lacasse and Nadim (1997)
Undrained strength ratio (S_u/σ_v')	5~15	Lacasse and Nadim (1997), Duncan (2000)
Standard penetration test blow count (N)	15~45	Harr (1987), Kulhawy (1992)
Electric cone penetration test (q_c)	5~15	Kulhawy (1992)
Mechanical cone penetration test (q_c)	15~37	Harr (1987), Kulhawy (1992)
Dilatometer test tip resistance (q_{DMT})	5~15	Kulhawy (1992)
Vane shear test undrained strength (S_v)	10~20	Kulhawy (1992)
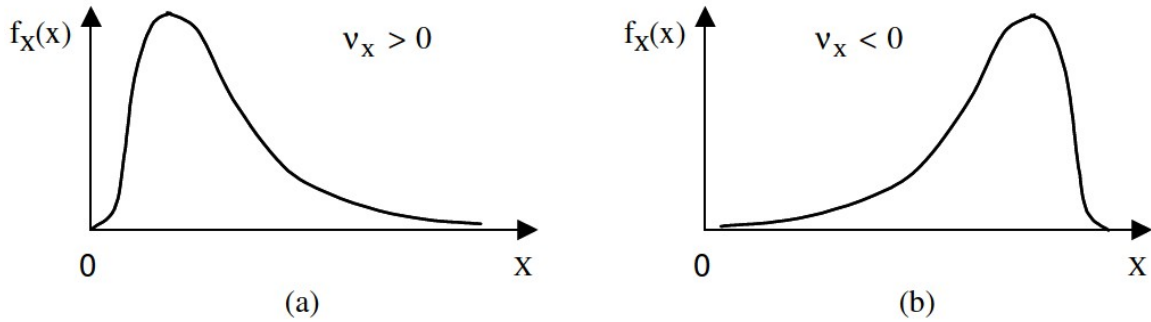
Fig. 3.1 Example of positively (a) and negatively (b) skewed distributions

The skewness of a random variable X is the third standardized moment, denoted by v and is defined as

$$v_x = \int_{-\infty}^{+\infty} \frac{(x-\mu_x)^3}{\sigma_x^3} \cdot f_x(x) \cdot dx \qquad (3.27)$$

where $f_x(x)$ is the probability density function of a random variable x.

Considering the data as reported by El Ramly et al. (2005), the skewness coefficient of the effective friction angle could be zero, and the skewness coefficient of the effective cohesion is about 1.7~4.0. It means that, in most cases the probability density function of effective

angle can be considered as symmetric distributed (like normal distributed), and the probability density function of cohesion can be considered as non symmetric distributed (like log normal distributed).

The mean value, standard deviation, and coefficient of variation are interdependent: knowing any two of them, the third can be known. In practice, a convenient way to estimate the moments of the parameters with little available data is to assume that the coefficient of variation is similar to the previously measured values from other data sets about the same parameter.

7). Autocorrelation length: Autocorrelation length θ is also called spatial correlation length. It is scale of fluctuation, which describes the spatial variability of a soil property in both horizontal and vertical directions. A large value of autocorrelation length will imply a smoothly varying field, while a small value will imply a ragged field. This is a very important parameter for random field modeling.

Leng (2000) summarized some values of autocorrelation length in both horizontal and vertical directions from different areas, shown in Table 3.2.

Table 3.2 Some values of autocorrelation length

Area and soil type	Soil property	Horizontal θ	Vertical θ
Indian sand	Standard penetration resistance	30.5m	7.8m
Bear paw shale	Liquid limit	2m	
Hongkong marine clay	Water content		1m
	Cohesion		<1m
San Francisco bay mud	Water content		2.7m
North sea moraine soil	cone penetration resistance	40m	
Chicago moraine soil	Water content	<91.4m	<0.6m
Chicago clay	Undrain shear strength		0.79
Japanese saturate clay	Undrain strength		1.25~2.86m

8). Correlation coefficient. Pairs of random variables X and Y may be correlated or independent; if correlated, the likelihood of a certain value of the random variable Y depends on the value of the random variable X. For example, the strength of sand may be correlated with density, and the top blanket permeability may be correlated with the grain size. The

covariance $Cov[X, Y]$ is analogous to the variance but measures the combined effect of how two variables vary together. The definition of the covariance is:

$$Cov[X,Y] = E[(X - \mu_X)(Y - \mu_Y)] \tag{3.7}$$

which is equivalent to:

$$Cov[X,Y] = \iint (X - \mu_X) \cdot (Y - \mu_Y) \cdot f(X,Y) dx dy \tag{3.8}$$

In the above equation, $f(X, Y)$ is the joint probability density function of the random variables X and Y. To calculate the covariance from data, the following equation can be used:

$$Cov[X,Y] = \frac{(X - \mu_X)(Y - \mu_Y)}{N} \tag{3.9}$$

To provide a non-dimensional measure of the degree of correlation between X and Y, the correlation coefficient $\rho_{X, Y}$ is obtained by dividing the covariance by the product of the standard deviations:

$$\rho_{X,Y} = \frac{Cov[X,Y]}{\sigma_X \sigma_Y} \tag{3.10}$$

The correlation coefficient may vary in the range from -1.0 to +1.0. A value of 1.0 or -1.0 indicates that there is perfect linear correlation between X and Y, given a value of X, the value of Y can be determined. The correlation coefficient zero indicates that there is no correlation between variables X and Y, which means that the variables are independent. A positive value indicates the variables X and Y increase or decrease at the same time; a negative value indicates that one variable decreases as the other increases.

According to theory and practice, for the same layer soil, there is always negative correlation between c and φ (Lumb, 1969). This is because of the difference of clay content: higher values of c are associated with lower values of φ when clay content is higher, and vice versa.

However, in some cases the correlation was found to be insignificant. Lumb (1969) concluded that the assumption of independence of strength parameters simplifies the strength interpretation considerably, and leads to conservative results if the correlation is negative in fact. Instead, the results of Cherubini (1998) indicate a significant negative correlation of $\rho_{c'\varphi'} = $ -0.6 between effective cohesion and friction angle for drained triaxial tests on Blue Matera clays. The same strong value of the correlation coefficient was

reported by Schad (1985) for marl in Urbach and was confirmed by Speedie (1956). Hence it seems that a value of about -0.6 is realistic for the soil parameters cohesion and friction angle.

3.2.2 Probability distributions

The terms probability distribution and probability density function (PDF) or the notation $f_X(X)$ refer to a function that defines a continuous random variable. The Taylor's series and point estimate methods described herein to determine the moments of performance functions require only the mean and standard deviation of random variables and their correlation coefficients, and knowledge of the form of the probability density function is not necessary. However, in order to ensure that estimates made for these moments are reasonable, it is recommended that the engineers plot the shape of the normal or lognormal distribution after assuming the expected value and standard deviation. This can easily be done easily with spreadsheet software or Matlab.

A probability density function has the property that for any X, the value of $f(x)$ is proportional to the likelihood of x. The area under a probability density function is unity. The probability that the random variable x lies between two values x_1 and x_2 is the integral of the probability density function taken between the two values. Hence:

$$P(x_1 < x < x_2) = \int_{x_1}^{x_2} f(x)\,dx \qquad (3.11)$$

The cumulative distribution function CDF or $F_x(x)$ measures the integral of the probability density function from minus infinity to x:

$$F_x(x) = \int_{-\infty}^{x} f(x)dx \qquad (3.12)$$

Thus for any value x, $F_x(x)$ is the probability that the random variable x is less than the given x. It must be a continuous non-decreasing function with values in the interval [0, 1].
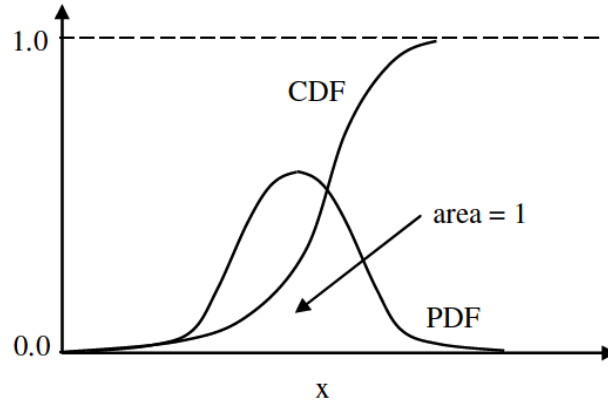
Fig. 3.2 CDF and PDF of a continuous random variable

In slope probabilistic analysis, the first step is to determine the probability characteristics of every random variable. The soil shear strength parameters cohesion c and friction angle φ are a pair of random variables, which have the strongest influence on the slope stability analysis. There are two kinds of statistical method for building the probability distributions of c and φ. The first is the least square method, which can calculate the means and standard deviations of c and φ from some groups test results directly; the second is to calculate the c and φ of every group test, and then calculate their means and standard deviations.

The soil shear strength is always expressed by Mohr-Coulomb criterion as

$$\tau = c + \sigma \tan \varphi \qquad (3.13)$$

where: τ is the soil shear strength, σ is the normal stress applied in slide mass.

The main characteristics of a random variable can be completely described if the probability density function and its associated parameters are known. In many cases, unfortunately, the form of the distribution function is unknown and often an approximated description is necessary. Several continuous distributions, which play an important role in civil engineering as well as in numerous other engineering fields, can be used as a good approximation for a random variable. These continuous distributions are applied when the random variables can take any value within some range, such as the normal and the shifted lognormal distributions.

The normal distribution or Gauss distribution is a symmetric probabilistic distribution most frequently used in engineering. It is commonly assumed to characterize many random variables where the coefficient of variation is less than about 30 percent. Its probability density function $f_x(x)$ is defined in terms of mean μ_x and standard deviation σ_x as:

$$f_x(x) = \frac{1}{\sqrt{2\pi}\sigma_x} \cdot exp\left[-\frac{1}{2} \cdot \left(\frac{x-\mu_x}{\sigma_x}\right)^2\right], \quad -\infty < x < +\infty \qquad (3.14)$$

A random variable X is log normally distributed, when its natural logarithm, $\ln(X)$, is normally distributed. The lognormal distribution for the random variable X may be defined in terms of its mean value μ_x, standard deviation σ_x and skewness coefficient v_x. The formula for the probability density function of the lognormal distribution is given by:

$$f_x(x) = \frac{1}{\sqrt{2\pi}x\sigma_x} \cdot exp\left[-\frac{1}{2} \cdot \left(\frac{\ln x-\mu_x}{\sigma_x}\right)^2\right], \quad x > 0 \qquad (3.15)$$

The lognormal distribution is generally accepted to reasonably model many soil properties, because it is strictly non-negative. It often provides a reasonable shape in cases where the coefficient of variation is larger than 30% (Consolata Russelli, 2008).

Moreover, soil properties such as cohesion and friction angle are often measured as a geometric mean over a certain volume, whose distribution tends to be lognormal distribution by the central limit theorem.

3.3 Basic theory of reliability analysis

3.3.1 Failure probability of slope

Generally speaking, the safety analysis of any engineering project contains the relationship study of "Supply" and "Demand". When these two factors are represented by symbols "X" and "Y" respectively, the structure will be safe if X > Y, and unsafe if X < Y. When X-Y = 0, it is called the limit state. This relationship can be given as Eq. 3.16.

$$M = X - Y \qquad (3.16)$$

For a slope, the resistance force R and load L on failure mass can be expressed as "Supply" and "Demand". Once the resistance force R is less than the load L, the slope will fail. Because of the uncertainties of the geological parameters and application forces, R and L are considered as random variables. The relationship of the safety factor *FS*, probability failure P_f and the probability density functions of resistance force and load are shown in Fig. 3.3. Mean value of *FS* is defined as the distance of the means of resistance force and load, and the possibility (or probability) of the slope failure P_f is indicated by the overlap of the probability density functions of resistance force and load.
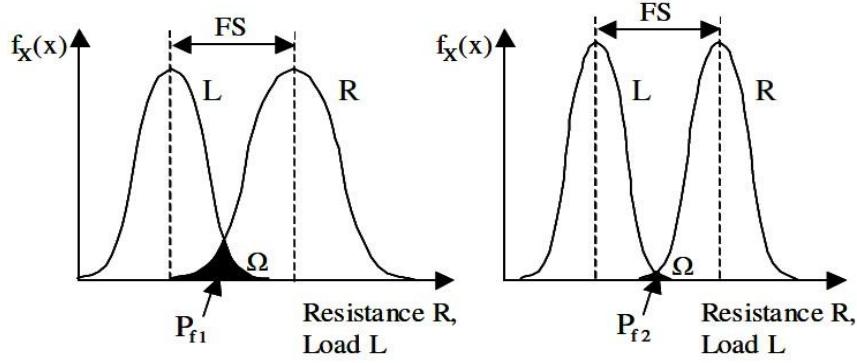
Fig. 3.3 Safety factor versus failure probability

In Fig. 3.3, the means of safety factor from two different situations are the same, but the failure probabilities are different which depend on following two aspects:

1). the relative position of the probability density functions of R and L: If the distance between $f_x(R)$ and $f_x(L)$ is longer, the overlap will be less, and the failure probability P_f will be smaller. Conversely, the P_f will be bigger. The relative position of $f_x(R)$ and $f_x(L)$ is always measured as the safety margin $(\mu_R - \mu_L)$ or the ratio of the means of R and L (μ_R/μ_L).

2). the dispersions of the probability density functions of R and L. When the relative position of the probability density functions of R and L is constant, the distributions of $f_x(R)$ and $f_x(L)$ are more dispersive, the overlap will be larger and the failure probability P_f will be bigger. The dispersions of $f_x(R)$ and $f_x(L)$ are always described by the standard deviations of R and L $(\sigma_R$ and $\sigma_L)$.

In short, the failure probability of slope is relative to the first two moments of resistance force and driving force,

$$P_f = \propto f(\mu_R/\mu_L, \; \sigma_R, \; \sigma_L) \tag{3.17}$$

3.3.2 Definition of reliability index

Harr (1987) defines the engineering definition of reliability as follows: "Reliability is the probability of an object (item or system) performing its required function adequately for a specified period of time under stated conditions." As it applies in the present context, the reliability of a slope can be defined as follows: The reliability of a slope is the probability that the slope will remain stable under specified design conditions. The design conditions include: for example, the end-of-construction condition, the long-term steady seepage

condition, rapid drawdown, and earthquake with a specified magnitude.

For representing conveniently, the resistance force R and load L are assumed as independent normal distributed variables N (μ_R, σ_L) and N (μ_R, σ_L). Therefore, the limit state equation M=R-L is also normal distributed, N (μ_M, σ_M), where

$$\mu_M = \mu_R - \mu_L \tag{3.18}$$

$$\sigma_M^2 = \sigma_R^2 + \sigma_L^2 \tag{3.19}$$

Therefore, the purpose of the probabilistic analysis of slope is to determine the probability of M < 0.

$$P_f = P(M = R - L < 0) = \int_{-\infty}^{0} f(M) dM \tag{3.20}$$

Based on the probabilistic and statistical theory, it is not difficult to prove that above integral can be expressed as the function of μ_M/σ_M, i.e.

$$P_f = 1 - \Phi(\mu_M/\sigma_M) \tag{3.21}$$

In reliability theory, it can be represented as reliability index β, i.e.

$$\beta = \mu_M/\sigma_M \tag{3.22}$$

For further expatiate on the geometric meaning of reliability index, we lead in standard variables:

$$R' = (R - \mu_R)/\sigma_R \tag{3.23}$$

$$L' = (L - \mu_L)/\sigma_L \tag{3.24}$$

Substitute Eq. 3.23 and 3.24 into the function 3.16, we get

$$M = \sigma_R R' - \sigma_L L' + \mu_R - \mu_L \tag{3.25}$$

In the standard variables space (Fig. 3.4), the safe state and unsafe state are separated by the failure face M = 0.
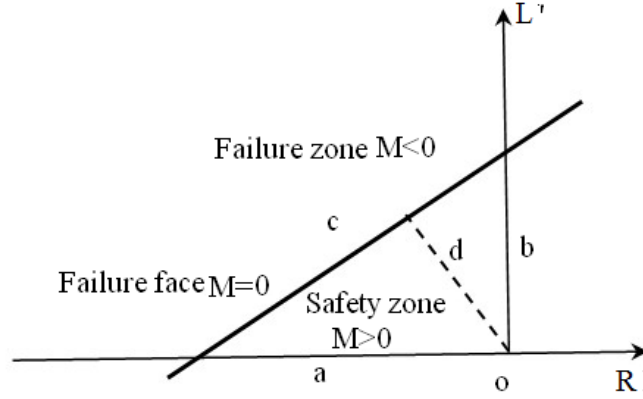
Fig. 3.4 Limit state surface in standard variables space

From the geometric relationship in Fig. 3.4, the parameters *a*, *b* and *c* can be determined as follows:

$$a = (\mu_R - \mu_L)/\sigma_R \tag{3.26}$$

$$b = (\mu_R - \mu_L)/\sigma_L \tag{3.27}$$

$$c = \frac{\mu_R - \mu_L}{\sigma_R \sigma_L} \cdot \sqrt{\sigma_R^2 + \sigma_L^2} \tag{3.28}$$

Thus, the safety degree or the reliability of slope can be measured by *d*, the minimum distance between the original point and limit state line, according to the geometric knowledge,

$$d = \left| \frac{ab}{c} \right| = \frac{(\mu_R - \mu_L)}{\sqrt{\sigma_R^2 + \sigma_L^2}} = \frac{\mu_M}{\sigma_M} = \beta \tag{3.29}$$

In above discussion, the state function is assumed as a linear function about two independent normal distributed variables. When the number of variables increased from 2 to 3, the calculation of reliability index β can be extended from 2 dimensions to 3 dimensions using Eq. 3.29. If the random variables are not normal distributed or independent, they should be transformed into independent normal distributed variables through some means (Ang and Tang, 1984).

If the probability density function of safety factor is normally distributed, the corresponding reliability index β is defined as (Chowdhurg, 1984; Tabba, 1984; Fell et al., 1988):

$$\beta = (\mu_{FS} - 1)/\sigma_{FS} \tag{3.30}$$

where μ_{FS} is the mean of safety factor and σ_{FS} is the standard deviation of safety factor. If the probability density function of safety factor is log normally distributed, the reliability index of slope can be given as Eq. 3.31 (Wolff and Wang, 1992).

$$\beta = ln\left(\frac{\mu_F}{\sqrt{1+(\sigma_F/\mu_F)^2}}\right)/\sqrt{ln(1+(\sigma_F/\mu_F)^2)} \tag{3.31}$$

The relationship of the reliability index β and failure probability P_f is shown in Fig. 3.5.
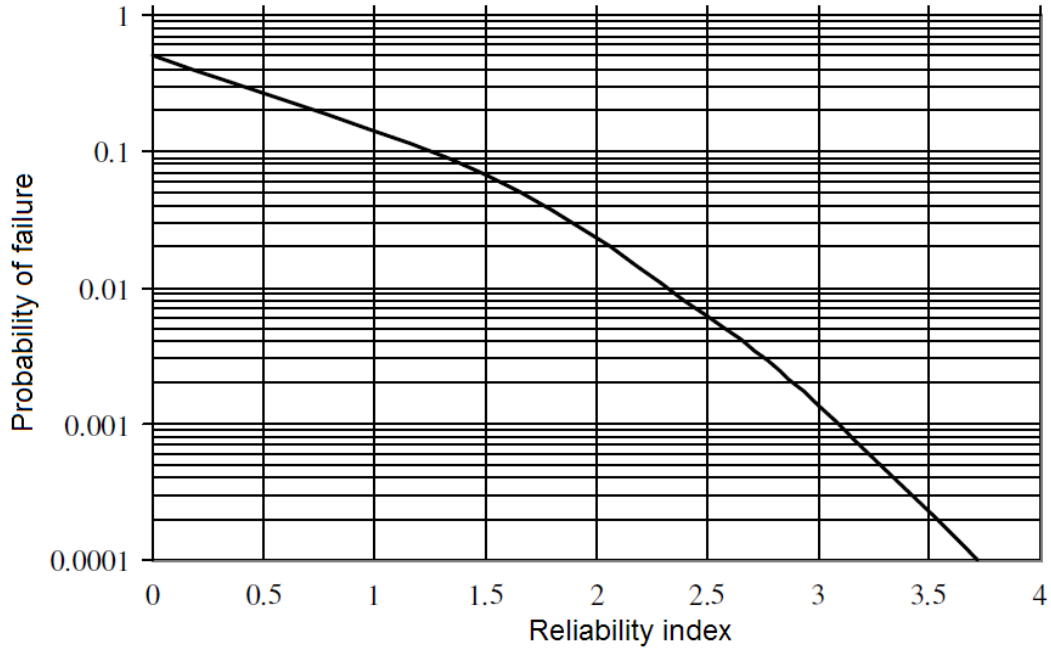
Fig. 3.5 Failure probability P_f versus reliability index β for a normal distribution

3.3.3 Definition of the performance function

The reliability is a kind of measurement that the structure can obtain intended function or the system can run normally in one period under some load condition. According to US Army Corps of Engineers (1997) "The term 'failure' is used to refer to any occurrence of an adverse event under consideration, including simple events such as maintenance items. To distinguish adverse but non-catastrophic events (which may require repairs and associated expenditures) from events of catastrophic failure (as used e.g. in the dam safety factor context), the item probability of unsatisfactory performance is sometimes used."

Slope stability calculations need to be performed to ensure that the resisting forces are greater than the forces tending to cause a slope to fail. In slope reliability analysis, the performance function of slope stability is always defined as

$$g(X) = R - L = g(x_1, x_2, \ldots, x_n) \tag{3.32}$$

where, x_i ($i=1, 2, \ldots, n$) are n input variables which impact the slope reliability, like shear strength properties, pore water pressures, slope geometry and other soil and slope properties. The function $g(X)$ reflects the performance or state of the slope. The slope will be safe when $g(X) > 0$; unsafe or failure when $g(X) < 0$; limit state when $g(X) = 0$, which is also called the limit state function of slopes.

If the joint probability density function of the variables x_i in performance function is $f_{x_1, x_2 \ldots, x_n}(x_1, x_2, \ldots, x_n)$, the probability of safety is

$$P_s = \int_{g(X)>0} \ldots \int f_{x_1, \ldots, x_n}(x_1, x_2, \ldots, x_n) dx_1 dx_2 \ldots dx_n \tag{3.33}$$

In the same way, the probability of failure is

$$P_f = \int_{g(X)<0} \ldots \int f_{x_1, \ldots, x_n}(x_1, x_2, \ldots, x_n) dx_1 dx_2 \ldots dx_n \tag{3.34}$$

In slope probabilistic analysis, Li and Lumb (1987) and Lowe, et al. (1998) defined the limit state of performance function as following two expressions:

$$F(x_1, x_2, \ldots, x_n) - 1 = 0 \tag{3.35}$$

$$\ln F(x_1, x_2, \ldots, x_n) = 0 \tag{3.36}$$

where $F(x_1, x_2, \ldots, x_n)$ is the safety factor function about x_i ($i=1, 2, \ldots, n$), it is the ratio of the maximum shear strength and the mobilized shear stress. When $F(X) > 0$, the slope is safe; when $F(X) < 0$, the slope is unsafe. Therefore, the performance function of slope stability analysis can be defined by different form if different safety factor calculation method is chosen (e.g. Simplified Bishop Method, Spencer method, Morgenstern-Price Method and etc.). Otherwise, there may be no explicit performance function if numerical simulation method is used in slope stability analysis.

3.4 Determination of geotechnical parameters based on real time monitoring data

The usual means of determination of geotechnical parameters are laboratory and in situ experiments, or the use of empirical classification systems in rock. The results of all methods are fraught with uncertainties due to uncertainty factors such as heterogeneity, representative experimental conditions, etc. Therefore, sometimes the simulation results, like displacements, based on these parameters are much different with the results from field

tests. To reduce these uncertainties, the inverse analysis based on the comparison of real time monitoring data and numerical simulation results can be used to determine the geotechnical parameters.

Recent research in the area of real-time monitoring of landslides development focus on the application of micro sensors (MEMS) in ad hoc wireless sensor networks operated in an interoperable spatial data infrastructure (SDI) according to the sensor web enablement (SWE) guidelines of the OGC (Open Geospatial Consortium), like the SLEWS-Sensor based Landslide Early Warning System (Fernandez-Steeger et al., 2009; Azzam, et al., 2011). Apart from motion detection, the SLEWS sensor nodes also provide a 3D acceleration data to evaluate direction and value of the peak acceleration (Klapperich et al., 2011).
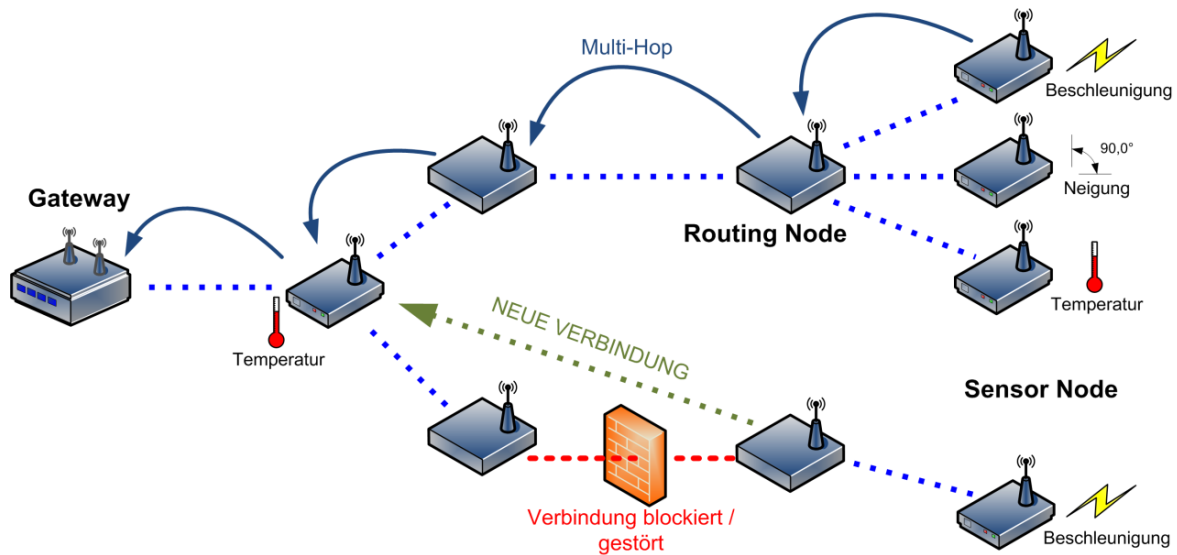
Fig. 3.6 Structure of an ad hoc wireless sensor network (Fernandez-Steeger et al., 2009)

Real-time monitoring systems can help people to understand the failure mechanisms of slopes induced by heavy rainfall or earthquake, and invert the input parameters of the slope stability analysis model. Through comparison of numerical solutions and real-time data, the mechanical parameters can be inferred by inversion method, which are in turn to determine the safety factor or the degree exploitation needed to DIN 1054.

Inverse methods are divided into analytical approaches, numerical simulation-such as FEM, FDM and BEM, etc. Here, the equations describing the system behavior can be inverted in the manner that the material parameters as a result and the measured quantities occur as input. Figure 3.7 shows a schematic of the inversion method, which takes advantage of the back-analysis.
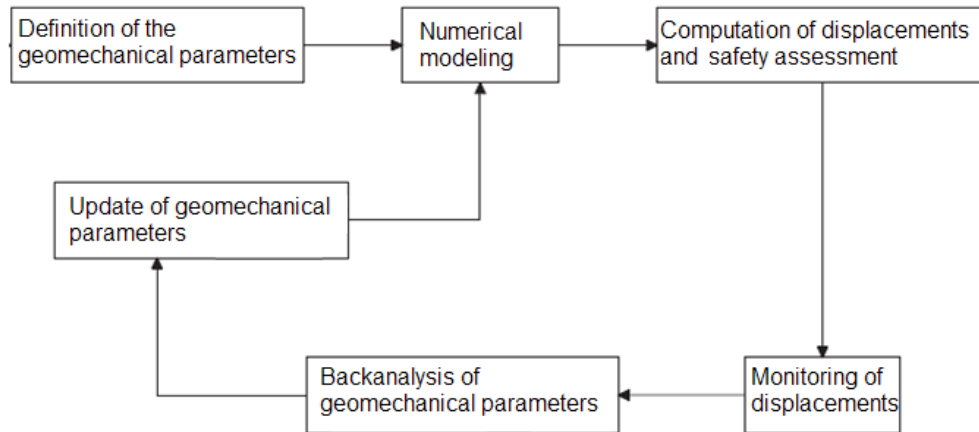
Fig. 3.7 Scheme of the observational method using back analysis in the process

The measured data to validate or update the input values (such as the geomechanical parameters) using models based on the numerical simulation. An example of a homogeneous embankment under earthquake loading will be shown in follows, and the application of real-time measurements to improve the modeling by means of inversion. The numerical simulation is performed with the software FLAC.

Figure 3.8 shows the selected example with 25 °slope angle, length of 200 m, left height of 35 m, and right height of 80 m. The initial input soil parameters are listed in Table 3.3 (dilation is disregarded).

Table 3.3 The soil parameters

Density (kg/m^3)	Bulk (Pa)	Shear (Pa)	Cohesion (Pa)	Friction angle °	Dilation °	Tension (Pa)
2000	5.1e8	2.3e8	2.5e4	25	0.0	0.0
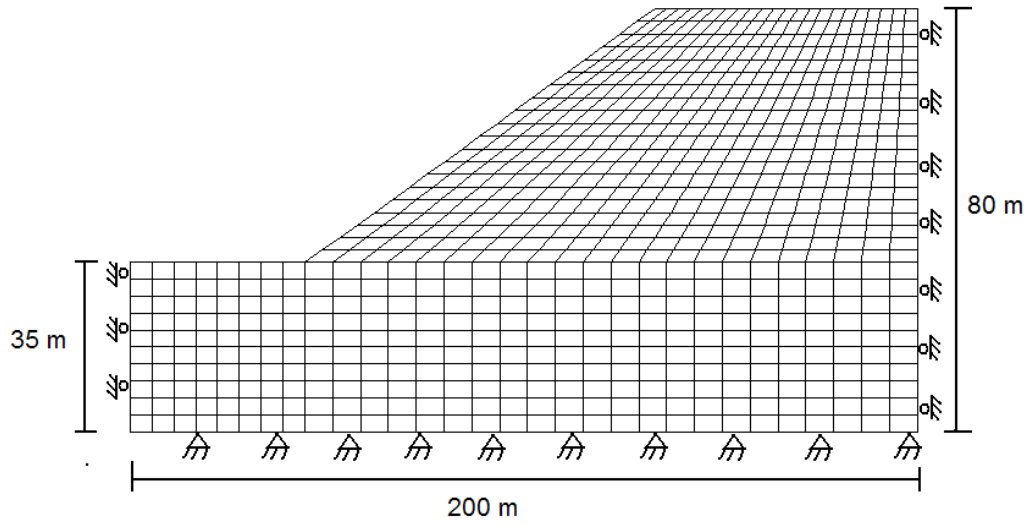
Fig. 3.8 Finite difference mesh of the slope

Fig. 3.9 shows a relative displacement of one point of the sliding mass by numerical simulation. The solution is converged to a certain displacement, and it means this is a stable slope.
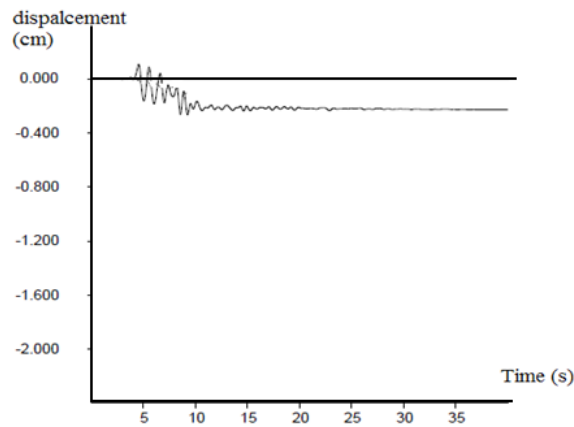
Fig. 3.9 Relative displacement at one point by numerical simulation

In the following step, the geotechnical slope parameters are modified by inversion based on the comparison of displacement history of the numerical simulation and real-time monitoring, until the results from monitoring and numerical simulation are very close. At last, the developed numerical model can used to analyze a deformation development in a long time or due to a higher-magnitude earthquake, helping to improve the warning system.

The inversion analysis based on real time monitoring data and numerical simulation is a practical way to reduce the uncertainty of slope modeling.

4. Slope Stability Analysis based on the Integration of GIS and FLAC

Introduction

The numerical simulation technique, such as the finite difference or finite element has developed incredibly fast and is extensively applied in slope stability analyses. However, in most numerical simulations, the modeling of complex slope topography and the determination of most vulnerable cross section is difficult to materialize. FLAC; the prevailing finite difference program used for numerical simulations of slope stability cannot use geospatial data directly without being processed beforehand. To bypass the lengthy preprocessing, mostly the 2D models instead of 3D or simplified geological models are adopted in numerical simulations, which affect the results significantly. The difficulty of this preprocessing hinders the application of numerical simulation techniques in geotechnical engineering seriously. Therefore, a simpler and more precious modeling technique of slopes stability needs further study.

GIS provides various excellent functions of capturing, inputting, manipulating, transferring, visualizing, combining, querying, analyzing, modeling, and outputting of the geospatial data. With the development of many kinds of topography measuring techniques, such as LiDAR, satellite imagery, stereographic surveys and GPS, GIS is applied more and more to slope stability analyses. However, most of the researchers use a statistical method to quantify the relationship between slope failure and the influential factors while GIS is used only to perform regional data preparing and processing. Little research has been conducted on the integration of GIS and a deterministic numerical simulation technique for slope stability analysis. Xie et al. (2004, 2006) developed a column-based three dimensional limit equilibrium slope stability analysis model to calculate the 3D safety factor based on GIS grid. Dahal et al. (2008) carried out a deterministic distributed analysis using GIS to calculate the probability of slope failure. In both these studies, the deterministic calculations were performed by means of GIS with input of geometrical data, data on shear strength parameters, unit weight and physical parameters. Due to limitations of complex algorithms and iteration procedures in GIS only simple models like limit equilibrium models have been conveniently applied.

Aringoli et al (2008) tried to combine the GIS technique and commercial numerical simulation code to conduct the deterministic slope stability analysis. Contrary to Xie et al. (2004, 2006) and Dahal et al. (2008), Aringoli et al (2008) performed the deterministic

calculations outside GIS; two programs Surfer-8 and GiD-8 were applied to edit and transform GIS data into numerical simulation software. This technique needs to deal with the problem of data conversion among three different programs, which increases the difficulty of operation. Consequently a procedure to integrate GIS and a commercial finite difference code FLAC in slope stability analysis has been developed. Surfer-8 is applied to deal with the topographic data of slope and a script has been written using FISH programming language for transforming the topographic data into FLAC directly. The reliability of the coupling of GIS and numerical simulation technique is demonstrated by the Xuecheng slope stability analysis, after investigating both 2D and 3D models.

4.1 Overview of FLAC

FLAC [ITASCA 2005] is the abbreviation of "Fast Lagrangian Analysis of Continua" and is developed by ITASCA. The FLAC software is based on the explicit finite difference method which can simulate the behavior of many materials such as soils, rocks and structural buildings.

4.1.1 Application range of FLAC

The application range of FLAC is very extensive, because it is equipped with 11 built-in constitutive models, five optional facilities, several kinds of structure element as well as a built in language FISH.

The 11 available models for FLAC are divided into three groups: null model, elastic models (isotropic and transversely isotropic) and plastic models (Drucker-Prager, Mohr-Coulomb, ubiquitous-joint, strain-hardening/softening, bilinear strain-hardening/softening ubiquitous-joint, double-yield and modified Cam-clay). Every element of the numerical model can be defined by different material model, and the property parameters of the material can be linear or non linear distributed.

Furthermore, there are also following five optional facilities in FLAC:

1). Static mode: this is a default mode in FLAC, and the static solution can be obtained through the dynamic relaxation.

2). Dynamic mode: user can directly input the values of acceleration, velocity or stress as the boundary or initial conditions of system.

3). Creep mode: there are six creep modes can be applied to simulate time-dependent

material behavior, including both viscoelastic and viscoplastic modes.

4). Seepage mode: this facility can be used to simulate the flow of underground water, the dissipation of pore pressure and the coupling of deformable porous median and the viscous liquid inside. This mode can be coupled with the static, dynamic or thermal modes.

5). Thermal mode: it can simulate the heat conduction and thermal stress.

FLAC also can simulate various structures. For general rock, soil or other material, the eight point hexahedron element can be adopted. In FLAC grids, the interface is accepted. The grids on the both sides of interface can separate or slide. Therefore it can simulate the joint, fault or some other physic boundaries easily.

Totally, there are four kinds of additional structure element in FLAC: beam, anchor, pile and shell. They can be used to simulate the artificial structures in geotechnical engineering, like support, liner, anchor, rock bolt, geotextile, friction pile, sheet pile and etc.

Another highlight of FLAC is the inner language FISH. It can be used to define some new variables or functions, and meet the user's new demands. It can help user to realize following functions:

1). It can be used to define the distribution rule of material property (e.g. non linear or random distribution).

2). It can be used to define some new variables, and trace its change law during the simulation and plot or print it out.

3). it can be used to design user's own element forms.

4). It can be used as servo control in numerical tests.

5). It can be used to define special boundary conditions.

6). Based on the built-in FISH variables and functions, user can obtain the parameters of nodes or elements, like coordinates, displacements, velocities, material parameters, stress, strain, unbalanced forces and so on.

4.1.2 Comparison with finite element methods

Compared with some finite element methods, FLAC have following advantages:

1). FLAC adopts mix discrete method to simulate the yield or plastic flow of material, it is more reasonable than the reduced integration method generally used in finite element methods.

2). the dynamic equation applied in FLAC is very suitable to simulate the dynamic problems, for example, vibration, failure, large deformation and so on.

3). over the years, certain "traditional" ways of doing things have taken root: for example, finite element programs often combine the element matrices into a large global stiffness matrix, whereas this is not normally done with finite differences because it is relatively efficient to regenerate the finite difference equations at each step. FLAC uses an "explicit" time marching method to solve the algebraic equations, but implicit, matrix-oriented solution schemes are more common in finite elements.

There are still some disadvantages in FLAC:

1). FLAC needs more time than finite element method to reach convergence for the linear problem.

2). the convergence velocity of FLAC depends on the ratio of maximum natural period and the minimum natural period of system. Therefore, the simulation efficiency of some problems is very low, like the models which include the elements with different size or material elastic modulus.

In a word, the most obvious disadvantage of FLAC compared with finite element methods is that it is more time consuming.

4.2 Brief description of the Strength Reduction Method

One approach of computing factor of safety with FLAC is by Strength Reduction Method (SRM). In SRM, the safety factor is defined as the shear strength margin, which is also adopted in conventional limit equilibrium method and is widely accepted by engineers for practical applications. The process of strength reduction technique is discussed as follows.

For Mohr-Coulomb failure criterion, the shear strength τ_f is given as:

$$\tau_f = c + \sigma_n \cdot tan\,\varphi \qquad (4.1)$$

where σ_n is the effective normal stress, c is the cohesion, and φ is the angle of internal friction.

The reduced shear strength τ_m along the failure surface is expressed as follows:

$$\tau_m = \tau_f/f \tag{4.2}$$

By substituting Eq. 4.2 into Eq. 4.1, we get:

$$\tau_m = c/f + \sigma_n \cdot tan\,\varphi/f \tag{4.3}$$

The value of f is adjusted until the slope fails, where the ultimate f is the factor of safety. In FLAC, the convergence criterion to determine the simulation attaining equilibrium is to achieve a state when the maximum node unbalanced force approaches zero. The unbalanced force is the sum of forces acting on a node from its neighboring elements. If a node is in equilibrium, these forces should sum to zero. Thus, the unbalanced force is a measure of how far from equilibrium a particle node is.

To determine if a simulation has reached equilibrium or not, the numerical mesh is searched for the node with the greatest unbalanced force. The maximum unbalanced force is then normalized by the gravitational body force acting on the node. In a numerical simulation the unbalanced force never gets zero and so acceptable lower limit must be chosen. For this study, a simulation was considered to have converged to an equilibrium state when the normalized nodal unbalanced force of every node in the mesh was less than 10^{-3}.

For quickly obtaining the reference value of f, the bracketing and bisecting procedure was used. First, the upper and lower brackets were established. The initial lower bracket was a trial value of f for which the solution converged. The initial upper bracket was a trial value of f for which the solution did not converge. Next, a middle value between the upper and lower brackets was tested. When the solution converged, the lower bracket was replaced by this new value. On the contrary, it replaced the upper bracket. The process was repeated until the difference between upper and lower brackets was less than 10^{-3}.

After the reference value of f is obtained, it is then used for further calculation with the examination of graphic output of yield zone developed within the slope in order to determine the slip surface during failure. Smaller incremental values of f are required in the successive steps to determine the possible failure surface.

The processing of geospatial data using GIS software for use in FLAC and application of shear strength reduction technique for Xuecheng Slope is demonstrated in the following text.

4.3 Stability analysis of Xuecheng slope

In this section, the integration of GIS and FLAC is demonstrated by the Xuecheng slope

stability analysis.

4.3.1 Project overview

The study area is located in the southwest of China, part of the Qinghai-Tibet Plateau and develops eastward the edge of Qionglai Mountain. The exposure soil of this area is predominated by Paleozoic Devonian terrain and Quaternary loose deposits and presents a complex structural setting. The extensional Quaternary tectonic has produced a general and intense uplift of the area, and the velocity of this uplift has increased in recent years. The bedrock comprises of thick sequence of phyllites which are divided into strongly weathered and moderately weathered.

The study area belongs to subtropical monsoon climate. Data from the weather station indicates that the average temperature is 11.4 ℃. The annual average precipitation is 609.6 mm, the maximum annual precipitation is 709.1 mm (1992), and the maximum daily precipitation is 55.9 mm (12, Aug. 1982). 69% of rainfall concentrates in the months from May to September of every year.

Since the beginning of 20th century, many catastrophic slope failures have occurred in this area (Huang 2009), where earthquake is the most frequent trigger. Wenchuan Earthquake induced about 20,000 landslides in 2008 and damaged the vegetation on slope surface and structure of the subsurface of many slopes, which are brought to the margin of failure; one of them is the Xuecheng slope, which needs stability estimation urgently.

The Xuecheng slope is located at the back of Xuecheng middle school in Xuecheng town, Sichuan province, and its coordinates are N31°33′00″ and E103°18′34″ (Fig. 4.1). The elevation of the Xuecheng slope varies from 1,604 to 1,778 m. It is a steep slope with a gradient of 30-45 °, and the slope aspect is about 330 °. Based on the geological investigations, the soil of slope consists of 8-10 m thick quaternary alluvial deposits composed of rubble mixed with 20-30% silt. Devonian age phyllites predominate as the bedrock. The slope surface is sparsely vegetated with grass, shrubs, and some scattered planted fruit trees.

Fig. 4.1 Location and view of Xuecheng slope

Before the 2008 earthquake, the Xuecheng slope was stable integrally, and there was no obvious deformation. Impacted by the earthquake, some cracks and deformation appeared in the middle and crest of the slope, and that too concentrated in the shallow layer (Fig. 4.2).
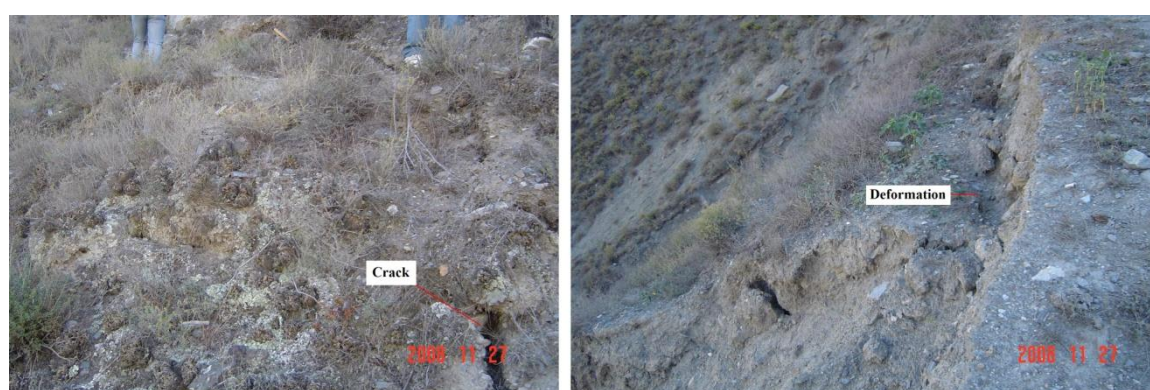
Fig. 4.2 Crack and deformation in the middle and crest of slope

The geotechnical parameters of the slope were obtained from numerous analyses carried out during the geognostic surveys derived from in situ and laboratory tests (Table 4.1). The gravity is set to 9.81 m/s^2, and the interface between soil and bedrock is considered approximately parallel to the ground surface of the slope having a depth of 10 m.

Table 4.1 Mechanics parameters of the slope in different layer

layer	Weight (kN/m^3)	Cohesion (kPa)	Friction angle (°)	Bulk (GPa)	Shear (GPa)	Tension (MPa)
Soil	19.5	20	34	3.04	1.65	0.01
Bedrock	20.1	90	37	28.4	18.7	0.7

4.3.2 Preparation of GIS data

Xuecheng slope is a natural slope modified by human; therefore the topography of this slope is very complicated, unlike man made slopes (e.g. dams or banks). Thus, it is difficult to construct the precise slope model directly using FLAC. In this study, the GIS technique is applied to overcome this difficulty.

GIS data can be collected from many sources, i.e. GPS, satellite images and different kinds of maps. The topographic data of 1:1000 resolution having elevation interval of 1 m for Xuecheng slope was used (Fig. 4.3).
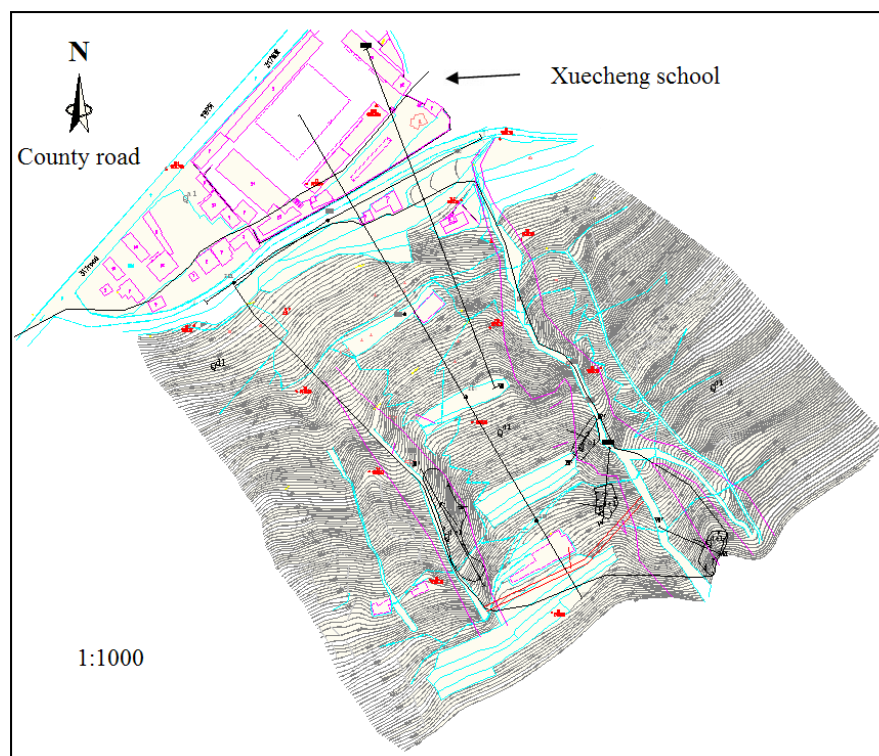
Fig. 4.3 Contour line map of Xuecheng Slope

The graphic program Surfer-8 was used for assigning elevation attribution to the contour lines. Then a digital elevation Model (DEM) was generated from the elevation data (Fig. 4.4), in which the spatial coordinates (*x, y, z*) of each superficial point were interpolated with the kriging method to obtain a uniform distribution of the nodal values to cover the whole area. The resultant map was stored as a grid formation data; comprised of rows and columns of cells, with each cell storing a single value of elevation. The elevation is represented by RGB (red, green, blue) colors which make the slope and aspect of the Xuecheng slope visually clearer. Red indicates a higher elevation, and blue represents a lower elevation.
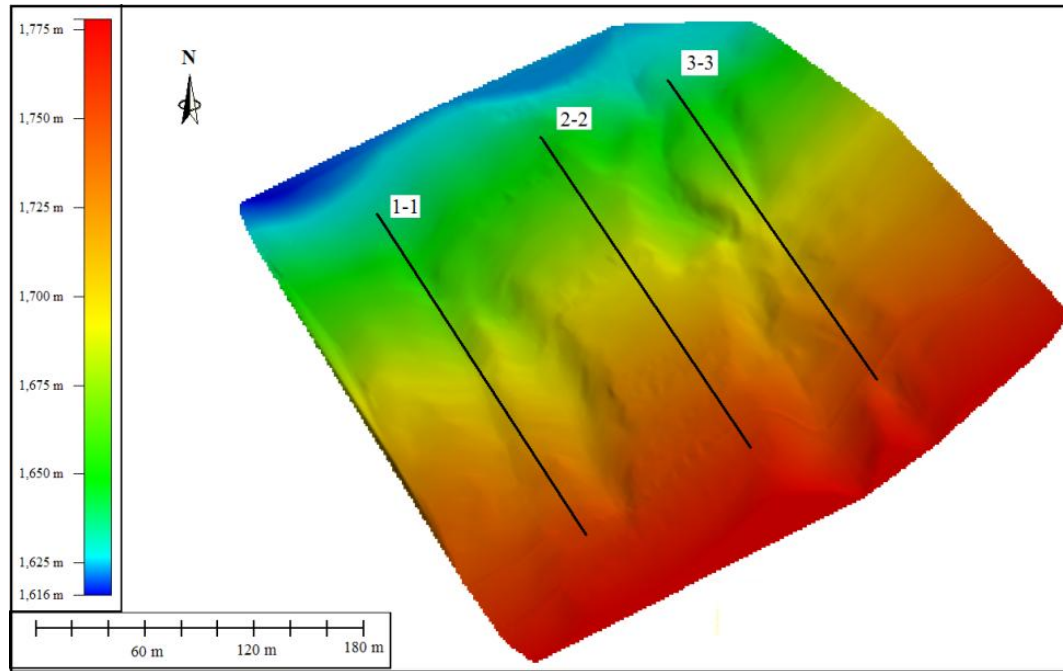
Fig. 4.4 Digital elevation map of Xuecheng slope

4.3.3 Slope stability analyses in 2D

4.3.3.1 Numerical modeling of slope in 2D

In 2D slope stability analysis, the safety factor of the whole slope is determined by the safety factor of a particular cross section; therefore choosing and modeling of the most vulnerable cross section in the potential slide mass are the most critical steps. Applying cross section extraction function of Surfer-8 program, profile of a cross section can be obtained by drawing a line on the digital elevation map, and the distance vs. elevation data of this cross section can be stored as an ASCII data. A program for automatically generating the FLAC 2D slope models from the ASCII data was developed using FISH language. Thus any cross section model in the map can be simulated by this process easily, quickly and precisely.

Three representative cross sections distributed in the west, middle and east of the slope respectively (Fig. 4.4) were constructed to perform the numerical simulation. In construction of 2D numerical models based on GIS, the elevation data of 20 meters interval was chosen. If a higher resolution of the model is required, shorter interval of elevation data can be chosen. The profiles and the 2D numerical models of these three cross sections are shown in Fig. 5-7, where the green plots are the profiles of slope cross sections constructed using GIS software, and the plots at the right side of profiles are the finite deference models of the corresponding cross sections. The elements number of each numerical model is 2964, and the element in the

rock layer is much coarser than the soil layer.
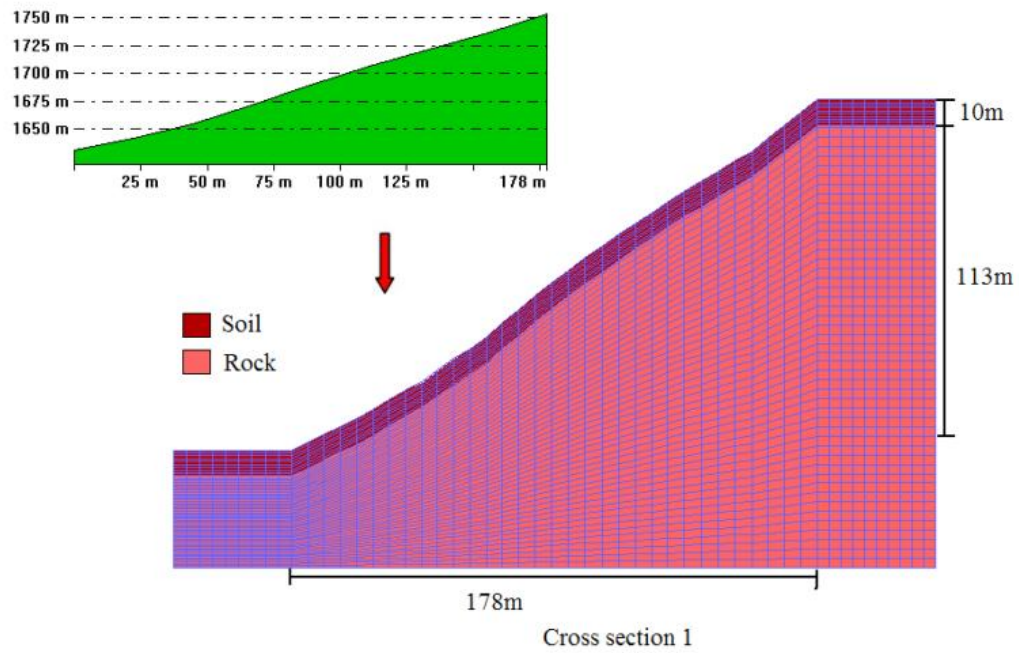
Fig. 4.5 Profile and the 2D numerical slope model about Cross Section 1
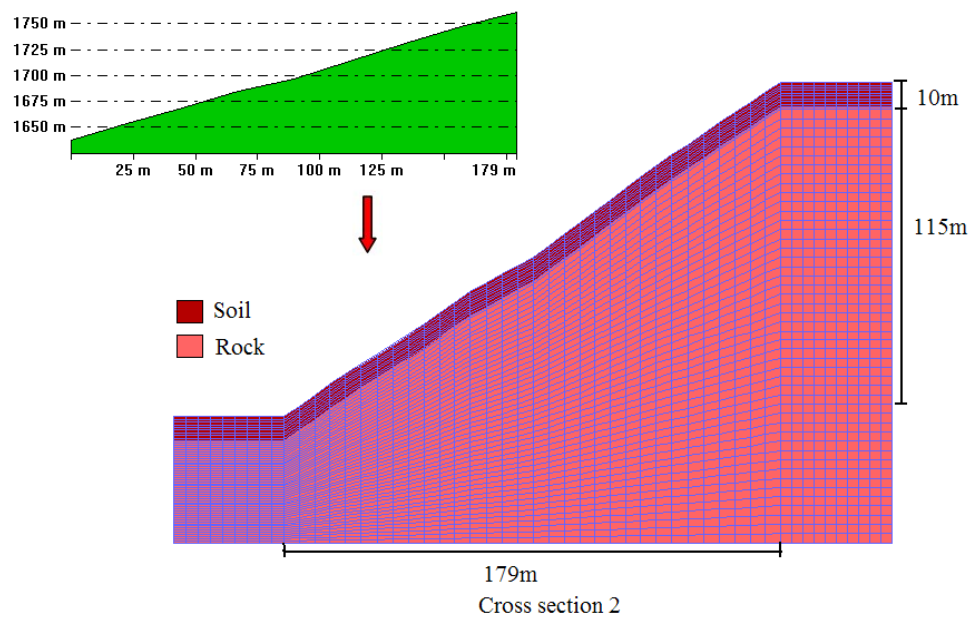
Fig. 4.6 Profile and the 2D numerical slope model about Cross Section 2
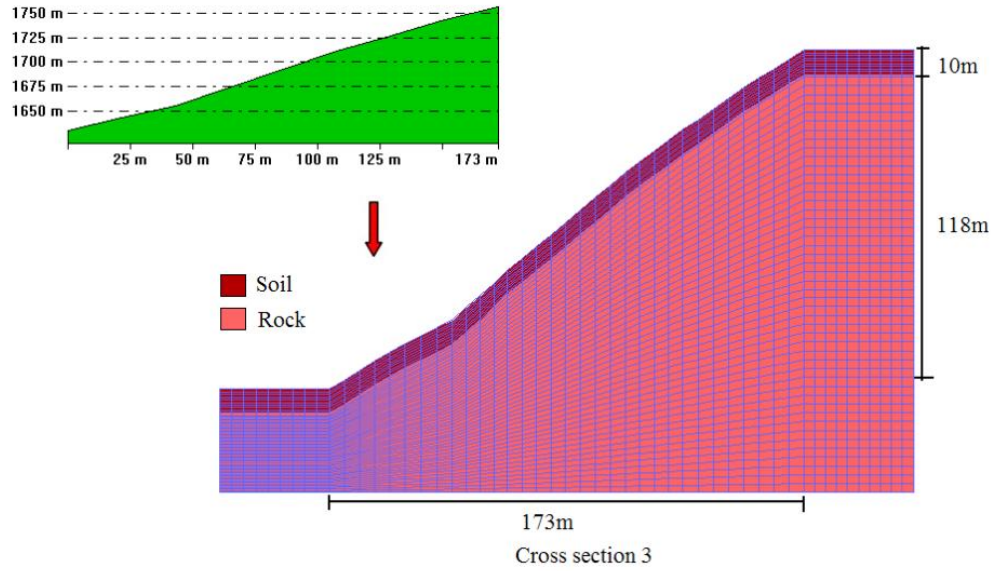
Fig. 4.7 Profile and the 2D numerical slope model about Cross Section 3

The Mohr Coulomb constitutive model was used in the numerical simulation. For the deformation and failure to occur at shallow level of the slope and because the tectonic stress dissipates in the long term geologic process, the horizontal tectonic stress is ignored, and the mesh of the soil is constructed denser than that of the bedrock. These calculations are plane strain problems ignoring the lateral deformation. The boundary conditions of the slope models are: left and right boundaries are fixed only in x direction and the bottom is fixed both in x and y directions.

4.3.3.2 Results of stability analysis of slope in 2D

Simulations were performed for a series of trial factors of safety with c and φ reduced according to Eq. 4.3. Fig. 4.8 shows the normalized unbalanced force obtained as the shear strength is reduced in 5,000 steps based on cross section 1.
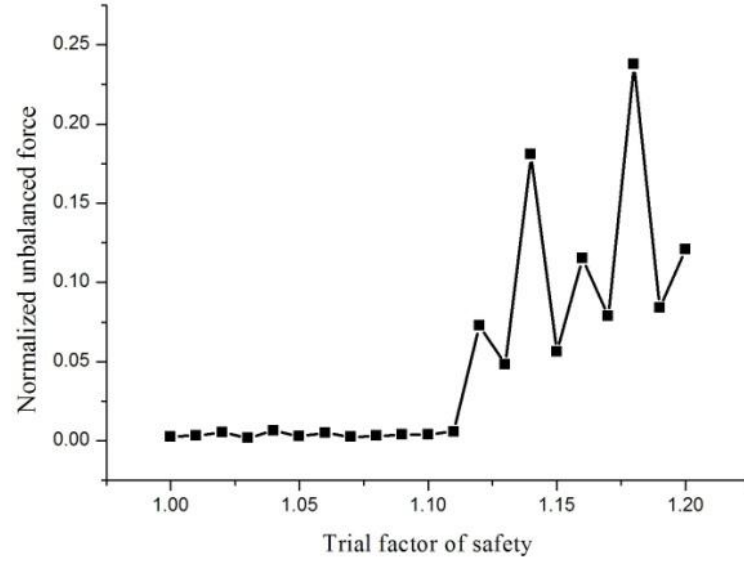
Fig. 4.8 Unbalanced force as the trial factor of safety is increased in 5,000 steps

For trial factors of safety up to 1.11, simulations converged to equilibrium with an unbalanced force of the order of 10^{-3}. However, when the trial factor of safety was increased to 1.12 the simulation no longer converged, with the unbalanced force exceeding 10^{-3}. As the strength was reduced further, the unbalanced force continued to increase.

The sharp break in the unbalanced force in Fig. 4.8 shows that there is no ambiguity in identifying the trial factor of safety at which the slope fails. This is a consequence of using a linear elastic-perfectly plastic constitutive model, a model with a sudden transition from elastic to plastic behavior.

The safety factors of the Xuecheng slope at the three cross sections using the Strength Reduction Method compared with limit equilibrium methods (LEM) are shown in Table 4.2. Generally, the safety factor by Strength Reduction Method is a little smaller than the limit equilibrium method. Comparing the safety factors of three cross sections, one can see the safety factor of Cross Section 3 is the smallest and close to 1.0, which means that the potential failure possibly will occur in the area along Cross Section 3 (i.e., at eastern side of this slope).

Table 4.2 Factors of Safety by SRM and LEM

Cross section	SRM	Ordinary	Bishop	Janbu	Morgenstern Price
No.1	1.11	1.207	1.242	1.207	1.231
No.2	1.15	1.254	1.281	1.256	1.269
No.3	0.98	1.101	1.129	1.103	1.122

Fig. 4.9 shows the slope state of the three cross sections and the *x* displacement contours of Cross Section 3. For all of the cross sections, the shear failure distributes in the interface between the soil and bedrock. In Cross Section 3, not only the shear yield, but also the tension yield appeared, and the tension yield distributes on the crest of slope and connects with the shear yield through the whole slide mass, which means that slope at the Cross Section 3 failed. The *x* displacement of Cross Section 3 reached to 3.5 cm in 5000 steps simulation and concentrated in the upper part of the soil layer.
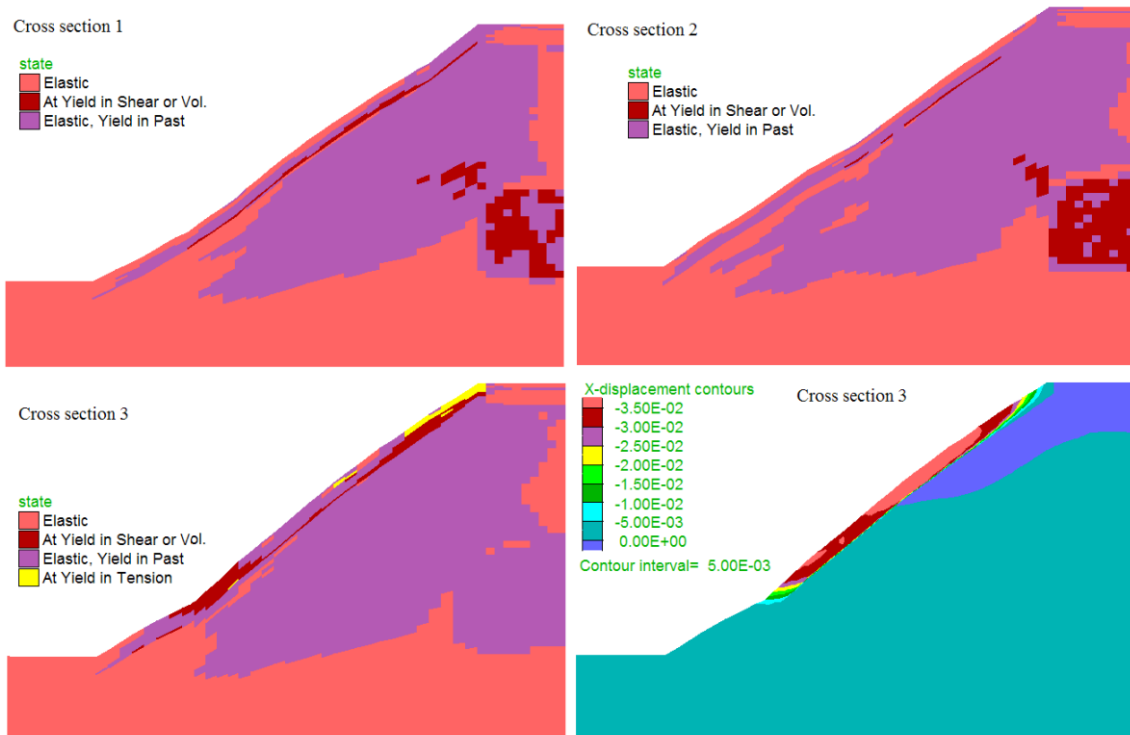
Fig. 4.9 Results of the numerical simulation in 2D

4.3.4 Slope stability analyses in 3D

4.3.4.1 Generation of 3D slope numerical model

For complex and heterogeneous slopes, 1D or 2D slope stability analysis is inappropriate and leads to oversimplification with inaccurate results, and 3D analysis is required for an accurate evaluation of the slope stability. In this case, a 3D numerical simulation was carried out for Xuecheng slope.

For building 3D numerical model, all the data having values at the coordinates *x*, *y* and *z* of the topographic map are needed. After gridding of the DEM data, the bottom face of the map needs to be reconstructed based on the scope of slope and size of the expected numerical

element. After that, the grid map is converted into ASCII data, and the program developed using the FISH language of FLAC3D is run for generating 3D finite difference mesh from ASCII data. In this case, the numerical model is made up of wedge elements (Fig. 4.10). The analyzed horizontal zone is 366 m×276 m, and the element size of *x-y* coordinates in horizontal plane is 6 m×6 m. Like 2D models, the slope is divided into 10 m thick soil and bedrock. For the deformation and failure to occur in the shallow part of the slope, the mesh of soil is made denser than that of the bedrock.
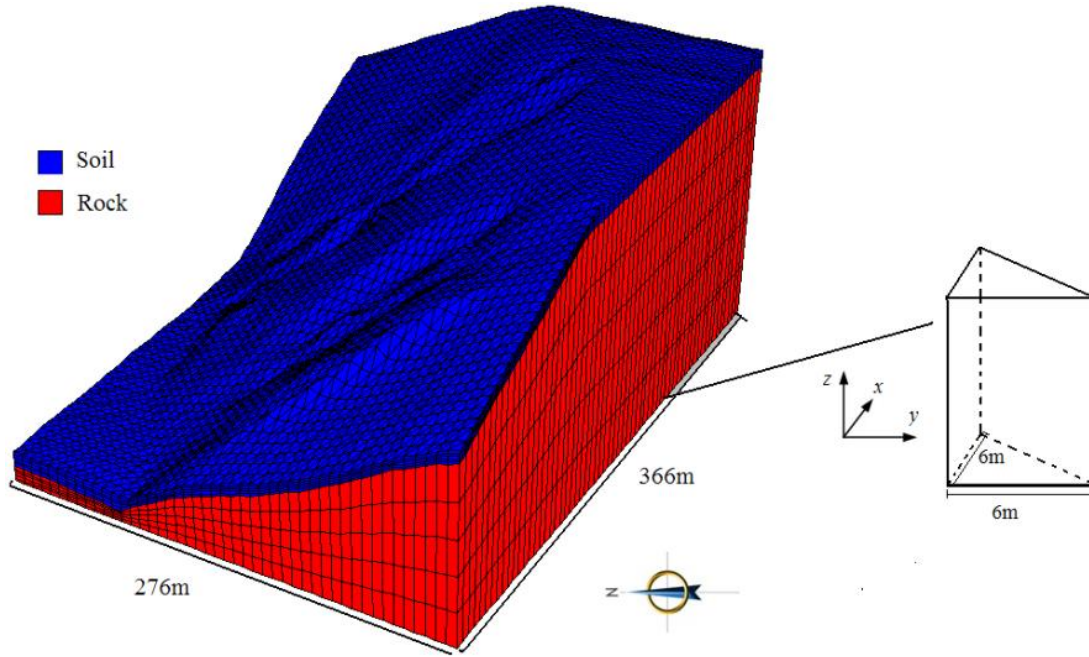
Fig. 4.10 3D wedge slope model by FLAC3D

4.3.4.2 Results of slope stability analysis in 3D

After building the numerical model based on GIS, the slope stability analysis is performed. In the numerical simulation, the boundary conditions employed are: the side boundaries are fixed in the corresponding direction, and the bottom is fixed in *x, y* and *z* directions. The failure criterion of the slope is the Mohr-coulomb criterion and the mechanical properties are listed in Table 4.1. In FLAC3D, the convergence criterion to determine if the simulation has reached equilibrium is the ratio of the maximum unbalanced force to the gravitational body force acting on the node becomes less than 10^{-5}.

The 3D safety factor of Xuecheng slope was calculated to be 1.3 through the FLAC3D Strength Reduction Method, which is higher by 13% than the maximum 2D safety factor (i.e. 1.15). Based on the fact that generally the difference of the safety factor calculated by means

of 2D and 3D models is about 20-30%, it is crucial to develop a 3D model for important assessments of slope stability using GIS (Xie et al 2003).

After the shear strength got reduced by a coefficient of 1.3, the displacements in x, y and z directions and the slope state are shown in Fig. 4.11. The major displacements are concentrated in the eastern side of slope (represented by Cross Section 3). The shear yield distributes on the surface at foot hill, and the tension yield concentrates on the surface of hill crest.

Furthermore, the accuracy of results depends upon the accuracy of input data, and the resolution of geospatial data, but high resolution geospatial data requires more processing time. Compared with 2D analysis, 3D numerical simulation requires significantly more time to reach equilibrium state in FLAC.
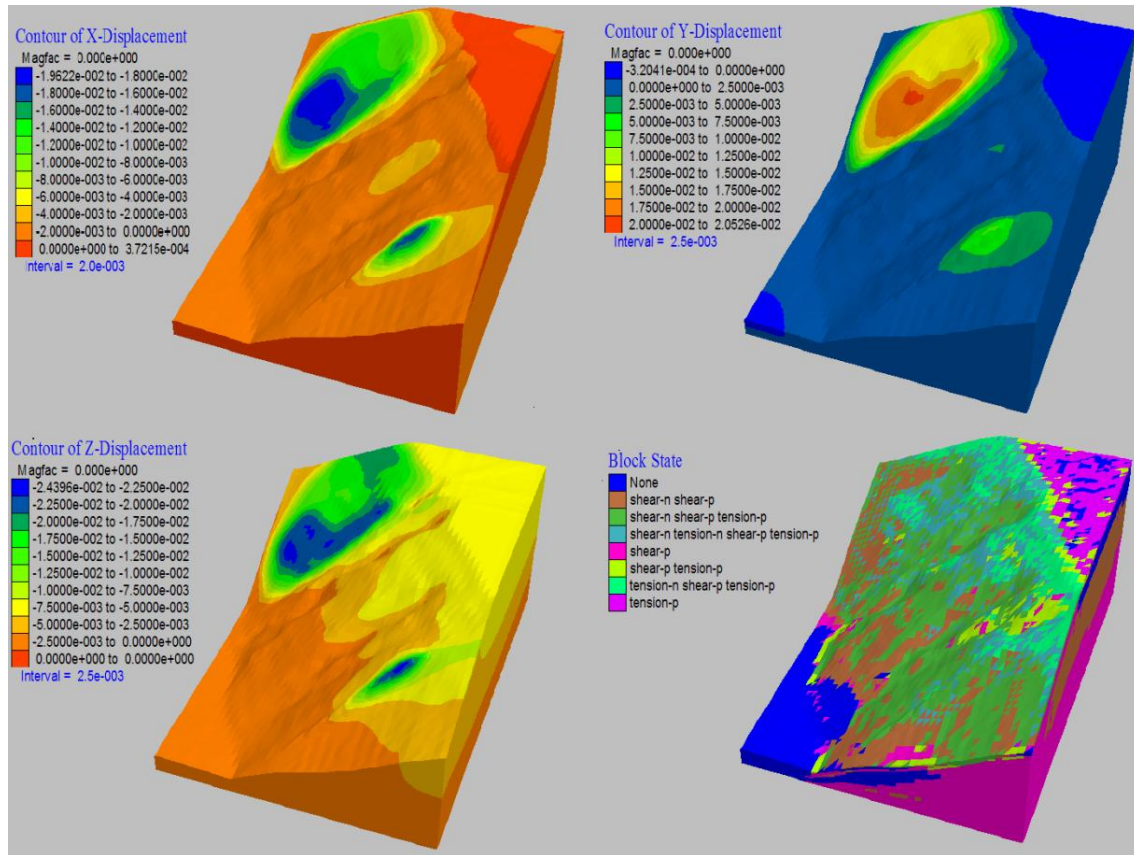
Fig. 4.11 Representations of max vertical displacements (in meters) and the yielding zones, when shear strength reduction coefficient is1.3

4.4 Conclusions

Using the outstanding spatial processing function of GIS and the excellent capability of

numerical simulation of FLAC, a convenient slope stability analysis procedure is proposed. In current study GIS is used effectively as a spatial database for storing, displaying, and updating the input data. The calculations of slope stability are performed outside GIS. For transforming the GIS topography data into the commercial finite difference code FLAC smoothly, Surfer-8 and scripts developed using FISH language are applied and discussed. Surfer-8 is used to grid the raw maps, and generate the DEM of slope. Fish language script is written to overcome the problem of data format and data structure conversion from GIS into FLAC. In FLAC complicated numerical models can be easily applied due to the use of complex algorithms, iteration procedures, and the third dimension in the conventional, two-dimensional GIS. And the representation and spatial distribution of results in FLAC can be shown visually in 2D and 3D.

Based on the case study of Xuecheng slope, this integration technique is demonstrated to have high reliability. It can be used to generate 2D slope numerical models in seconds along desired lines. Furthermore, it can be used very effectively in 3D modeling as well, no matter how complex the topography of slope is.

From the comparison of the numerical simulation results, one can conclude that the safety factor calculated through 2D analysis is a little conservative as compared to that of 3D, because in 2D the assumption of plane strain model without considering the horizontal restrict in the vertical direction of the plane is adopted. 3D numerical slope stability analysis can be performed to obtain the safety factor, and to seek the potential failure surface for the whole slope, and even to simulate the volume of failure mass which is very valuable for reinforcing of design. Through 2D numerical simulation one can only obtain the safety factor, and can seek the potential failure line for some particular cross section which has been selected in advance. Therefore, for a relative important slope, it is recommended to conduct 3D stability assessment, even though 3D analyses require more time.

5. Slope Probabilistic Analyses based on Strength Reduction Method

Introduction

Reliability in slope stability analysis is affected by various factors such as uncertainty associated with soil properties and uncertainty associated with the methods (or models) used. This chapter is to address the reliability of the safety factor due to soil uncertainty, including the probability density function and the correlation of soil properties. Model uncertainty is addressed in a simple manner by applying a rigorous method-numerical simulation method. In the present study, soil properties cohesion c and friction angle φ are represented as random variables because they have the strongest influence on slope stability.

Probabilistic analyses are usually used to evaluate statistical distribution of the safety factor of slope based on known statistical characteristics of input variables. In this chapter, three most popular probabilistic methods in slope stability analysis: Monte Carlo Simulation (MCS), First Order Reliability Method (FORM), and the Point Estimate Method (PEM) are applied combined with Strength Reduction Method which has been discussed in chapter 4. These techniques are demonstrated by three slope cases: one is homogenous slope with two independent random variables; second is a homogenous slope with two correlated random variables; and the third one is two-layered slope with four random variables. Based on the comparison of results, the accuracy and feasibility of different probabilistic methods are discussed. All of the probabilistic analysis processes are programmed using FISH programming language in FLAC.

5.1 Probabilistic methods applied based on Strength Reduction Method

5.1.1 Monte Carlo Simulation

Monte Carlo Simulation is a method used to obtain the probability distribution of dependent random variables given the probability distribution of a set of independent random variables. In this technique, the soil mechanical parameters such as cohesion c and internal friction angle φ are considered as independent random variables and sampled thousands times from its known (or assumed) probability distribution. Subsequently, thousands of safety factors considered as dependent random variables are obtained through numerous slope deterministic stability analyses based on these input samples, thus the mean value, standard deviation and probability distribution of the safety factor are evaluated.

As we known, MCS is a time consuming method, which need thousands of deterministic

analyses repeating. Strength Reduction Method also needs much iteration to get the safety factor, and the time consuming depends on the number of elements in model. Therefore, most of time, researchers applied MCS based on the limit equilibrium methods. For simplify, MCS combined with LEM is called MCS-LEM in the present study, and MCS directly combined with SRM is called traditional MCS-SRM.

For reducing the time consumption, development of a simplified MCS-SRM is disscused in this chapter. In each deterministic analysis, only the stability situation of slope is estimated according to the convergence criterion of numerical simulation, without the exact safety factor calculation. After deterministic analyses are repeated adequate times, the failure probability P_f will be m/n, where m is the times of slope failure, and n is the total number of simulations.

The equilibrium state of slope is defined as (just as used in Strength Reduction Method): after adequate steps of simulation, if the normalized nodal unbalanced force of every node a in the mesh is less than 10^{-3}, it means the slope is stable and vice versa. The process of MCS which has been programmed using FISH language is shown in Fig. 5.1.
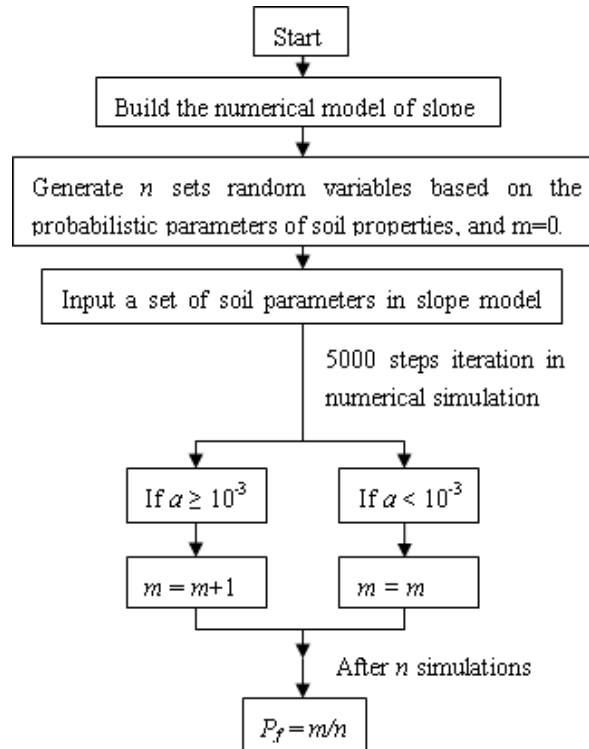
Fig. 5.1 Flow chart of MCS

Through this technique, only the mean of safety factor μ_{FS} is calculated by the mean of soil

parameters and the probability of failure is achieved directly. To get the other characteristic parameters of safety factor (e.g. variability), the cumulative distribution function (CDF) of safety factor *FS* can be applied based on the assumed distribution function of safety factor. And then the probability of failure P_f is presented as the probability of safety factor less than 1.0, as Eq. 5.1.

$$P_f = \text{CDF}(1; \mu_F, \sigma_F) \tag{5.1}$$

Based on Eq. 5.1, the standard deviation of the safety factor σ_{FS} can be calculated, and furthermore the reliability index can be calculated through the probability and statistical theory.

Monte Carlo Simulation is a relative accurate method, which is close to the real answer and suitable as reference for comparison with other probabilistic methods results. However, to obtain any real confidence, the model needs a large number of simulations. The accuracy of MCS results depends on the number of simulations carried out for the input parameters considered. Bennet and Ang (1986) suggested that confidence coefficient is 95% to insure the tolerance error ε. The relationship of error with the number of simulations *N* and failure probability is shown in following equation:

$$\varepsilon = \left[2(1 - P_f)/(N \cdot P_f) \right]^{1/2} \tag{5.2}$$

From Eq. 5.2, one can see when the probability failure gets constant, *N* is bigger with the smaller tolerance error ε; when the error is constant, P_f is bigger with smaller *N*. Hence improving the accuracy requires an increase in the number of simulations (Woodward, 1999). Simply:

$$N \geq 100/P_f \tag{5.3}$$

5.1.2 First Order Reliability Method

The first relatively simple alternative to MCS is the First Order Reliability Method (FORM), also well-known as the Hasofer-Lind method. It is based on the Taylor series expansion of the safety factor or the performance function at the critical points on the failure surface, known as design point. This method provides analytical approximations for the mean and standard deviation of a parameter of interest as a function of the mean and standard deviations of the various input variables, and their correlations. It is a simple method, but the distribution function for the safety factor also need to be assumed beforehand to estimate the failure

probability.

In FORM, the performance function for the slope stability is always determined as the safety factor function about the soil properties. Its Taylor's series expansion about the expansion point gives

$$F(X) = F(X^*) + \sum_{i=1}^{n}(x_i - x_i^*)\frac{\partial F}{\partial x_i}|_{X^*} + \sum_{i=1}^{n}\frac{(x_i-x_i^*)^2}{2}\frac{\partial^2 F}{\partial x_i^2}|_{X^*} + \cdots \tag{5.4}$$

where $X=(x_1, x_2,\ldots, x_n)$ is the input random variables, $F(X)$ is the safety factor function, and the derivatives are evaluated at X^*, which are considered as linearization points or critical points. After truncation from second order terms, the first-order Taylor's series is:

$$F(X) = F(X^*) + \sum_{i=1}^{n}(x_i - x_i^*)\frac{\partial F}{\partial x_i}|_{X^*} \tag{5.5}$$

If truncated from third order terms, the Eq. 5.5 will become the second order Taylor's series. This method is called Second Order Reliability Method (SORM) with a higher accuracy than FORM, but requires more calculation effort than FORM.

Considering the variances or standard deviations of random variables X as known, the mean value of the performance function is obtained by evaluating the function at the mean values of the random variables μ_X as follows:

$$\mu_F = F(\mu_X) + \frac{1}{2}\sum_{i=1}^{n}\sum_{j=1}^{n}\left(\frac{\partial F}{\partial x_i}\cdot\frac{\partial F}{\partial x_j}\right)\cdot COV(x_i, x_j) \tag{5.6}$$

where $COV(x_i, x_j)$ is the covariance of x_i and x_j. If the x_i and x_j are independent variables, the $COV(x_i, x_j)$ will be 0.0.

The variance of the performance function are given approximately by the following equations

$$Var(F) = \sum_{i=1}^{n}\left(\frac{\partial F}{\partial x_i}\Big|_{x_i^*}\right)^2\cdot Var(x_i) + 2\cdot\sum^{n}\sum_{i\neq j}^{n}\left(\frac{\partial F}{\partial x_i}\Big|_{x_i^*}\cdot\frac{\partial F}{\partial x_j}\Big|_{x_j^*}\right)\cdot Cov(x_i, x_j) \tag{5.7}$$

where

$$x_i^* = \mu_{x_i} - \alpha_i\beta\sigma_{x_i} \tag{5.8}$$

$$\alpha_i = \frac{\partial F}{\partial x_i}|_{x^*}\sigma_{x_i}/\sum_{i=1}^{n}\left(\frac{\partial F}{\partial x_i}|_{x^*}\sigma_{x_i}\right)^2 \tag{5.9}$$

where α_i is the directional derivative of failure face at point $X^*=(x_1^*, x_2^*, \ldots, x_n^*)^T$ in space X, and σ_{x_i} is the standard deviation of the random variable x_i,

FORM is based on the Taylor series expansion of the performance function. However, Strength Reduction Method is a stress-strain analysis method without explicit performance function, which is like a "black box". Therefore, in this study, finite difference method approximates the solutions to differential equations by replacing derivative expressions with approximately equivalent difference quotients.

$$\frac{\partial F}{\partial x_i}\big|_{x^*} = \left[F\left(x_1^*, x_2^*, \ldots x_i^* + \sigma_{x_i}, \ldots, x_n^*\right) - F\left(x_1^*, x_2^*, \ldots, x_n^*\right)\right]/\sigma_{x_i} \quad (5.10)$$

In FORM an iterative solution is usually required to find the expansion point. The process of this iteration is shown as follows:

1). suppose the initial expansion point $X^{(0)} = \left(x_1^{(0)}, x_2^{(0)}, \ldots, x_n^{(0)}\right)$ which are the means of the soil parameters;

2). calculate the safety factor function $F^{(0)} = F(x_1^{(0)}, x_2^{(0)}, \ldots, x_n^{(0)})$, $F^{(i)} = F(x_1^{(0)}, x_2^{(0)}, \ldots, x_i^{(0)} + \sigma_{x_i}, \ldots, x_n^{(0)})$ by Strength Reduction Method, and we can get $n+1$ safety factors;

3). apply these $n+1$ safety factors to calculate the μ_F and $\frac{\partial F}{\partial x_i}\big|_{x^*}$ using Eq. 5.10;

4). use Eq. 5.9 and 5.10 to calculate the expansion point $X^{*(0)}$, and use Eq. 5.7, 5.8 and 3.30 or 3.31 to calculate the reliability index $\beta^{(k)}$, where the superscript k means the kth iteration;

5). determine the convergence condition

$$\left|\beta^{(k)} - \beta^{(k+1)}\right| < \varepsilon \quad (5.11)$$

ε is always set as 0.05. If Eq. 5.11 cannot be satisfied, new iteration point should be generated by the interpolation method as follow:

$$x^{(k+1)} = x^{(k)} + \left(x^{*(k)} - x^{(k)}\right)\frac{F(x^{(k)})-1}{F(x^{(k)})-F(x^{*(k)})} \quad (5.12)$$

And then return to step (2), until the convergence condition is satisfied. The usual output of FORM is the reliability index given by Eq. 3.30 or 3.31.

5.1.3 Point Estimate Method

Point Estimate Method is a computationally straightforward technique for uncertainty analysis, and is capable of estimating statistical moments of a model output involving several stochastic variables, whether correlated or uncorrelated and symmetric or asymmetric. The basic idea of this method is to replace the probability distributions of continuous random variables by discrete equivalent distribution having the same first three central moments to calculate the mean value, standard deviation and skewness of a performance function, which depends on the input variables. To do this, generally two point estimates are considered with one standard deviation on either side of the mean value from each distribution representing the random variables. Then the performance function is calculated for every possible combination of the point estimates, producing 2^n solutions, where n is the number of the random variables involved. Then the mean value, standard deviation and skewness of the performance function can be found from these 2^n solutions.

In this study, the Strength Reduction Method is applied to calculate the safety factor on the estimation points. First of all, the locations of the sampling points for every random variable should be estimated. To do this, one should first evaluate the so-called standard deviation units ξ_{Xi+} and ξ_{Xi-}, which depend on the skewness coefficient v_{x_i} of the input variables and are given by

$$\xi_{Xi+} = \frac{v_{x_i}}{2} + \left[1 + \left(\frac{v_{x_i}}{2}\right)^2\right]^{1/2} \, , \ \xi_{Xi-} = \xi_{Xi+} - v_{x_i} \tag{5.13}$$

If the input variables are symmetrically distributed, the standard deviation units will be both equal to unity.

If the variable X is lognormally distributed, the skewness coefficient v can be calculated using the following formulas

$$\sigma^2 = \ln\left(1 + \frac{var(X)}{\mathrm{E}(X)^2}\right) \tag{5.14}$$

$$v = \left(e^{\sigma^2} + 2\right)\sqrt{e^{\sigma^2} - 1} \tag{5.15}$$

Knowing the mean value and standard deviation of the input variables, the corresponding sampling point locations x_{i+} and x_{i-} can be calculated as follows:

$$x_{i+} = \mu_{x_i} + \xi_{Xi+} \cdot \sigma_{x_i}, \ x_{i-} = \mu_{x_i} - \xi_{Xi-} \cdot \sigma_{x_i} \tag{5.16}$$

After that, the weights P_i, also called probability concentrations, can now be determined to obtain all the point estimates. As the probability density function encloses an area of unity, then the weights must also sum to unity and they have to be positive. The weights of the random variables are given by different expressions depending on the number of the input variables and on the correlation.

For a single random variable, the weights are easily calculated using the standard deviation units as

$$P_{x+} = \frac{\xi_{x-}}{\xi_{x+}+\xi_{x-}}, \ \ P_{x-} = 1 - P_{x+} \tag{5.17}$$

When the random variable is symmetric then the weights are both equal to 0.5.

For two correlated random variables (Rosenblueth, 1981), the weights are given as follows

$$P_{s_1 s_2} = P_{x_{s_1}} \cdot P_{x_{s_2}} + s_1 \cdot s_2 \cdot \left(\rho_{x_1 x_2} / \left(\left(1 + \left(\frac{v_{x_1}}{2} \right)^3 \right) \cdot \left(1 + \left(\frac{v_{x_1}}{2} \right)^3 \right) \right)^{1/2} \right) \tag{5.18}$$

where $P_{s_1 s_2}$ are the associated weights, with $P_{x_{s_1}}$ and $P_{x_{s_2}}$ being the weights for the input variables evaluated as single variables. s_1 and s_2 take positive sign for points greater than the mean value of the variables and negative sign for points smaller than the mean value. $\rho_{x_1 x_2}$ is the correlation coefficient between the variables X_1 and X_2, when the variables are uncorrelated then $\rho_{x_1 x_2}$ will be zero. For two uncorrelated random variables, where the weights can be evaluated as

$$P_{s_1 s_2} = P_{x_{s_1}} \cdot P_{x_{s_2}} \tag{5.19}$$

Now, it is possible to determine the deterministic analysis F(X) at each sampling point located at X_{i+} and X_{i-}.

Finally the first three moments of the safety factor, the mean value, the standard deviation and the skewness can be determined respectively using the following equations

$$\mu_{FS} = \sum_{i=1}^{2^n} P_i \cdot FS_i \tag{5.20}$$

$$\sigma_{FS} = \sqrt{\sum_{i=1}^{2^n} P_i \cdot (FS_i - \mu_{FS})^2} \tag{5.21}$$

$$\nu_{FS} = \frac{1}{\sigma_{FS}^3} \sum_{i=1}^{2n} P_i \left(FS_i - \mu_{FS}\right)^3 \tag{5.22}$$

Unfortunately, Eq. 5.18 has some evident drawbacks. First of all, if the skewness coefficient of the input variables has different sign then the radicand under the square root can be negative, which is mathematically impossible. This can happen for example if one input variable has a negatively skewed distribution and the other a symmetrically or positively skewed distribution. Secondly if the skewness coefficient of the input variables is equal to -2 then the denominator of the second term of Eq. 5.18 tends to infinity, giving then infinite weights. Moreover this formula can sometimes give negative values. It is unacceptable, because the weights are described as probability values, which are always positive by definition. For example, negative values of the weights can occur when the random variables are symmetric and perfectly correlated (i.e. $\rho = \pm 1$).

To overcome the problem in Rosenbluth's formula 5.18, a better definition for two correlated random variables, being symmetrically distributed, is given by Christian et al. (1999), where the weights can be evaluated as

$$P_{+-} = P_{-+} = P_{x_{1\pm}} \cdot P_{x_{2\mp}} \cdot \left(1 - \rho_{x_1 x_2}\right), \ P_{--} = P_{++} = P_{x_{1\pm}} \cdot P_{x_{2\pm}} \cdot \left(1 + \rho_{x_1 x_2}\right) \tag{5.23}$$

For n symmetrically distributed and correlated random variables, Christian et al. (1999) defined the weights as

$$P_{s_1 s_2 \dots s_n} = \frac{1}{2^n} \cdot \left[1 + \sum_{i=1}^{n-1} \sum_{j=i+1}^{n} \left(s_i \cdot s_j \cdot \rho_{ij}\right)\right] \tag{5.24}$$

In the next sections, three examples were selected for studying the reliability and uncertainty of slope's factor of safety using Monte Carlo simulation, First Order Reliability Method and Point Estimate method. The first example illustrates the stability of a homogeneous slope with two independent input variables, the second illustrates the stability of the same homogenous slope but with two correlated input variables, and the third illustrates the stability of a non-homogeneous slope with four input variables.

5.2 Slope stability analysis of case 1

The first case deals with the study of stability analysis of a homogenous soil slope with a length of 40 m and a depth of 30 m. The slope is divided into 740 elements in FLAC2D shown in Fig. 5.2. Movement is allowed vertically on both lateral boundaries, while the constraint is imposed in both directions of the base boundary. The soil parameters cohesion c

and fiction angle φ are considered as two independent random variables. More specifically, the soil type is what can be called a grossly uniform soil, in which the whole mass is of the same consistency throughout and whose properties show no marked trend with depth or distance.
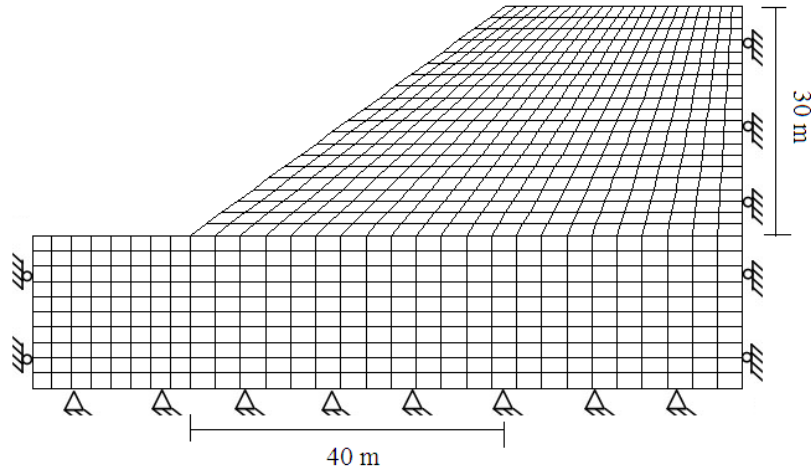
Fig. 5.2 Finite difference model of a homogeneous soil slope

All of the soil properties are taken as constants, while the parameters c and φ are taken into account as independent normal or log normal random variables. In this chapter, the values of coefficient of variations (CV) are assumed according to their proposed range by Harr (1977) (Table 5.1). Knowing the mean value and the coefficient of variation of cohesion and friction angle, it is possible to define their standard deviations and shapes of the probability density functions (Fig. 5.3).

Table 5.1 Soil properties for the example 1

γ (kN/m^3)	Bulk (GPa)	Shear (GPa)	μ_c (kPa)	CV_c	μ_φ (°)	CV_φ
19.5	1.8	1.2	20	0.25	25	0.20

(a)   (b)
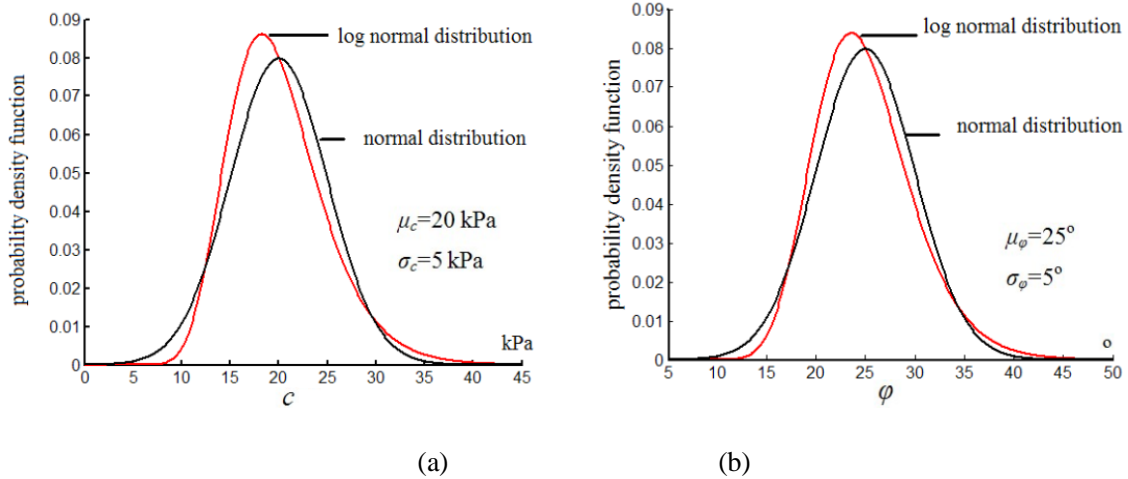
Fig. 5.3 (a) Distributions about cohesion c and (b) distributions about friction angle φ

5.2.1 Monte Carlo Simulation results for case 1

For the probabilistic slope stability analysis, Monte Carlo Simulations are initially performed. First, the mean of safety factor is calculated by Strength Reduction Method based on the mean value of soil properties. Fig. 5.4 presents the simulation result for example 1. The critical failure surface is found automatically as the max shear strain rate zone, so it is not necessary to specify the shape of the failure surface in advance (e.g. circular, log spiral, piecewise linear, etc.). The calculated factor of safety for this slope is 1.07. The deterministic analysis therefore showed that the failure of the slope was imminent.
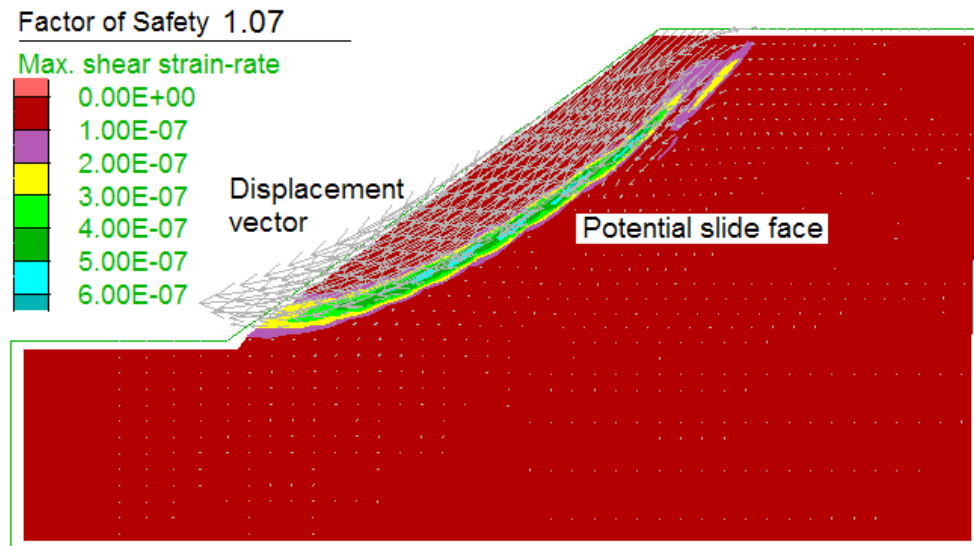
Fig. 5.4 Simulation results of a homogenous slope by SRM

To perform the reliability analysis based on Monte Carlo Simulation, thousands of samples

of the soil parameters should be generated.

1). for the normally distributed input variables, a set of standard normally distributed variables should be generated first.

There are many algorithms to generate the standard normal variables. In this study, the Box-Muller method (Box and Muller, 1958) is applied. It uses two independent random numbers U and V distributed uniformly on (0, 1). Then the two independent standard random variables X and Y:

$$X = \sqrt{-2 \ln U} \cos(2\pi V) \tag{5.25}$$

$$Y = \sqrt{-2 \ln U} \sin(2\pi V) \tag{5.26}$$

will both have the standard normal distribution, and be independent. This formulation arises because for a bivariate normal random vector (X, Y), the squared norm $X^2 + Y^2$ will have the chi-square distribution with two degrees of freedom, which is an easily generated exponential random variable corresponding to the quantity $-2\ln(U)$ in these equations; and the angle is distributed uniformly around the circle, chosen by the random variable V.

The standard normal variable can be transformed into normal variable with the corresponding mean value and standard deviation as Eq. 5.27.

$$x_i = \sigma_{x_i} z_i + \mu_{x_i} \tag{5.27}$$

where, z_i is the standard normal variable, x_i is a normal variable, and μ_{x_i} and σ_{x_i} are its mean value and standard deviation respectively.

2). for the log normally distributed variables, we can produce a series normal random variable y first and then transfer it to lognormal random variables following the given Eq. 5.28:

$$F = e^y \tag{5.28}$$

where F is a series log normal random variable. The relationship of mean values and standard deviations of F and y are given by:

$$\sigma_y = \sqrt{ln(1 + V_F^2)} \tag{5.29}$$

$$\mu_y = ln\left(\mu_F / \sqrt{1 + V_F^2}\right) \tag{5.30}$$

$$V_F = \sigma_F / \mu_F \tag{5.31}$$

During the generation of the random samples, there are some issues that should to be noticed. For example, in practical engineering all of the soil parameters are non-negative, and the friction angle is less than 90 °. In the present thesis, all the generated negative soil parameter samples are replaced by a very small value of 0.1, and the friction angle which are greater than 90 °are replaced by 89 °.

The accuracy of MCS depends on the number of calculations carried out for the input parameters considered. Hence improving the accuracy requires an increase of the simulations number. The appropriate sample size of soil properties should be determined beforehand since its strong influence on the accuracy of the MCS. For this purpose, the samples with different sizes ranging from 50 to 2,000 were generated and the associated probability of failure P_f was calculated, when both of the input soil properties c and φ were assumed as normal distributed. Fig. 5.5 shows the relationship between sample size (generated number) and the probability of failure. It is clearly shown in this figure that there is no significant difference in the calculated (P_f) when the sample size exceeds 1,000. Therefore, the sample size of 1,000 was chosen in this study.
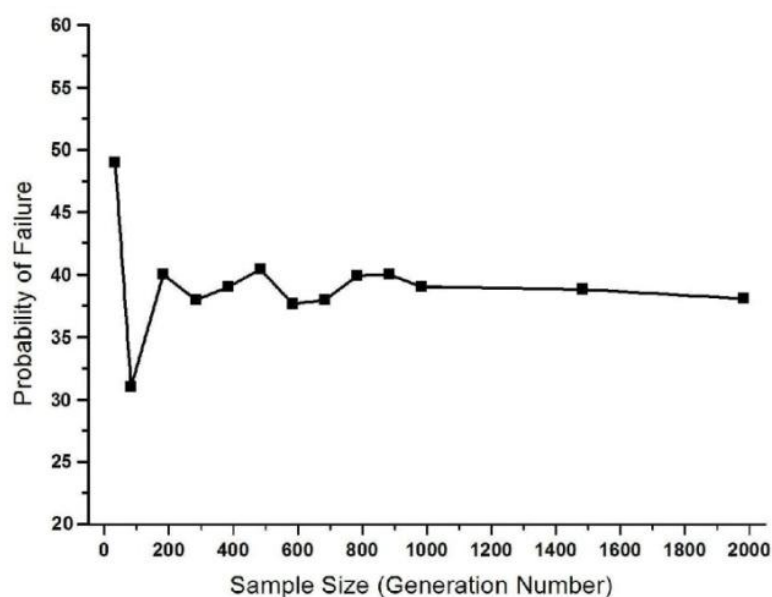
Fig. 5.5 Relationship of the probability failure and sample size

After the sample size is determined, the traditional MCS-SRM is carried out first. One thousand cohesion and friction angle values are generated according to each different random variable distribution, and then one thousand safety factors are calculated. The histograms of the safety factor shown in Fig. 5.6 are based on different random variable distributions. Comparing these two diagrams shows that when the input random variables

are normally distributed, the probability density function of the safety factors tends to be normally distributed; in turn, when the input random variables are log normally distributed, the probability density function of the safety factors tends to be log normally distributed. The means of these two different distributed safety factors are the same, and there is only slight difference between the standard deviations.
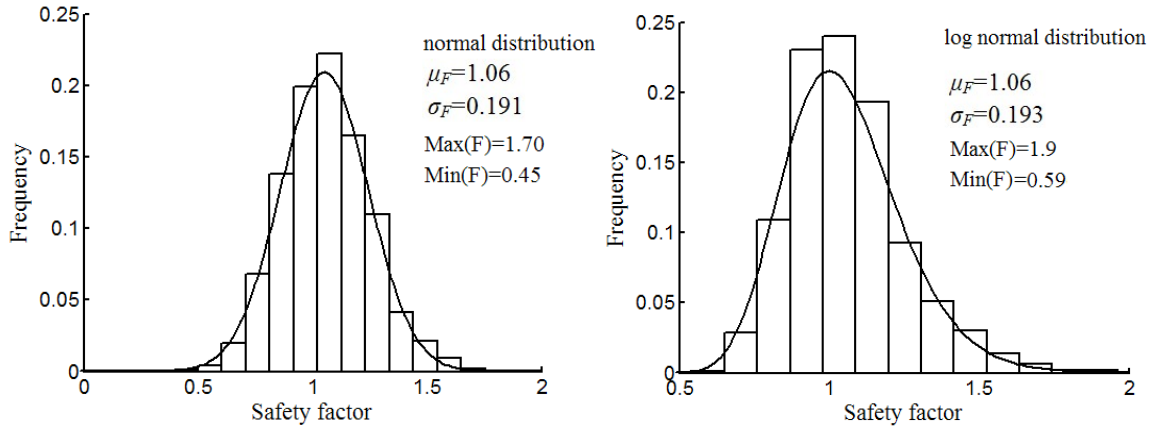
Fig. 5.6 Frequency and probability density function by traditional MCS-SRM

After that, the MCS-LEM is also carried out. In the present study, one of the LEM, Morgenstern Price method is applied as the deterministic method, and the number of samples is also determined as 1000. The histograms by different distributed random variables are shown in Fig. 5.7. Comparing these two diagrams reveal that when the input random variables are normally distributed, the probability density function of the safety factors also tends to be normally distributed and vice versa. The mean and standard deviation of safety factors by log normally distributed random variables are obviously greater than the results by normally distributed random variables. For log normally distributed random variables, the maximum value of safety factor reaches 25.75, which is non sensitive in practice.
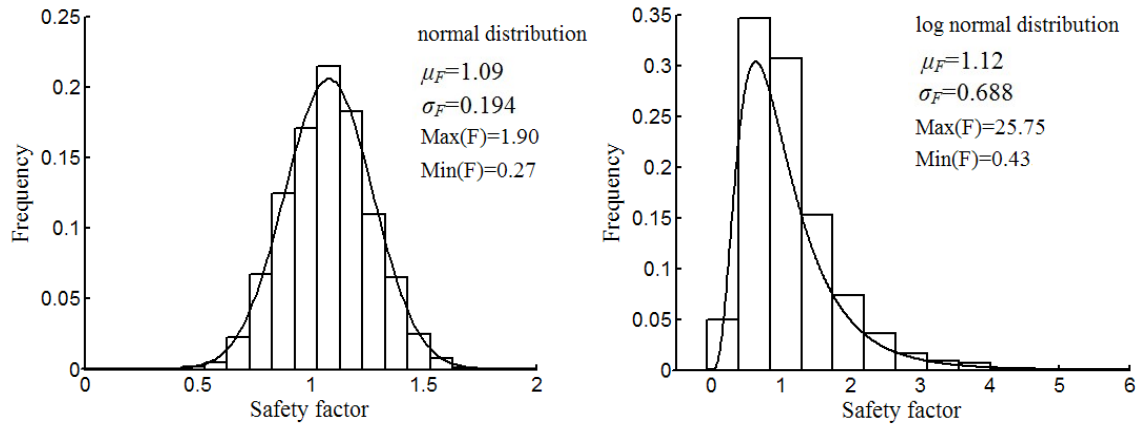
Fig. 5.7 Frequency and probability density function by MCS-LEM

From these two kinds of MCS studies, we can conclude that: the normal distributed random variables will generate the normal distributed safety factors, and the log normal distributed random variables will generate the log normal distributed safety factors. This rule will be adopted in the whole thesis.

At last, the simplified MCS-SRM developed in above section is carried out. After thousand of soil properties c and φ are generated and thousand of slope stabilities are estimated, the probability of failure is obtained, and the statistical results are calculated based on the assumed probability density functions of safety factor. The probability density function distributions of safety factor by simplified MCS-SRM are shown in Fig. 5.8.

The results and the time consumption of different methods and different distributed random variables are compared in Table 5.2.
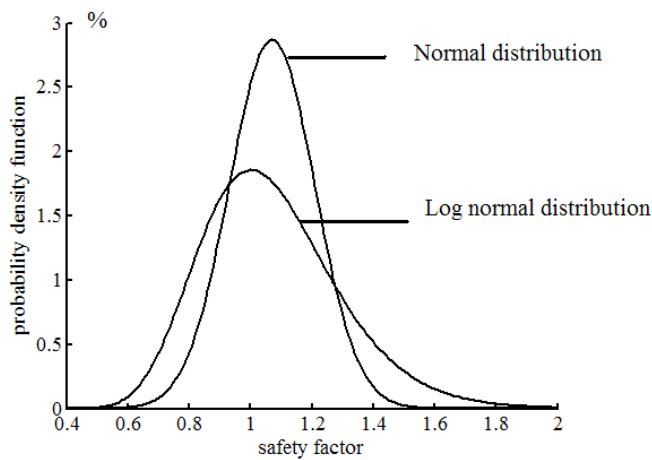
Fig. 5.8 Assumed probability density function distributions of safety factors for simplified MCS-SRM

Table 5.2 Statistical results predicted by 1,000 MCS for case 1

Methods	Normal distribution				Log normal distribution				Time consuming
	P_f (%)	μ_{FS}	σ_{FS}	β	P_f (%)	μ_{FS}	σ_{FS}	β	
Traditional MCS-SRM	37.6	1.06	0.191	0.31	40.8	1.06	0.193	0.23	20 hours
Simplified MCS-SRM	38.4	1.07	0.139	0.50	39.5	1.07	0.227	0.22	4 hours
MCS-LEM	32.5	1.09	0.194	0.46	33.8	1.12	0.688	-0.08	4 seconds

Comparing the statistical values of Table 5.2, it becomes evident that the results by traditional MCS-SRM are very similar as simplified MCS-SRM, but the time consumption is 5 times that of the simplified MCS. Both of the value and discreteness of safety factor by LEM are greater that of MCS, but only needs seconds to obtain the results. Therefore, MCS-LEM is absolutely the fastest method for slope probabilistic analysis, but the MCS-SRM integrates the advantage of numerical simulations and has a higher accuracy. The simplified MCS-SRM proposed in the present study reduces the time consuming significantly and retains the high accuracy.

5.2.2 First Order Reliability Method results for case 1

It was highlighted that the simplest alternative to MCS is the FORM, which produces a linearization around the critical points of the input soil parameters. This section will show the process of FORM applied to case 1 that is already considered.

Considering the slope safety factor formula as a function of two independent random variables cohesion c and friction angel φ, the Taylor's series expansion for the safety factor about the expansion value c^* and φ^* truncated after the first order terms is given by

$$F = F(c^*, \varphi^*) + (c - c^*)\frac{\partial F}{\partial c}|_{c^*} + (\varphi - \varphi^*)\frac{\partial F}{\partial \varphi}|_{\varphi^*} \tag{5.32}$$

where the first term is determined by substituting the expansion value of c^* and φ^*, while the derivative of the second term is evaluated at c^* and φ^*. The mean value and the variance of the safety factor are obtained using the following equations

$$\mu_F = F(\mu_c, \mu_\varphi) \tag{5.33}$$

$$\text{Var}(F) = \text{Var}(c).\left(\frac{\partial F}{\partial c}|_{c^*}\right)^2 + \text{Var}(\varphi).\left(\frac{\partial F}{\partial \varphi}|_{\varphi^*}\right)^2 \tag{5.34}$$

For log normal soil properties, the mean and standard deviation of the equivalent normal cohesion and friction angle are shown in follows based on the R-F method. Both of the mean

and standard deviation values are reduced slightly compared with the original ones.

$$\mu_{c'} = 19.4 \text{ kPa}, \ \sigma_{c'} = 4.9 \text{ kPa}$$

$$\mu_{\varphi'} = 24.5°, \ \sigma_{\varphi'} = 5.0°$$

Now it is possible to evaluate the variance and the standard deviation of the safety factor through the process in section 5.1.2. It is important to remember that FORM does not provide any skewness coefficient, so no information about the shape of the probability density function of the safety factor is given. The rule of the distribution of safety factors following the distribution of input random variables as suggested above is adopted here. Through the calculation of FORM, the probability density function distributions for different distributed safety factor are shown in Fig. 5.9 and the statistical values of different types of soil properties are shown in Table 5.3.
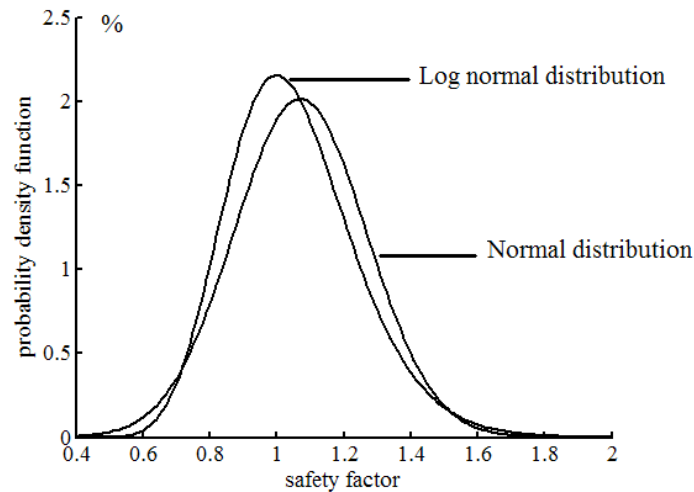
Fig. 5.9 Assumed probability density function distributions of safety factors by FORM

Table 5.3 Statistical values by FORM for case 1

Input variables	μ_{FS}	σ_{FS}	β	$P_f (\%)$
Normal distribution	1.07	0.198	0.35	35.4
Log normal distribution	1.05	0.193	-0.08	43.7

From Table 5.3, one can see that the mean of safety factor by the log normal distributed variables is lower than the result by normal distributed variables because of the equivalent normalization of the input variables. The estimated P_f by the log normal distributed variables is greater than the result by normal distributed variables because of the different probability

density function. The probability of failure by normal distribution from FORM is a little smaller than MCS, but the probability of failure by log normal distribution from FORM is a little greater.

5.2.3 Point Estimate Method results for case 1

In order to assess the slope stability related to the first case, the two point estimate method is applied now. The procedure for implementing the PEM and the corresponding calculations are described step by step in this section.

The relationship between the dependent variable safety factor *FS* and the random variables *c* and φ is considered. The two sampling point locations for *c* and φ have to be computed. First of all, the standard deviation units, giving locations of the sampling points to the right and to the left of the mean value, are evaluated using Eq. 5.29 and 5.30, and then the weights P_i are determined by Eq. 5.31.

1). for normal distributed random variables, the standard deviation unites are unity, and the corresponding sampling point locations can be evaluated with Eq. 5.16.

$c_+ = 25$ kPa, $c_- = 15$kPa

$\varphi_+ = 30^\circ$, $\varphi_- = 20^\circ$

The weights P_i, giving each of the four point estimates of soil parameters considered as single random variable, are then determined using Eq. 5.17, thus obtaining

$P_{c+} = P_{c-} = P_{\varphi+} = P_{\varphi-} = 0.5$

Then the associated weights need to be found, considering the input parameters as multiple uncorrelated variables. Eq. 5.19 gives the following weights

$P_{c+\varphi+} = P_{c+\varphi-} = P_{c-\varphi+} = P_{c-\varphi-} = 0.25$

2). for log normally distributed random variables, first the skewness coefficient *v* of the input variables should be obtained using Eq. 5.14 and 5.15.

$v_c = 0.7656$, $v_\varphi = 0.608$

The standard deviation units which depend on the skewness coefficient *v* of the input variables *c* and φ are given by Eq. 5.13.

$\xi_{c+} = 1.4536$, $\xi_{c-} = 0.688$

$\xi_{\varphi+} = 1.3492$, $\xi_{\varphi-} = 0.7412$

The corresponding sampling point locations are

$c_+ = 27.268$ kPa, $c_- = 16.56$ kPa

$\varphi_+ = 31.746^o$, $\varphi_- = 21.294^o$

Then the associated weights and safety factors for different combination of the cohesion and friction angle are shown in Table. 5.4.

Table 5.4 Associated weights and safety factor for different variables combinations

Combinations	$c_+\varphi_+$	$c_+\varphi_-$	$c_-\varphi_+$	$c_-\varphi_-$
Associated weights P	0.1139	0.2074	0.2407	0.4380
Safety factor	1.429	1.057	1.250	0.8941

The values of the safety factor are then evaluated at both sampling point locations of c and φ, and the first three moments of the safety factor can be evaluated using Eq. 5.20 and 5.21, where $n = 2$. After that, based on the assumed probability density function of safety factors, the probability of failure is obtained. The results are presented in Table 5.5 and Fig. 5.10.

Table 5.5 Statistical values by PEM for case 1

Input variables	μ_{FS}	σ_{FS}	β	P_f (%)
Normal distribution	1.07	0.189	0.37	35.5
Log normal distribution	1.07	0.190	0.32	37.4
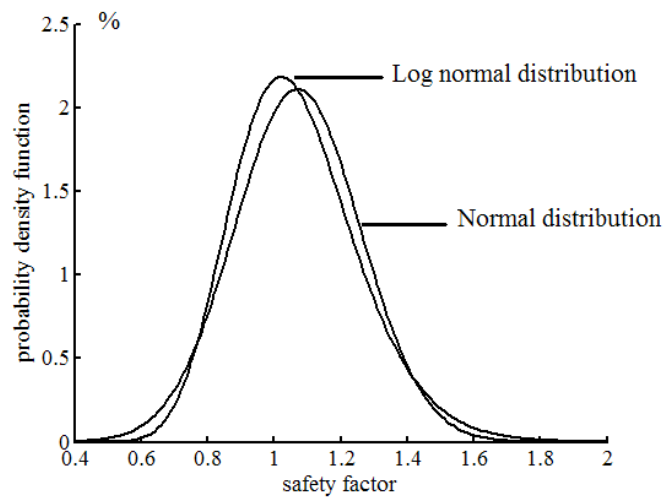
Fig. 5.10 Assumed probability density function distributions of safety factors for PEM

From Table 5.5, the mean value is exactly the same as the deterministic analysis results (i.e.,

1.07). In addition, the estimated failure probability P_f obtained from the log normal distributed input variable is a little higher than that of the normal distributed input variable.

Considering the results of simplified MCS-SRM as reference, one can see that the accuracy of probabilities of failure by PEM is greater than FORM. The PEM may be better to capture the behavior of non linear functions. And as a non-iterative procedure, the PEM overcomes the convergence problems of the FORM, thus being less time consuming. There is another advantage compared with FORM, the PEM can handle the asymmetric random variables directly without equivalent normalization involved.

5.3 Slope stability analysis of case 2

It is well accepted that there exists a negative correlation between cohesion and friction angle of a soil mass. Soil properties are generally modeled as perfectly uncorrelated random variables and the results could therefore be uncertain. To perform a proper analysis involving correlated random variables, it is necessary to generate random numbers which will simulate the correlation structure of soil properties.

The geometry of the second example is the same as the first one, the effective soil cohesion and friction angle both are considered as normal random variables and the correlation coefficient between these two parameters is considered as varying from -1.0 to 0.

5.3.1 Monte Carlo Simulation results for case 2

In the second case, the correlation between effective cohesion c and friction angle φ is taken into account. Therefore these two correlated random variables should be generated based on the method shown as follows.

First, generate two sets of standard normal variables, X_1 and X_2. And then according to Eq. 5.35 produce a set of standard normal variables X_a which correlate with X_1.

$$X_a = X_1\rho + \sqrt{(1-\rho^2)}X_2 \qquad (5.35)$$

where ρ is the correlation coefficient of these two input variables X_1 and X_a.

Then transform X_1 and X_a into normal variables with the corresponding mean value and standard deviation as Eq. 5.27.

After thousand generations of the random variables, the simplified MCS-SRM is carried out for different correlation coefficient. The statistical values of the safety factor are listed

in Table 5.6 for different correlation coefficients ranging from -1.0 to 0.0.

The mean value of safety factor is the same as the deterministic one, but by increasing the correlation coefficient, the failure probability increases slightly, from around 27.7% when cohesion and friction angle totally negatively correlate up to around 38.4% when the soil parameters are independent.

Table 5.6 Influence of $\rho_{c\varphi}$ on the statistical results by simplified MCS-SRM

ρ	μ_{FS}	σ_{FS}	β	$P_f(\%)$
-1.0	1.07	0.118	0.593	27.7
-0.9	1.07	0.127	0.551	29.2
-0.8	1.07	0.139	0.504	30.4
-0.7	1.07	0.145	0.483	31.0
-0.6	1.07	0.151	0.464	32.2
-0.5	1.07	0.158	0.443	32.8
-0.4	1.07	0.162	0.432	33.3
-0.3	1.07	0.165	0.424	33.4
-0.2	1.07	0.170	0.412	34.1
-0.1	1.07	0.178	0.393	34.6
0	1.07	0.239	0.293	38.4

Fig. 5.11 shows the influence of the correlation coefficient variation on the shape of the normal fit of the safety factor. The curves become narrow for lower correlation coefficients, thus decreasing the variability of the safety factor and increasing the peak of the fit.
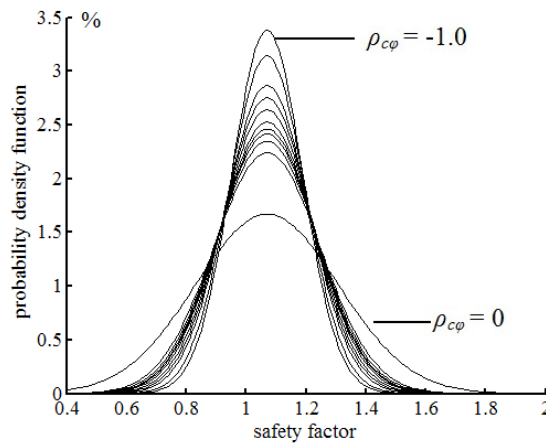
Fig. 5.11 Influence of the correlation coefficient variation on the normal fit of safety factor for simplified MCS-SRM

5.3.2 First Order Reliability Method results for case 2

For FORM method, considering now the safety factor of slope as a function of two correlated soil parameters cohesion c and friction angle φ, the Taylor's series expansion for the safety factor about the expansion values μ_c and μ_φ, truncated after the first order terms, is given by Eq. 5.5.

Considering the correlation between cohesion and friction angle, the mean value and variance of safety factor are obtained using Eq. 5.36 and 5.37.

$$\mu_{FS} \approx F\left(\mu_{x_1}, \ldots, \mu_{x_n}\right) + \frac{1}{2} \cdot \left(\frac{\partial F}{\partial c} \cdot \frac{\partial F}{\partial \varphi}\right) \cdot Cov(c, \varphi) \tag{5.36}$$

$$Var(FS) \approx \left(\left.\frac{\partial F}{\partial c}\right|_{c^*}\right)^2 \cdot Var(c) + \left(\left.\frac{\partial F}{\partial \varphi}\right|_{\varphi^*}\right)^2 \cdot Var(\varphi) + 2 \cdot \left(\frac{\partial F}{\partial c} \cdot \frac{\partial F}{\partial \varphi}\right) \cdot Cov(c, \varphi) \tag{5.37}$$

At last, the results are shown in Table 5.7. Varying the correlation coefficient from -1.0 to 0, the standard deviation of safety factor increases up to around 0.198 for $\rho_{c\varphi}=0.0$, while the mean value is always constant and equal to 1.07. Therefore, the probability of failure increases from 25.1% to 35.5%.

Table 5.7 Influence of $\rho_{c\varphi}$ on the statistical results of slope stability by FORM

$\rho_{c\varphi}$	$Cov(_{c,\varphi})$	μ_{FS}	σ_{FS}	β	$P_f(\%)$
-1	-25	1.07	0.110	0.636	25.1
-0.9	-22.5	1.07	0.122	0.574	27.2
-0.8	-20	1.07	0.133	0.526	28.8
-0.7	-17.5	1.07	0.142	0.493	30.2
-0.6	-15	1.07	0.152	0.461	31.3
-0.5	-12.5	1.07	0.160	0.438	32.2
-0.4	-10	1.07	0.169	0.414	33.0
-0.3	-7.5	1.07	0.177	0.396	33.8
-0.2	-5	1.07	0.184	0.380	34.4
-0.1	-2.5	1.07	0.191	0.367	34.9
0	0	1.07	0.198	0.354	35.5

The normal distribution is assumed to draw the probability density curves of the safety factor results of table 5.7, then the same conclusions of Fig. 5.11 about the shape of the curves and

the variability of the safety factor with the correlation between the input soil parameters would come out as (in Fig. 5.12).
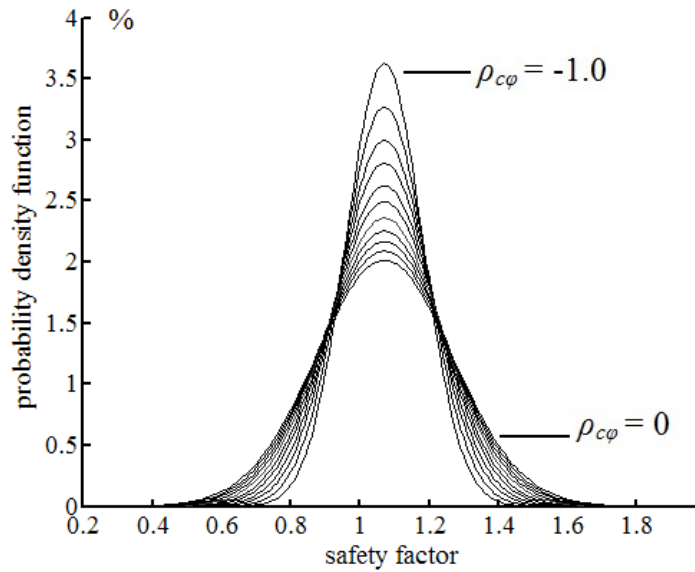
Fig. 5.12 Influence of the correlation coefficient variation on the normal fit of safety factor for FORM

5.3.3 Point Estimate Method results for case 2

If the soil parameters c and φ are correlated, then Rosenblueth´s formula (5.18) cannot be applied for this case, because negative weights are found. For this reason Christian's formula (5.24) is used.

As c and φ are both symmetrically distributed, then computations of the sampling point locations and weights for single random variable are just the same as in case 1, only the associated weights are different.

Varying the correlation coefficient from -1.0 to 0.0, the associated sampling weights and the statistical values of the slope stability are listed in Table 5.8.

By increasing the correlation coefficient and considering the equivalent normal variables c and φ as input for the analysis, the mean value changes slightly (less than 0.2% difference for soil parameters with $\rho_{c\,\varphi'} = 0.0$ to $\rho_{c\,\varphi'} = -1.0$), while the standard deviation decreases significantly down to about 126% reduction for the case with $\rho_{c\,\varphi'} = -1.0$. The failure probability decrease to about 22.8% for a correlation of $\rho_{c\,\varphi'} = -1.0$. Fig. 5.13 shows the influence of the correlation coefficient variation on the shape of the normal fit of the safety factor.

Table 5.8 Statistical values of the slope stability from PEM for different correlation coefficients

$\rho_{c\varphi}$	$P_{c+\varphi+}$	$P_{c+\varphi-}$	$P_{c-\varphi+}$	$P_{c-\varphi-}$	μ_{FS}	σ_{FS}	β	p_f (%)
-1.0	0.000	0.5	0.5	0.000	1.07	0.094	0.747	22.8
-0.9	0.025	0.475	0.475	0.025	1.07	0.107	0.654	25.7
-0.8	0.050	0.450	0.450	0.050	1.07	0.119	0.588	27.8
-0.7	0.075	0.425	0.425	0.075	1.07	0.130	0.539	29.5
-0.6	0.100	0.400	0.400	0.100	1.07	0.139	0.504	30.7
-0.5	0.125	0.375	0.375	0.125	1.07	0.148	0.473	31.8
-0.4	0.150	0.350	0.350	0.150	1.07	0.156	0.449	32.7
-0.3	0.175	0.325	0.325	0.175	1.07	0.164	0.427	33.5
-0.2	0.200	0.300	0.300	0.200	1.07	0.175	0.400	34.5
-0.1	0.225	0.275	0.275	0.225	1.07	0.179	0.391	34.8
0.0	0.250	0.250	0.250	0.250	1.07	0.189	0.370	35.5
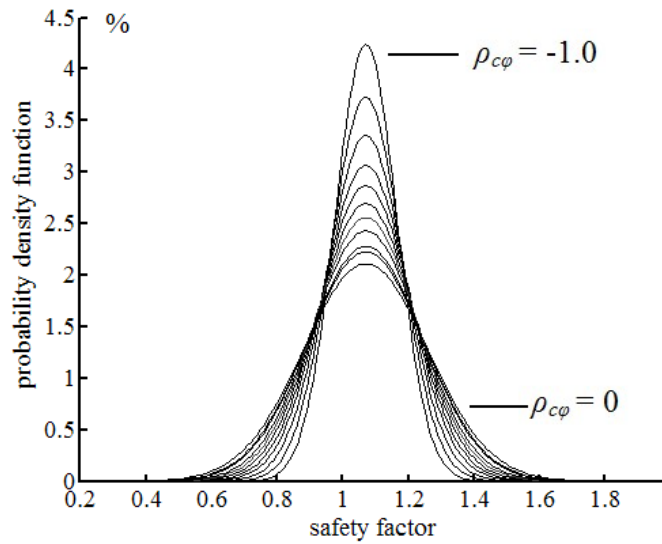
Fig. 5.13 Influence of the correlation coefficient variation on the normal fit of safety factor for PEM

Comparison of results

Comparison of the influence of correlation coefficient ρ on different methods is shown in Fig. 5.14. The probability of failure by MCS is the greatest, and the probability of failure by PEM is the smallest among these three methods. The curves of the probability of failure vs. correlation coefficient by methods of MCS and PEM are almost parallel, while the curves by the methods of FORM and PEM intersect gradually when the correlation coefficient tends to be 0.0. The probability of failure increases as the correlation coefficient increase

for all of these three methods.

Recapitulating all these observations, it is then possible to conclude that the choice of a negative correlation for the soil parameters is reasonable, because the uncertainty in the problem decrease considerably.
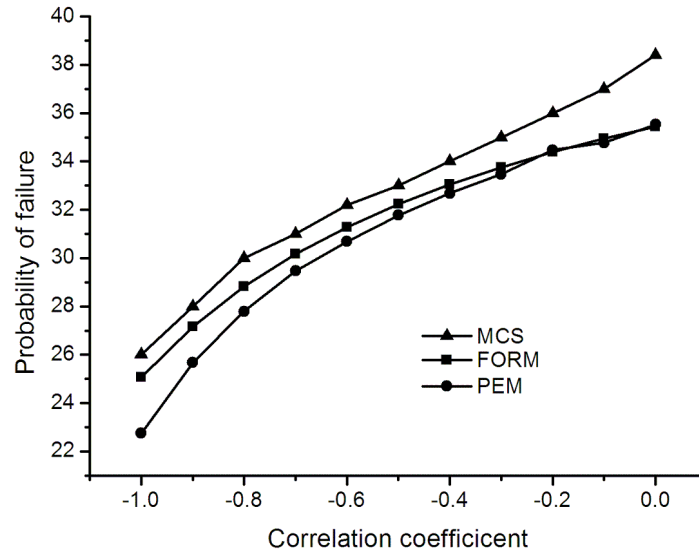
Fig. 5.14 Comparison of results by MCS, FORM and PEM for case 2

5.4 Slope stability analyses of case 3

This example is a two-layered slope with a length of 40 m and a depth of 30 m, and the depth of upper layer is 15m. The whole slope is divided into 1286 elements as in Fig. 5.15.
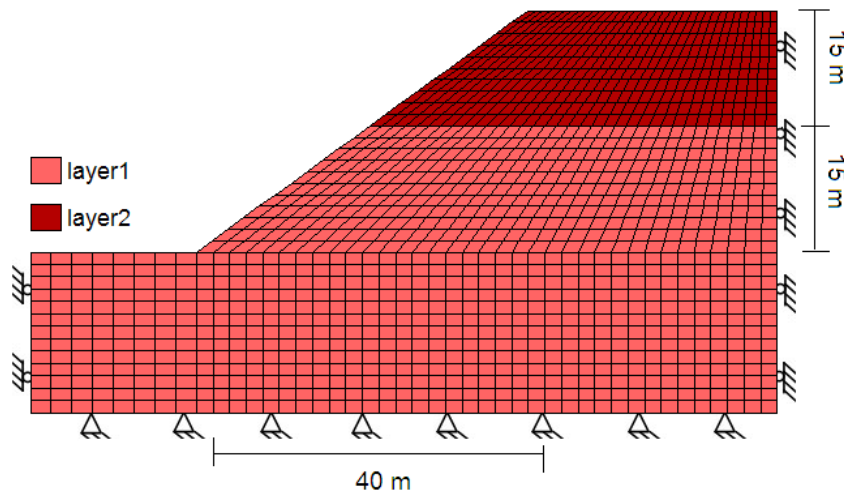
Fig. 5.15 Mesh of slope for case 3

In this case, the cohesion and friction angle of both layers are considered as random variables,

so, the number of input variables increases from 2 to 4. In example 1 and 2, the cohesion and friction angle of two layers soil are considered as three types: normal distributed variables, log-normal distributed variables and negative correlated normal distributed variables. The slope soil parameters are shown in Table 5.9.

Fig. 5.16 presents the simulation result for case 3 using Strength Reduction Method based on the mean value of soil properties, and the factor of safety is calculated to be 1.10.

Table 5.9 Soil properties for case 3

soil	γ (kN/m^3)	Bulk (GPa)	Shear (GPa)	μ_c (kPa)	CV_c	μ_φ (°)	CV_φ
Layer 1	2000	2.0	1.4	25	0.2	25	0.2
Layer 2	1950	1.8	1.2	20	0.2	20	0.2
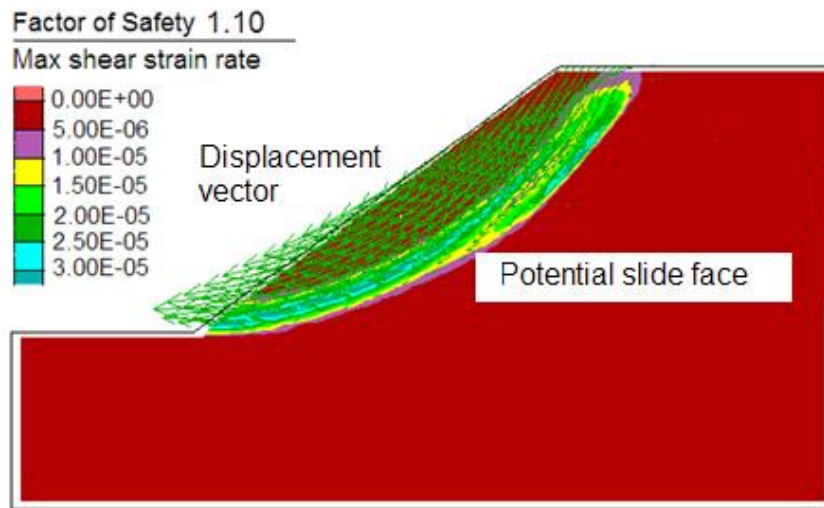
Fig. 5.16 Simulation result for two layered slope by SRM

The influence of the type of the soil properties on the calculated reliability index using three probabilistic analysis methods is shown in Table 5.10. One can see that, generally the results of PEM are closer to MCS than FORM. It means that the accuracy of FORM decreases as the number of input variables increases. For the probabilistic analysis of non homogenous slope with more input variables, MCS and PEM are very efficient.

Table 5.10 Reliability comparison between the three probabilistic methods for example 3

Methods	Normal distributed				Log-normal distributed				Correlated normal distributed (ρ=-0.6)			
	μ_{FS}	σ_{FS}	β	P_f	μ_{FS}	σ_{FS}	β	P_f	μ_{FS}	σ_{FS}	β	P_f
MCS	1.10	0.254	0.394	34%	1.10	0.210	0.409	34%	1.10	0.135	0.741	22%
FORM	1.10	0.147	0.680	24%	1.09	0.113	0.620	26%	1.10	0.108	0.926	17%
PEM	1.05	0.147	0.340	36%	1.05	0.150	0.333	36%	1.08	0.116	0.690	24%

5.5 Conclusions

This chapter presents general and user-friendly computational methods for reliability analysis of slope stability. "User-friendly" methods refer to those that can be implemented on a desktop PC by a non-specialist with limited programming skills; in other words, methods within reach of general practitioner. At last, following conclusions are presented:

First, MCS is the most accurate method, but it is too time consuming for practical purposes; consequently too expensive. For the simulation of uncertain inputs following arbitrary non-normal probability distribution functions and correlation structure, the translation model involving memoryless transform of the multivariate normal probability distribution function can cater for most practical scenarios.

Second, FORM is an approximate method with similar conservative results. It should be pointed out that the safety factor does not vary linearly, but exponentially with c and φ. The FORM procedure only considers linear functions, and then uncertainty is introduced in the safety factor calculations, giving less accurate results than MCS. Furthermore, equivalent normalization for non normal distributed variables and the iteration process make the FORM difficult for operation. PEM is chosen as alternative probabilistic method instead of MCS and FORM, because it requires much less computational effort than MCS. This approach does not require the determination and evaluation of partial derivatives of the safety factor function as FORM, thus being more straightforward to use. However there are also some drawbacks in calculation process when the variables are correlated and non-symmetric.

At last, there is much difference of the standard deviations of safety factor between the input variables with different correlations. Therefore considering the correlations of the soil parameters can decrease the uncertainty of the slope stability analysis significantly.

In practice, FORM and PEM can be used as a preliminary check for the failure probability of

slope stability. However, the MCS should be used in the analysis if the slope is of greater importance.

6. Spatial Variability and Slope Reliability Analysis

Introduction

Soil properties are highly spatial variable and rarely homogeneous by nature, i.e., soil properties vary from one point to another in space due to different deposition conditions and different loading histories (Elkateb et al., 2002). However, in slope stability analysis, most deterministic analysis methods and even probabilistic analysis methods ignore the spatial variations of soil properties and assume that soil parameters of the distinct soil layer are constant.

In 1984, the random field model was introduced into geotechnical engineering by Vanmarke. This model can effectively describe the spatial variations of soil properties by spatial correlation theory. However, the model is seldom applied with numerical simulation because of the complexity of the discretization process in the numerical model. Recently, a more rigorous method of probabilistic geotechnical analysis, the random finite element method (RFEM), which integrates the random field model and finite element method, has been developed and applied in geotechnical engineering (Fenton and Griffiths, 1993), Paice, 1997), and Griffiths and Fenton, 2000)). Griffiths, Fenton, Hicks and Spencer (2010), investigated the influence of the spatial variability of soil properties on the stability of saturated soil slope based on random field theory.

Unfortunately, RFEM has limited application because of its complex programming. Furthermore, the feasibility and accuracy of this method also need further study. Thus, in the present study, a more practical procedure for probabilistic slope stability analysis that considers the spatial variability of soil properties is presented. The local average subdivision is applied to discretize continuous random fields. Both of the stationary and the non stationary random field models for soil properties are investigated in this paper. For studying the influence of the local averaging on the probability of failure, in the first two cases, only one parameter soil cohesion is considered as random variable. In the case 3, the cohesion and friction angle of soil both are considered as random variable. After the random field modeling, the Monte Carlo simulation is applied to compute the probability of slope failure, and then the influence of local averaging on the probability of failure and the convergence of analysis is studied. The whole procedure is performed using a commercial finite difference code FLAC, which requires less programming.

6.1 Brief description of the random field model

6.1.1 Statistical model of soil

In the process of geotechnical probability analysis, the primary and the most difficult work is the statistical analysis about the soil properties, because it is the fundamental of geotechnical analysis and the soil properties are different in different point. Theoretically, the distribution of soil properties in space is not absolutely stochastically, but follows some regulars. If infinite surveys can be conducted, the distribution of soil properties would be determined exactly. While in practice no matter the geological work or laboratory work is finite, so it is unavoidable to extrapolate the whole situation from a handful of data. We have to apply the probabilistic and statistical stools to deduce the most feasible distribution of the geological characters which are considered as stochastic. The probability profile about the soil layer is more representative and can be used in the following geotechnical probabilistic analysis.

The probabilistic modeling of soil layer profile is fatal in slope probabilistic analysis which is not only to calculate the safety factor function, but also to determine the uncertainty of the safety factor. Therefore, the uncertainty about the geological parameters is deserved to quantify.
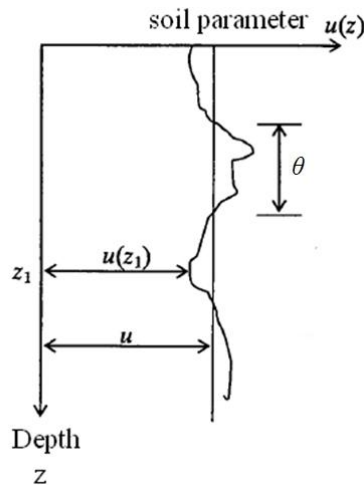
Fig. 6.1 Profile of soil property

As aforementioned, the uncertainty sources of the soil layer profile are: the inherent heterogeneity and variability of soil, the shortage of data about underground situation and the test error. In regular profile, the mechanical character of soil is determined by single value parameters, but ignoring their fluctuation. While in probabilistic profile, at least one property

of soil is treated as a random variable in one or more dimensions. Except for mean, standard deviation and variance, there is another parameter to describe the spatial variance of the soil layer character, i.e. the spatial correlation length θ (as Fig. 6.1), which indicates the fluctuation range of the parameter. The spatial correlation length represents the span in where the soil character remains sequence. A smaller θ indicates that the soil parameter fluctuate fast, otherwise, the parameter is relative steady in big range.

In the spatial variability analysis about the random field, the geostatistical method is the most efficient. It is based on the Regionalization Variable Theory, and applies the variability function to analyze the spatial variability of the geotechnical parameters.

6.1.2 Spatial variation

Spatial variation in a soil deposit can be characterized in detail, but only with a great number of observations, which normally are not available. Thus, it is common to model spatial variation by a smooth deterministic trend combined with residuals about that trend, which are described probabilistically.

Generally, considering the geometry of the geotechnical space as V ($V \in R^2$ or R^3), the actual soil mechanic parameter at location x (in one or more dimensions) is $z(x)$. $z(x)$ can be expressed as

$$z(x)=m(x)+R(x) \tag{6.1}$$

where $m(x)$ is a smooth trend at x, and $R(x)$ is residual deviation from the trend. The residuals are characterized as a random variable of zero-mean and some variance because there are too few data to do otherwise. This does not presume that soil properties actually are random. The variance of the residuals reflects uncertainty about the difference between the fitted trend and the actual value of soil properties at particular locations. Spatial variation is modeled stochastically not because soil properties are random but because information is limited.

Trends are estimated by fitting lines, curves, or surfaces, to spatially referenced data. The easiest way to do this is by regression analysis. Usually, $m(x)$ can be expressed as follow polynomial

$$m(x) = \sum_{l=0}^{k} a_l f_l(x) \tag{6.2}$$

where a_l is the coefficient of drift polynomial; $f_l(x)$ is the drift polynomial, $f_l(x) = x^l$; k is the exponent number of drift and always not more than two.

6.1.3 Random field

The application of random field theory to spatial variation is based on the assumption that the property of concern, $z(x)$, is the realization of a random process. When this process is defined over the space $x \in V$, the variable $z(x)$ is said to be a stochastic process. In this chapter, when V has dimension greater than one, $z(x)$ is said to be a random field.

A random field is defined as the joint probability distribution:

$$F_{x1,...,xn}(z_1, ..., z_n) = P\{z(x_1) \leq z_1, ..., z(x_n) \leq z_n\} \tag{6.3}$$

The joint probability distribution describes the simultaneous variation of the variables z within a space V_x. Let, $E[z(x)] = \mu(x)$ be the mean or trend of $z(x)$, and let $Var[z(x)] = \sigma^2(x)$ be the variance. The covariances of $z(x_1)$, ..., $z(x_n)$ are defined as:

$$Cov[z(x_i), z(x_j)] = E\left[[z(x_i) - \mu(x_i)] \cdot [z(x_j) - \mu(x_j)]\right] \tag{6.4}$$

A random field is said to be second order stationary (weak or wide-sense stationary) if $E[z(x)] = \mu$ for all x, and $Cov[z(x_i), z(x_j)]$ depends only on vector separation of x_i and x_j, and not on location. $Cov[z(x_i), z(x_j)] = C_z(x_i-x_j)$, in which $C_z(x_i-x_j)$ is the auto covariance function. The random field is said to be stationary (strong or strict stationarity) if the complete probability distribution, $Fx_1, ..., x_n(z_1, ..., z_n)$ is independent of absolute location, depending only on vector separations among the $x_i...x_n$. Strong stationarity implies second-order stationarity. In the geotechnical literature, stationarity is sometimes referred to as statistical homogeneity. If the auto covariance function depends only on the absolute separation distance and not direction, the random field is said to be isotropic.

A random field that does not meet the conditions of stationarity is said to be non-stationary. Loosely speaking, a non-stationary field is statistically heterogeneous. It can be heterogeneous in a number of ways. In the simplest case, the mean may be a function of location, for example, if there is a spatial trend that has not been removed. In a more complex case, the variance or auto covariance function may vary in space. Depending on the way in which the random field is non-stationary, sometimes a transformation of variables can convert a non-stationary field to a stationary or nearly stationary field. For example, if the mean varies with location, perhaps a trend can be removed.

In the field of geostatistics, a weaker assumption is made on stationarity than that described above. Geostatisticians usually assume only that increments of a spatial process are

stationary (i.e. differences $|z_1$-$z_2|$) and then operate on the probabilistic properties of those increments. This leads to the use of the variogram rather than the auto covariance function. Stationarity of the auto covariance function implies stationarity of the variogram, but the reverse is not true.

Like most things in the natural sciences, stationarity is an assumption of the method and may only be approximately true in the world. Also, stationarity usually depends on scale. Within a small region soil properties may behave as if draw from a stationary process, whereas the same properties over a larger region may not be so well behaved.

6.1.4 Correlation function

For a homogeneous soil layer, the random variable of parameter in position x_1 is $Z(x_1)$, the correlation characteristic of $Z(x_1)$ and $Z(x_2)$ can be expressed by the correlation function as follow:

$$\rho_Z(\tau) = \frac{Cov[Z(x_1),Z(x_2)]}{\sigma_{Z(x_1)}\sigma_{Z(x_1)}} = \frac{E\{[Z(x_1)-m(x_1)]\cdot[Z(x_2)-m(x_2)]\}}{\sigma_{Z(x_1)}\sigma_{Z(x_1)}} \tag{6.5}$$

The correlation function of homogeneous isotropic random field $\rho_x(t_1, t_2)$ is only related to $\tau = t_1$-t_2, independent to the individual t_1 and t_2. The homogeneous isotropic random field is the univariate function about τ.

According to the views of Vanmarcke et al., the correlation function of soil can be expressed by the single-index model, double-indexes mode, triangle mode, Exponential Cosine mode, Markovian mode and so on. Although the correlation modes of soil are very complex, there are some rules. For seeking the suitable correlation mode with universal meaning, the typical correlation functions were discussed in this chapter. In the following equations, where ρ is the correlation coefficient between the soil parameters at any two points separated by a distance τ in a random field with spatial correlation length θ.

1). Constant mode (Fig. 6.2)

$$\rho(\tau) = 1 \tag{6.6}$$

This is the perfect correlation, where the soil is isotropic without considering the variability.

2). White noise mode (Fig. 6.3)

$$\rho(\tau) = \begin{cases} 1 & \tau = 0 \\ 0 & \tau \neq 0 \end{cases} \tag{6.7}$$

When the soil properties vary fast, and without considering the correlation, this mode will be adopted.
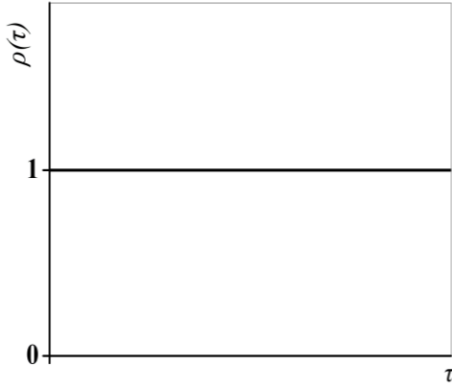
Fig. 6.2 Constant mode   Fig. 6.3 White noise mode
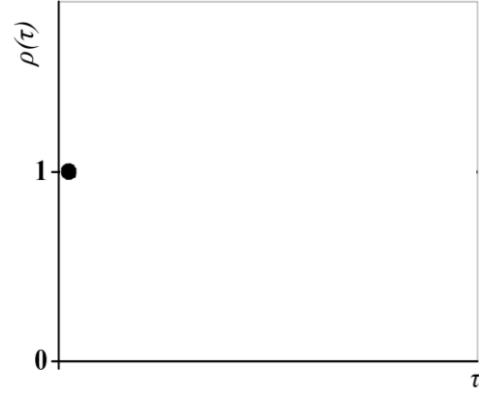
3). Cosine wave mode (Fig. 6.4)

$$\rho(\tau) = \cos 2\pi f \tau \qquad (6.8)$$

The soil properties vary as a cosine curve approximately. This situation seldom appeared in practice, it maybe indicates that there is periodicate geological process or physics and chemistry process during soil layer generation.

4). Triangle correlation mode (Fig. 6.5)

$$\rho(\tau) = \begin{cases} 1 - \tau/\theta & \tau \leq \theta \\ 0 & \tau > \theta \end{cases} \qquad (6.9)$$
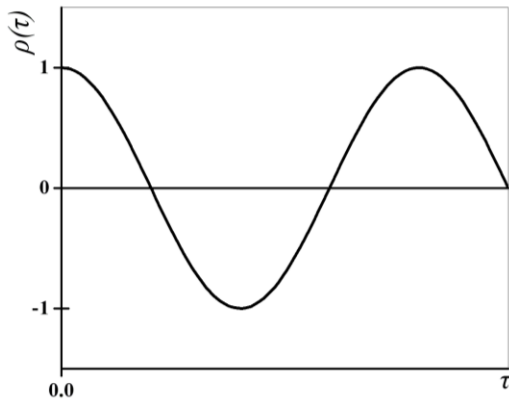
Fig. 6.4 Cosine wave mode   Fig. 6.5 Triangle correlation mode
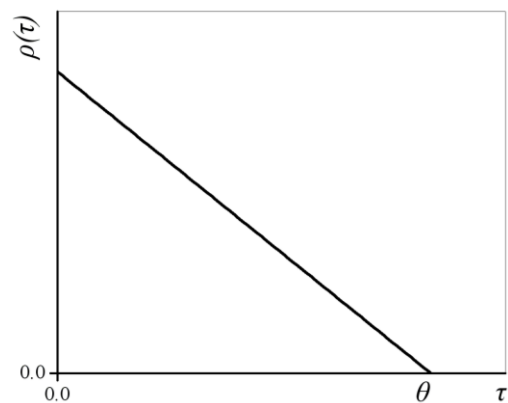
This mode is too simple, and has much difference with the real situation of the soil, so it is not representative.

5). Exponention cosine mode (Fig. 6.6)

$$\rho(\tau) = e^{-\frac{2}{\theta}|\tau|} \cos \omega \tau \qquad (6.10)$$

This correlation mode and its spectral density function have more adaptability. It is relative accurate, but the disadvantage is that the expression is two complex.

6). Markovian mode (Fig. 6.7)

In the present study, a Markovian spatial correlation function was used, of the form

$$\rho(|\tau|) = e^{-\frac{2}{\theta}|\tau|} \qquad (6.11)$$
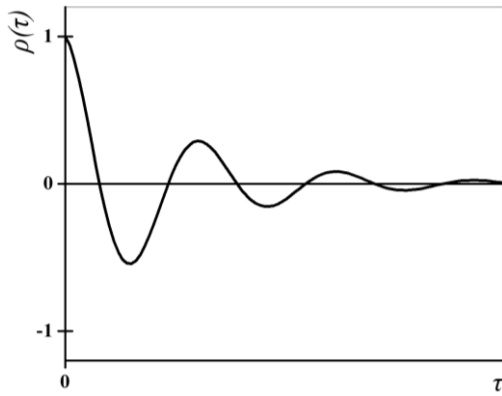
Fig. 6.6 Exponention cosine mode   Fig. 6.7 Markovian mode
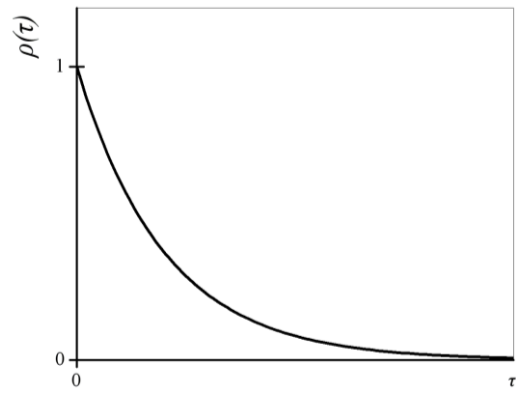
In the two-dimensional analysis presented in this chapter, the spatial correlation lengths in the vertical and horizontal directions are taken to be equaled (isotropic) for simplicity. And the correlation function from Eq. 6.11, repeated here in the form,

$$\rho = e^{-\frac{2}{\theta}\sqrt{\tau_x^2 + \tau_y^2}} \qquad (6.12)$$

where τ_x is the difference between the x coordinates of any two points in the random field, and τ_y is the difference between the y coordinates.

However, the actual spatial correlation structure of soil deposits is not usually well known, especially in the horizontal direction (e.g. Asaoka and Grivas, 1982; de Marsily, 1985; DeGroot and Baecher, 1993). In this chapter therefore, a parametric approach has been employed to study the influence of θ.

6.1.5 Variance reduction function

Actually, the stability of a soil slope tends to be controlled by the averaged soil strength rather

than the soil strength at a particular location along the slide surface, since soils generally exhibit plastic behavior (Li and Lumb, 1987). The effect of spatial averaging and spatial autocorrelation of soil properties on the stability of the slope has been noted in the literature (Vanmarke, 1977; Li and Lumb, 1987; El-Ramly et al., 2002).

Many different random field generator algorithms are available of which the following are perhaps the most common:

1). Fast Fourier Transform (FFT) method,

2). Turning Bands Method (TBM),

3). Local Average Subdivision (LAS) method.

If the problem at hand requires or would benefit from a local average representation, then the LAS method is the logical choice. In this technique, the local average value $z(v_i)$ of the random field $z(x)$ attributes the property in the unit body v_i.

$$z(v_i) = \frac{1}{v_i} \int_{v_i} z(x_i) dx \tag{6.13}$$

so, the random field $z(x)$ is discrete as n random variables $z(v_1)$, $z(v_2)$, …, $z(v_n)$, and described by the discrete parameters, as mean $E[z(v_i)]$, variance $Var[z(v_i)]$ and covariance $Cov[z(v_i)$, $z(vj)]$ (i, j=1, 2, …, n).

$$E[z(v_i)] = E\left[\frac{1}{v_i} \int_{v_i} z(x_i) dx\right] = \frac{1}{v_i} \int_{v_i} m(x) dx \tag{6.14}$$

Based on the correlation function theory, the variance should be reduced as follow

$$\sigma_T^2 = \sigma^2 \Gamma(T) \tag{6.15}$$

where σ^2 is the variance of point property, σ_T^2 is the variance after local averaged, T is the averaging domain and $\Gamma(T)$ is the variance reduction function.

$\Gamma(T)$ has follow mathematic meanings:

1). $\Gamma(0) = 1$;

2). For every $T \geq 0$, there is $0 \leq \Gamma(T) \leq 1$;

3). $\Gamma(-T) = \Gamma(T)$.

Variance reduction function reflects that: when the averaging domain increasing, the variance

of the average property will reduce. The variance reduction is related to the spatial correlation of soil properties. For a square finite element of side length T, it can be shown (Vanmarke, 1983) that for an isotropic spatial correlation field, the variance reduction factor is given by:

$$\Gamma(T) = \frac{\sigma_T^2}{\sigma^2} = \frac{4}{T^4} \int_0^T \int_0^T (T - \tau_x)(T - \tau_y) \, e^{-\frac{2}{\theta}\sqrt{\tau_x^2 + \tau_y^2}} \, d\tau_x d\tau_y \qquad (6.16)$$

In this chapter, a dimensionless spatial correlation length measure Θ is used, where

$$\Theta = \theta/T \qquad\qquad\qquad (6.17)$$

Numerical integration of this function leads to the variance reduction values shown plotted in Fig. 6.8.
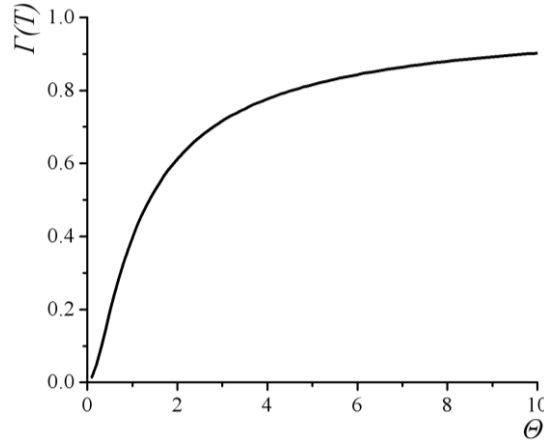
Fig. 6.8 Variance reduction function over Θ with a Markov correlation function

From Fig. 6.8, one sees that as the spatial correlation length compared with the averaging domain tends to infinity, the variance reduction factor reaches 1.0. At the other extreme, as the spatial correlation length tends to zero, the variance reduction factor reaches 0.0.

6.1.6 Calculation methods of spatial correlation length

In particular, the spatial correlation length (θ) describes the distance over which the spatially random values will tend to be significantly correlated in the underlying Gaussian field. Thus a large value of θ will imply a smoothly varying field, while a small value will imply a ragged field. The spatial correlation length can be estimated from a set of tested data taken over some spatial region simply by performing the statistical analyses on the log-data.

The values of spatial correlation length reported in literature are not numerous and regard

especially clay soils (Cherubini, 1997; Phoon and Kulhawy, 1999). It is possible, however, to state that the horizontal correlation length θ_h is more than one order of magnitude larger than the vertical one. In particular, for the vertical correlation length the values most frequently found are varying from 0.5 to 2 m whereas for the horizontal one the typical range is 30~60 m.

For calculate the spatial correlation length, there are mainly following methods: Recurrence Space Method, Curve Limit Method, Correlation Function Method, Statistical Simulation Method, Semi-variogram Method and so on.

6.2 Application of Random Field Method in slope stability analysis

The random field modeling of a two-layer slope is realized in the finite difference code FLAC. The slope is 20 m high with a slope angle of 45°. The elements of the soil are considered as proximate squares measuring 1×1 m (Fig. 6.9). The left and right boundaries are fixed in x-direction, and the bottom is fixed in both the x- and y-directions.
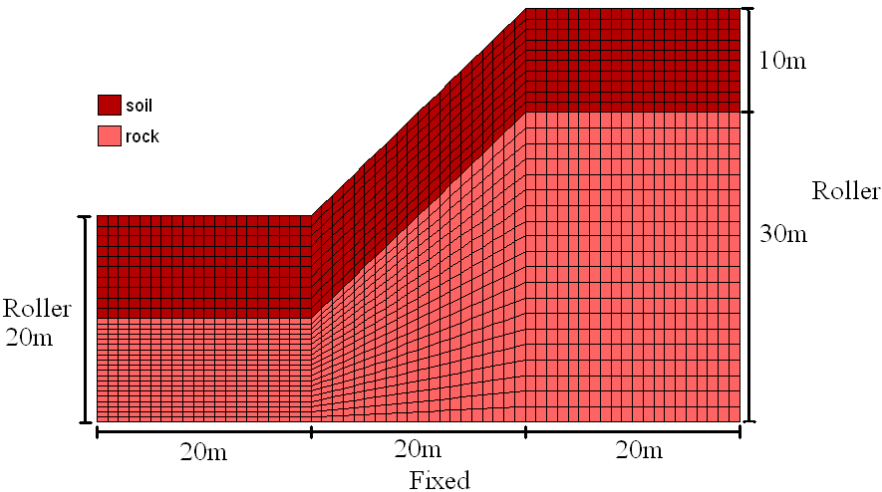
Fig. 6.9 Mesh used in slope stability analyses

The model is a linear elastic-perfectly plastic material with a Mohr-Coulomb failure criterion. For investigating the influence of spatial correlation on the probability of failure, all mechanical properties are considered as constant except for the cohesion of soil (Table 6.1).

Table 6.1 Mechanical parameters about the slope

Layer	Density (kg/m^3)	Bulk (Pa)	Shear (Pa)	Cohesion (Pa)	Friction angle ($^\circ$)
Soil	1950	1.8e9	1.2e9	-	22
Rock	2000	2.0e9	1.5e9	4.0e4	40

6.2.1 Case 1. Stationary random field model

In this case, the cohesion of soil c is assumed to be characterized statistically as random variables with a constant trend 21 kPa, and the standard variance σ_c is 4 kPa.

The safety factor of this slope using the Strength Reduction Method based on the trend value of soil cohesion (i.e., the residual deviation from the trend is zero) is 1.01, which means it is in the edge of failure. The simulation result for the slope presents in Fig. 6.10. Critical failure surface is found automatically as the max shear strain rate zone, and it is not necessary to specify the shape of the failure surface (e.g. circular, log spiral, piecewise linear, etc.).
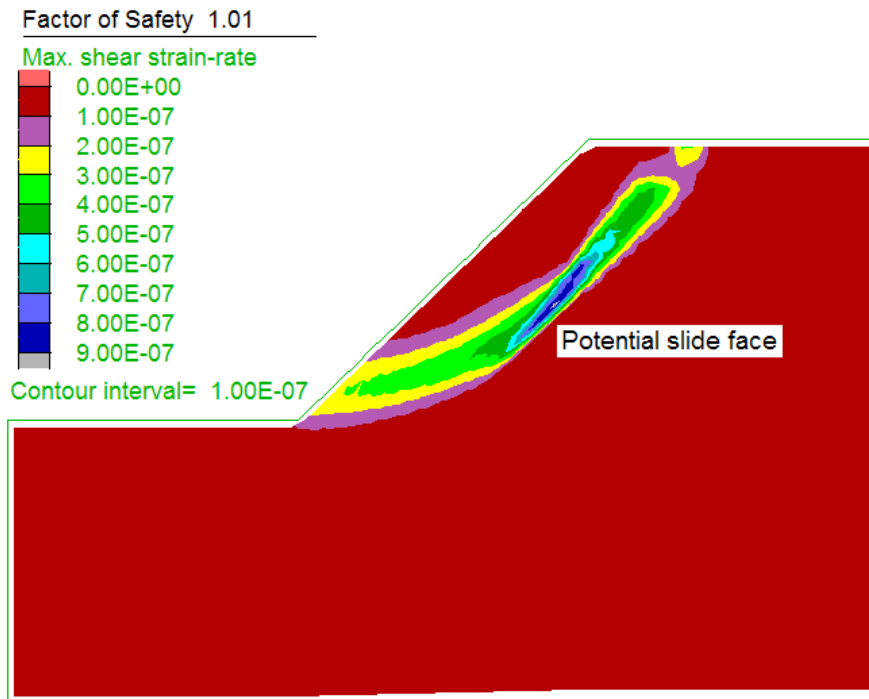
Fig. 6.10 Results of slope by Strength Reduction Method

When the random field method applied, the numerical solution algorithm requires that the continuous parameter field of cohesion c be discretized, and it is realized through the following transformation

$$c_i = m_{c_i} + R_{c_i} \tag{6.18}$$

in which c_i is the cohesion assigned to the ith element, trend m_{c_i} is the mean value of c in i^{th} element, and residual R_{ci} is a normal random variable with a mean of zero and a standard deviation of σ_T.

In the present study, the cohesion of soil is a stationary random field, and the trend in every element is a constant 21 kPa. The variance of the residual R_{ci} can be obtained by the local average subdivision based on the spatial correlation theory. In the two dimensional analysis presented in the following case study, the spatial correlation lengths in the vertical and horizontal directions are taken to be equal (isotropic) for simplicity.

In the first case, the averaging domain T is determined as the same of mesh size 1m, and the relationship between the variance reduction coefficient Γ and spatial correlation length θ is shown in Table 6.2 based on Eq. 6.16.

Table 6.2 Relationship between Γ and θ when T is 1 m

θ	0.1	0.2	0.5	1.0	2.0	4.0	5.0	8.0	10.0
$\Gamma(T)$	0.0138	0.048	0.1932	0.3965	0.612	0.7764	0.8156	0.8796	0.9020

Subsequent to determining the trend and residual deviation of cohesion in every element, the random values of cohesion can be generated by means of FISH program based on Eq. 6.18. The generations of two sets of random variables of cohesion based on different spatial correlation length are presented as the scattered points in Fig. 6.11, and the solid line presents the trend of cohesion in the depth of 1~10 m. The random variables are symmetrically distributed on both sides of the trend, and they are more dispersive when the spatial correlation length is greater.

a) θ=1m   b) θ=10m
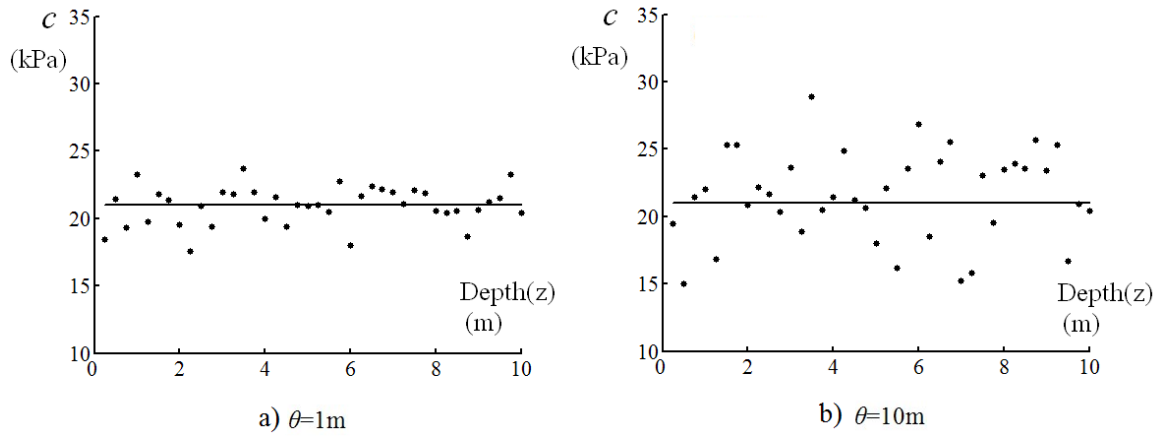
Fig. 6.11 Two sets of random variables with constant trend μ_c

The next step is to input the random variables generated by LAS to the slope mesh. This process also needs the help of FISH language in FLAC. The distribution of cohesion in slope with a relative lower spatial correlation length of θ_c=1.0 m is presented in Fig. 6.12 (a), and

the model with a relative higher spatial correlation length of $\theta_c=10$ m is shown in Fig. 6.12 (b). It should be emphasized that both these cohesion distributions come from the same normal distribution, only the spatial correlation lengths are different.

a) $\theta_c=1.0$m   b) $\theta_c=10$m
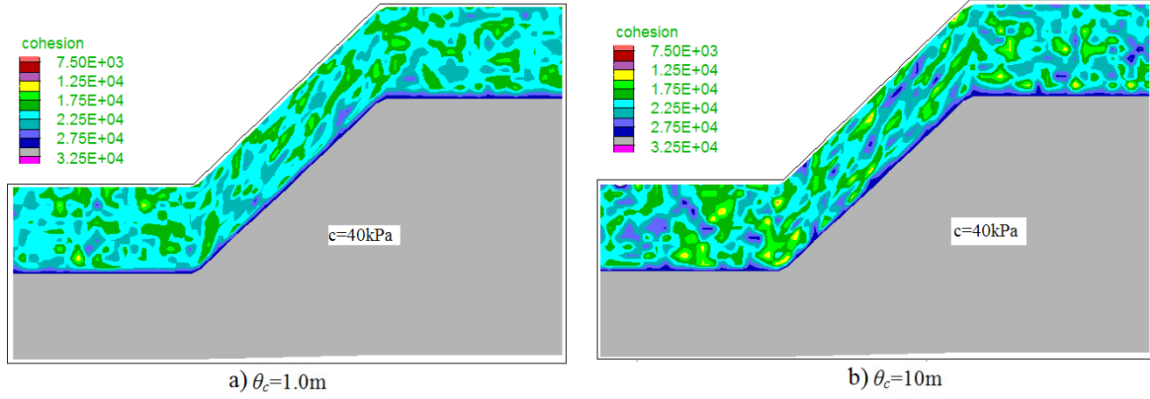
Fig. 6.12 Random field models of slope with constant trend and T is 1 m

In this section, stationary random field, whose first moment mean independent with the spatial position, is considered in slope probabilistic analysis. The analysis is performed using the mesh of Fig. 6.9. The random variables can be correlated to one another by controlling the spatial correlation length θ as described previously.

After the random field model of cohesion built, slope probabilistic analysis based on Monte Carlo simulation is performed. The random variables in different element are correlated to one another by controlling the spatial correlation length θ. For a given set of input cohesion parameters (mean, standard deviation and spatial correlation length), the slope stability analysis is repeated many times until the statistics of the output quantities of interest become stable. During each "realization" of the Monte Carlo process, each element in the soil is assigned a constant cohesion.

To perform the reliability analysis by Monte Carlo Simulation, the appropriate sample size of soil properties should be determined first. For this purpose different sample sizes ranged from 50 to 2000 were generated and the associated probabilities of failure p_f were calculated. Fig. 6.13 shows the relationship between the sample size (generated number) and the probability of failure, when the spatial correlation length is 0.1 m, 1 m and 10 m (i.e., reduction coefficient of variability is 0.0138, 0.3965 and 0.9021 respectively). It is clearly shown in this figure that when the spatial correlation length is 0.1 m, almost there is no significant difference in the calculated p_f as the sample size exceeds 500, but for the spatial correlation length 10 m, we need 1,000 samples to get the relative stable result. It

indicates that the spatial correlation length affects the convergence of the probabilistic analysis, and a longer correlation length need larger sample size to obtain the relative stable results.
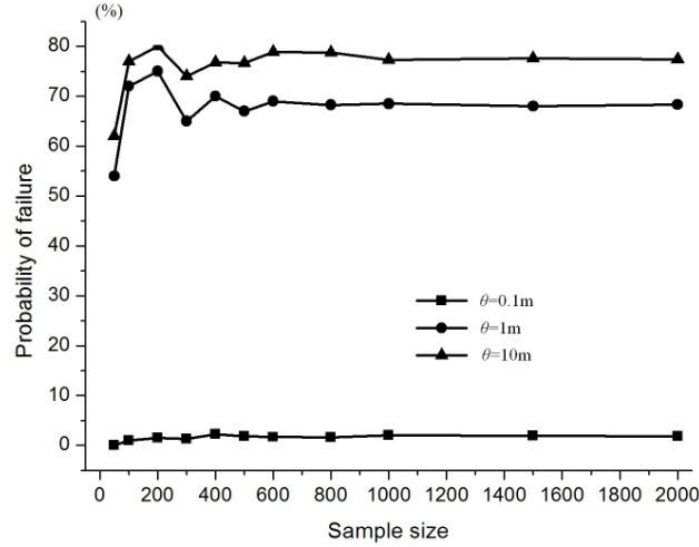
Fig. 6.13 Relationship between probability of failure and sample size

The correlation length θ of the random field, is in general the most difficult to evaluate. For this reason, a parametric study on the influence of this parameter was performed. Table 6.3 shows the influence of the spatial correlation length to the probability of failure, and the sample size of 1000 was chosen here in each case. One sees that for the mean of safety factor is more than 1.0, the probability of failure increase as the spatial correlation length increases (i.e., the reduction coefficient of cohesion increases).

Table 6.3 Probability of failure based on different θ when T is 1 m

θ (m)	0.1	0.2	0.5	1.0	2.0	4.0	5.0	8.0	10.0
P_f(%)	1.85	18.5	59.7	68.3	72.6	74.9	76.1	77.5	78.8

For study the influence of the averaging domain T on the probability failure of slope, in the second case, the averaging domain T is determined as 2 m, and the mesh size of the slope is the same as the Fig. 6.9. The relationship between the variance reduction coefficient Γ and spatial correlation length θ is shown in Table 6.4.

After generated the random values of cohesion according to local averaging subdivision, the distributions of cohesion in slope with a relative lower spatial correlation length of θ_c=1.0 m a relative higher spatial correlation length of θ_c=10 m are compared in Fig. 6.14. From the plot, one can see that when the spatial correlation length longer, the discreteness

of cohesion is greater.

Table 6.4 Relationship between Γ and θ when T is 2 m

θ	0.1	0.2	0.5	1.0	2.0	4.0	5.0	8.0	10.0
Γ	0.0037	0.0138	0.0699	0.1932	0.3965	0.6118	0.6718	0.7765	0.8158

a) θ_c=1.0m

b) θ_c=10m
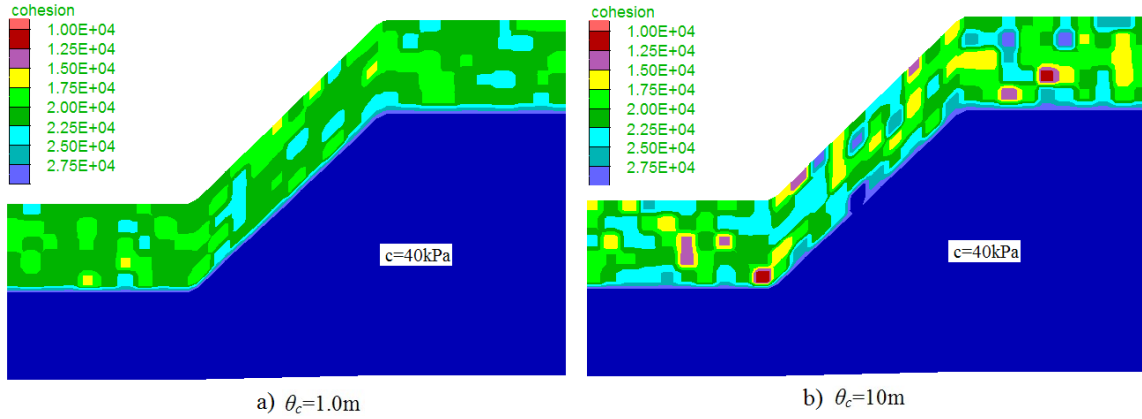
Fig. 6.14 Random field models of slope with constant trend and T is 2 m

Table 6.5 shows the probability of failure based on different spatial correlation length when T is 2 m, and the sample size of 1000 was chosen here in each case. One sees that for the mean of safety factor is more than 1.0, the probability of failure increase as the spatial correlation length increases (i.e., the reduction coefficient of cohesion increases).

Table 6.5 Probability of failure based on different θ when T is 2 m

θ (m)	0.1	0.2	0.5	1.0	2.0	4.0	5.0	8.0	10.0
P_f (%)	0.25	9	38.3	54.1	60	62.9	63.8	65.4	67.4

The results based on T=1 m and 2 m are present in Fig. 6.15. The figure of probability of failure vs. the spatial correlation length is a curve, and initially the probability of failure increase very fast with the spatial correlation length increase, at last, it is asymptotic in about 80% and 70%.

From Fig. 6.15, one can see that the average domain will influence on the probability of failure on some degree. When the T is greater, the probability of failure is smaller. Basically, we need to choose an average domain approximately equal the spatial correlation length.
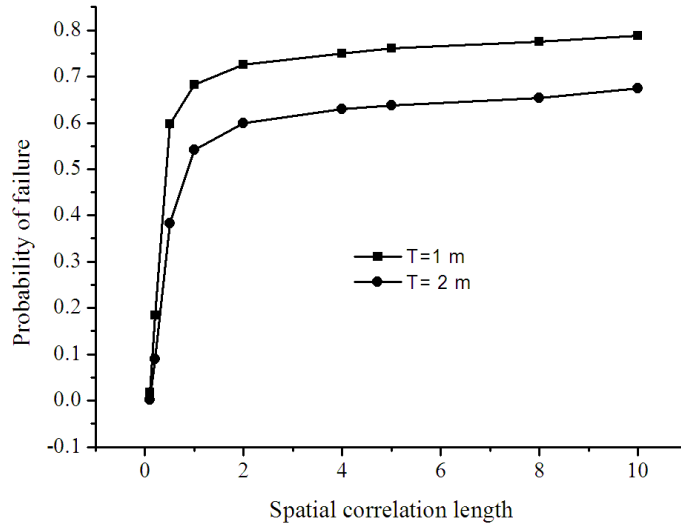
Fig. 6.15 Influence of the spatial correlation length to the probability of failure

6.2.2 Case 2. Non stationary random field model

Most of time, for the influence of earth stress and self weight, the property of sediment varies in depth (Leng Wuming, 2000). In this case the trend of the soil properties is assumed as a function of depth z, $m(z) = 9+2z$ kPa, and the standard variance of point σ_c is 4 kPa. Therefore, the cohesion of soil is a non stationary random field, and the trend is obtained by

$$m_{c_i} = \frac{1}{h} \int_{z_i}^{z_{i+1}} (9 + 2z)\, dz \tag{6.19}$$

where z_i is the height of the bottom of the ith element, and z_{i+1} is the height of the top of the ith element and h is the height of every element. Because $m(z)$ is a linear function, so m_{c_i} can be expressed as the cohesion value in the center of the ith element as Eq. 6.20.

$$m_{c_j} = 72 - 2j,\ (j{=}21, 22, \ldots, 30) \tag{6.20}$$

where j is the number of element along the depth of soil.

The variance of the residual R_{ci} is obtained by the local average subdivision as above case.

After determined the trend and residual deviation of cohesion in every element, the random value will be obtained based on Eq. 6.18. In Fig. 6.16, the scattered points show the generation of a set of random variables about cohesion, and the solid line presents the trend of cohesion in the range of 0~10 m depth. One sees that the trend is an oblique line, and the

random variables are randomly distributed in both sides of the trend.
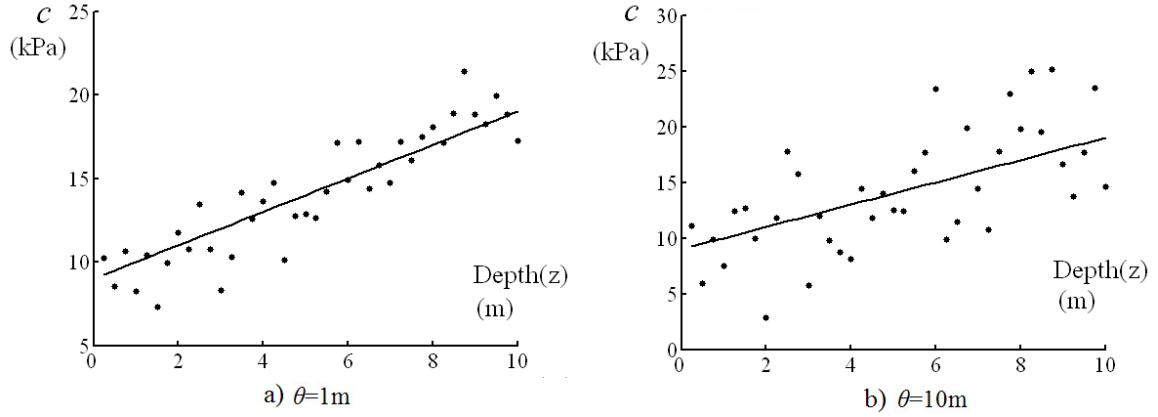
Fig. 6.16 Two set of random variables with inconstant trend μ_c

Next step is to input the random variables generated by LAS to the slope mesh. Fig. 6.17 (a) presents the distribution of cohesion in slope with a relative lower spatial correlation length of θ_c=1.0 m and Fig. 6.16 (b) shows the model with a relative higher spatial correlation length of θ_c=10 m.
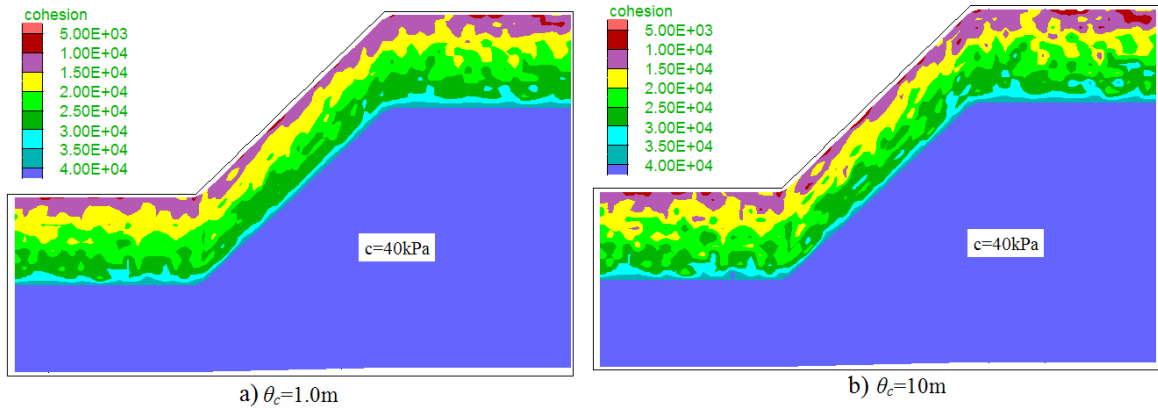
Fig. 6.17 Random field models of slope with inconstant trend

Fig. 6.18 presents the simulation result for slope using Strength Reduction Method based on the trend value of soil cohesion, (i.e. the residual deviation from the trend is zero). The critical failure surface is found automatically as the max shear strain rate zone. The safety factor of this slope is 1.05.

To determine the appropriate sample size of soil properties, different sample sizes ranged from 50 to 2000 were generated and the associated probabilities of failure p_f were calculated. Fig. 6.19 shows the relationship between the sample size (generated number)

and the probability of failure. It just like stationary random field, soil property with longer spatial correlation length needs larger sample size to get the stable result.
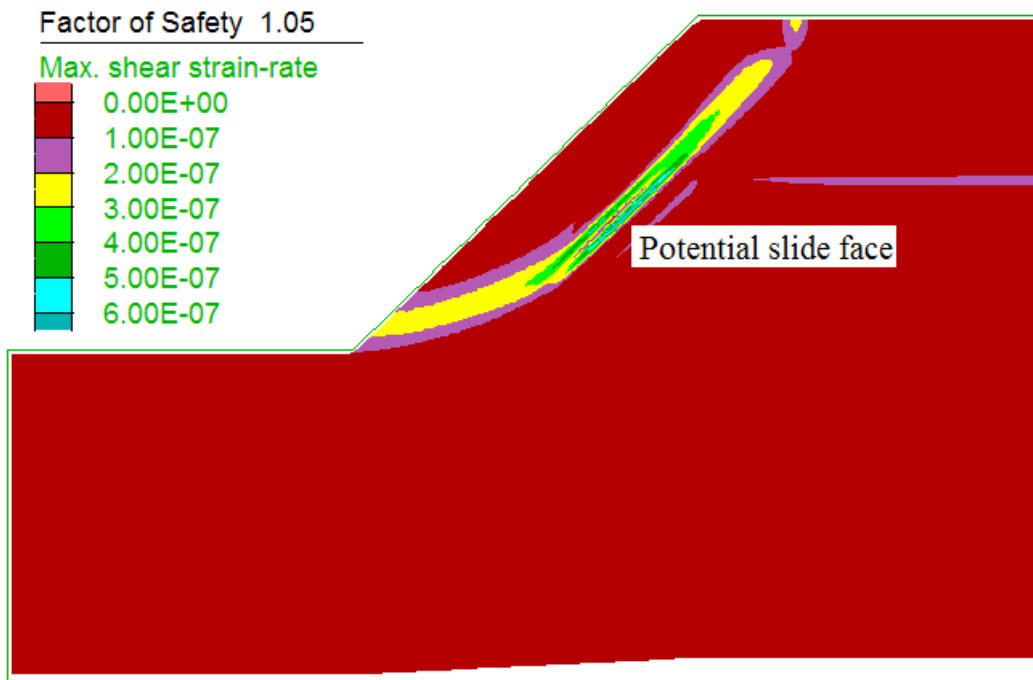
Fig. 6.18 Results of slope by Strength Reduction Method
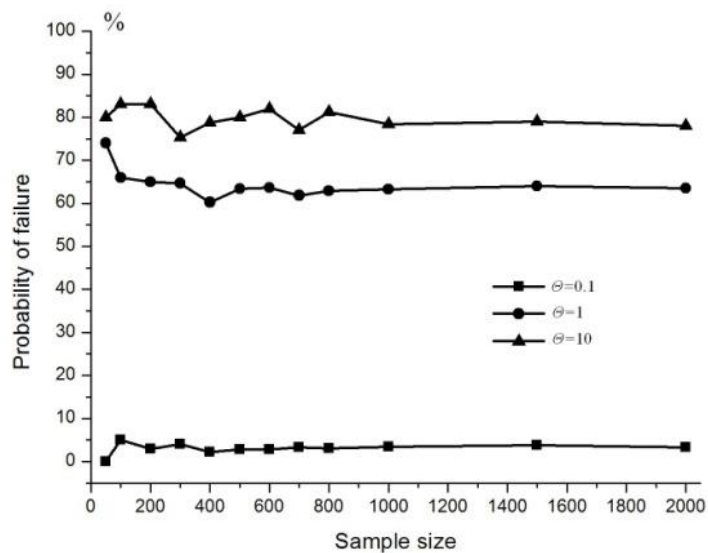
Fig. 6.19 Relationship between probability of failure and sample size

Fig. 6.20 shows the influence of the spatial correlation length to the probability of failure. The probability of failure at last asymptotic in about 80% as the spatial correlation length increases.
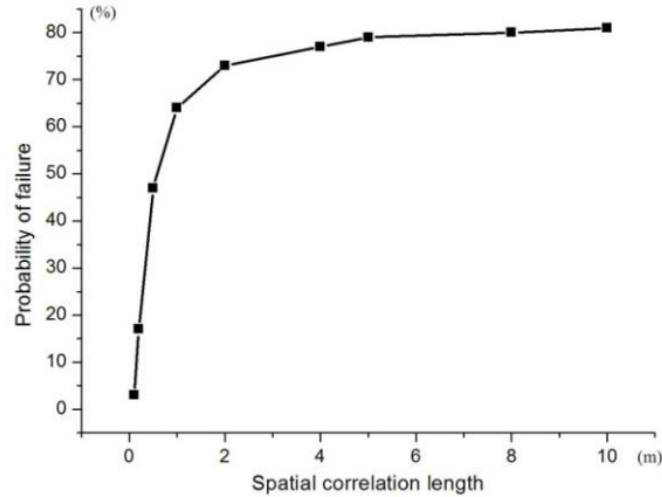
Fig. 6.20 Influence of the spatial correlation length to the probability of failure

6.2.3 Case 3. Double random field models

In this case, both cohesion and friction angle of soil, which impacted slope stability significantly, are considered as random variables and vary as the depth of soil. The mesh of the slope in Fig. 6.9 is applied. The trend of cohesion is 10+2z kPa, and the standard deviation of the cohesion is 4 kPa. The trend of friction angle is 16+2z °, and the standard deviation of the friction angle is 5°. The spatial correlation spatial lengths of cohesion and friction angle both are 2.0 m, and same in horizontal and vertical directions. The distributions of cohesion and friction angle are shown in Fig. 6.21.

Fig. 6.22 presents the simulation result for slope using Strength Reduction Method based on the trend value of soil cohesion, i.e. the residual deviation from the trend is zero. The critical failure surface is found automatically as the max shear strain rate zone. The safety factor of this slope is 1.04.

a) random field of cohesion

b) random field of friction angle
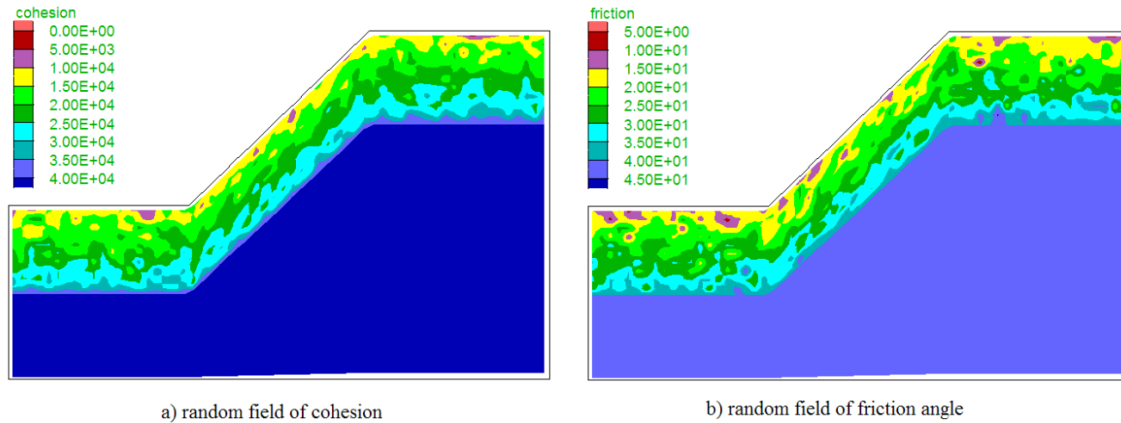
Fig. 6.21 Distributions of cohesion and friction angle
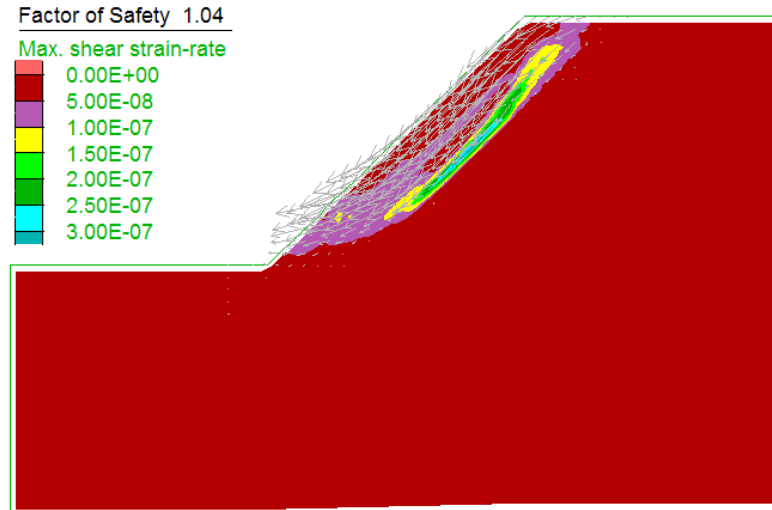
Fig. 6.22 Results of slope by Strength Reduction Method

To perform the reliability analysis by Monte Carlo Simulation, different sample sizes ranged from 50 to 2,000 were generated and the associated probability of failure p_f was calculated. Fig. 6.23 shows the relationship between the sample size (generated number) and the probability of failure. It is clearly shown in this figure that almost there is no significant difference in the calculated (p_f) as the sample size exceeds 500.
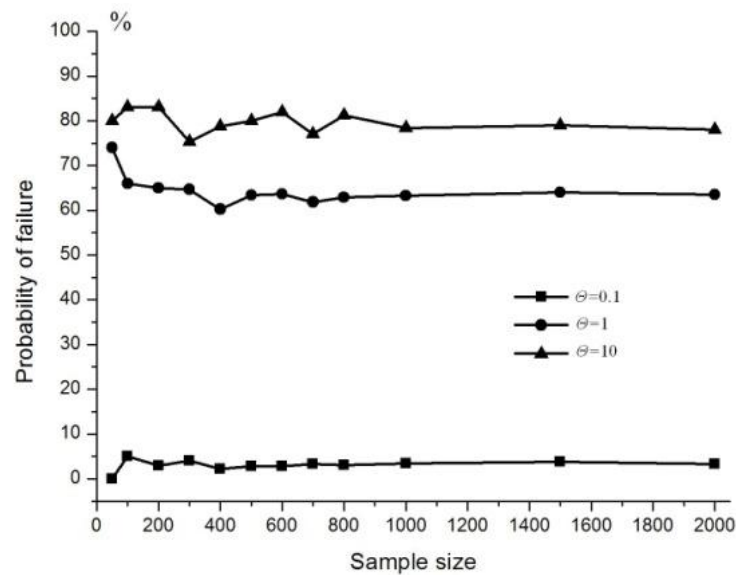
Fig. 6.23 Relationship between probability of failure and sample size

6.3 Conclusion

Modeling soil material properties properly is of crucial importance in geotechnical

engineering. The natural heterogeneity of soil can be fruitfully modeled using probability theory.

If an accurate description of the spatial variability is required, random fields may be employed. Their use in engineering problem requires their discretization. An efficient method has been presented for this purpose, namely local averaging method.

In this chapter, a numerical procedure for a probabilistic slope stability analysis based on a Monte Carlo simulation that considers the spatial variability of the soil properties is presented. The approach adopts the numerical simulation to determine the critical failure surface and to evaluate the safety of the slope. The analysis considers the spatial variability of soil property cohesion based on local averaging to discretize continuous random fields. The study focuses primarily on the non stationary random field to model the inhomogeneous soil. The importance of the spatial correlation structure of soil properties is highlighted and its effect on the stability of slope is studied.

7. Rock Slope Reliability Analysis based on Random Set Theory

7.1. Introduction

Uncertainty and variability are very common in geology engineering, especially in rock material which has many discontinuous joints. There are two sources of uncertainty in rock slope engineering-geometry and geomechnic. The former means the scattered values for discontinuity orientations and geometries such as discontinuity length and persistence; the latter means the variability of the geomechanical parameters of the rock mass as well as the discontinuous joints. Most probabilistic studies are focused on the geometric uncertainties based on the stochastic fracture network models (Dershowitz, 1988; Young, 1993; Meyer, 2002). Some researchers also try to deal with the second source of uncertainties in rock slope engineering by some classical probabilistic analysis methods. For example, Low (2007) has implemented First Order Reliability method and Monte Carlo Simulation to study the reliability of a rock slope in Hong Kong.

Besides probabilistic analysis methods, there are also non-probabilistic analysis methods to deal with the uncertainty in geotechnical engineering, such as Interval Analysis, Fuzzy Approach, Imprecise Probability Method based on p-box representation and Random Set Method. All of these methods are regarded as imprecise analysis methods.

In this study, by coupling Random Set Theory (RS) and Distinct Element Method (DEM), the Random Set Distinct Element Method (RS-DEM) has been developed and applied in the reliability analysis of a rock slope in China considering the uncertainty of rock material property. The safety factor of rock slope is assessed by Strength Reduction Method in a comerical distinct element code UDEC.

7.2. Random Set Theory

Random Set Theory provides a general framework for dealing with set-based information and discrete probability distributions. It yields the same results as Interval Analysis when only range information is available and under certain conditions results are similar to Monte Carlo simulations (Peschl 2004).

Suppose a system response is $F=X_1\times\ldots\times X_p$, where $\times$ indicates Cartesian product, F is the system response results, $X_1,\ldots X_p$ are the influence parameters of the system response. Because of the uncertainties, the influence parameters are not a single value, but a set with every possible value. Therefore, F is also a set impacted by the variation of parameters X.

Because of the imprecision, the set X is also composed by many subsets $A=\{A_j, j=1,\ldots, M\}$ which are called focal elements, and $m(A_j)$ is the basic probability assignment of A_j. So that $m(\Phi)=0$ and

$$\sum_j^M m(A_j) = 1 \qquad (7.1)$$

For example, in geotechnical engineering, each set A is the interval of one parameter values measured for one sample, and $m(A)$ is the frequency of this kind of sample occurring in all the samples. The parameter values measured from all samples compose the set X. Alternatively, the sets A_j could be ranges of a variable obtained from another source with relative credibility $m(A_j)$.

In probabilistic analysis method, all of the possible values of an input parameter conform to a certain probability distribution. While in Random Set approach, the parameters are composed of several intervals shown in Fig. 7.1 as an example. Only lower and upper limits of these intervals are considered as input variables in the deterministic model.
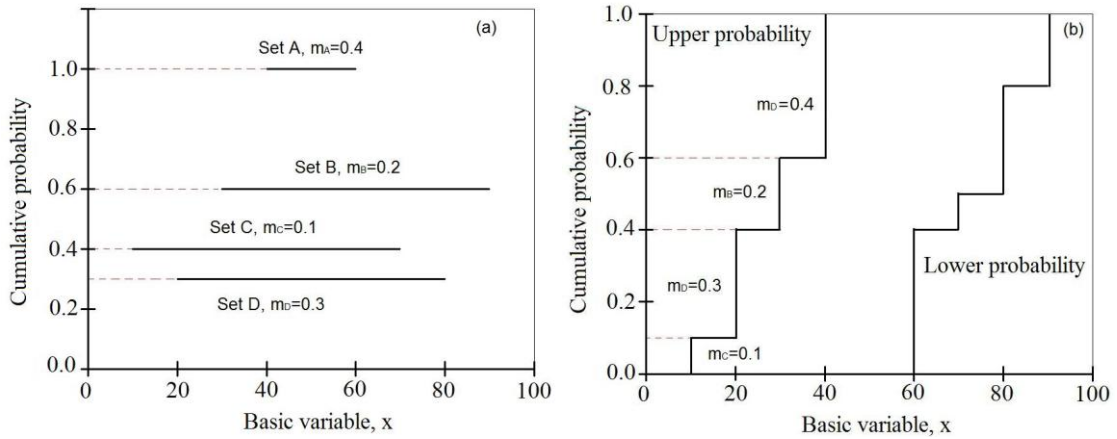
Fig. 7.1 Types of random set visualization: a) random interval b) p-box (after Nasekhian, 2011)

If $A_{1i},\ldots, A_{1j}$ are random sets on X_1 and $X_1,\ldots, X_p$ are stochastically independent, then the joint basic probability assignment is given by

$$m\left(A_{1i} \times \ldots \times A_{pj}\right) = m(A_{1i}) \times \ldots \times m(A_{pj}) \qquad (7.2)$$

In this chapter, Random Set Theory will be applied with Distinct Element Method in rock slope stability analysis.

7.3. Distinct Element Method in rock slope stability analysis

There are many discontinuous faces with different structure, and strength properties, like bedding plane, joint, fissure, soft and weak layer and fault in rock material. They induce great deal of difficulties in the rock slope stability analysis. Based on the situation of cementation and fill, the discontinuity joints can be divided into hard joints (no filled) and soft joints (filled). And according to the transfixion situation, the structure face can be divided into transfixion, half transfixion and non transfixion. In a low tectonic stress, the strength of rock is mainly controlled by the strength property of these discontinuous joints. Therefore, it is not reliable to apply the conventional soil slope stability analysis methods in rock slope directly.

For establishing the reasonable rock mechanical behavior model many numerical methods have been developed. All of these numerical methods can be divided into three groups: continuum modeling (e.g. finite element, finite difference), discontinuum modeling (e.g. distinct element, discrete element) and hybrid/coupled modeling. Stead et al. (2001) has reviewed these numerical techniques used in the rock slope stability analysis, including advances in computer visualization and the use of continuum and discontinuum numerical modeling codes.

Compared with the conventional rock slope stability analysis methods (e.g. Block Theory (Fu, 2000), limit equilibrium methods, rockfall simulation), the advantage of above numerical techniques are: the material deformation and failure are allowed, and complex behavior and mechanisms can be modeled; the effects of groundwater and pore pressures, dynamic events can be considered; block deformation and movement of blocks relative to each other are allowed. The limitation of numerical techniques is that, the users must be well trained and have extensive experience in programming and modeling. To overcome this limitation, many user-friendly slope stability numerical codes have been developed. In 1980's the ITASCA Company developed the Universal Distinct Element Code UDEC (Itasca, 2000), and has since been improved continually accordingly with the development of rock mechanics and computer.

Because of the complexity of the rock structure, it is impossible to exactly reflect the property of structure face and to conduct precise calculation. Therefore, for real slope engineering, generally only representative joints which have dominant influence on the slope stability are elected, according to the length, density, transfixion and orientation of the

structure faces. While for the rock cut by the joints with high density and diverse orientations, researchers always use an equivalent continuous medium to simulate it.

UDEC can employ several joint models which are used extensively, like perfect Elastic-Plasticity Model, Continuous Yield Model, Barton-Bandis Model and so on. The Strength Reduction Method applied in this chapter is based on Mohr-Coulomb model. The general shear yield, opening and the dilatancy of the joints all can be realized in this model.

The strength parameters c, and φ of deformable blocks and the joint faces both are reduced until the slope fails, and the last reduction coefficient at failure is the safety factor. In the process of calculation, when the ratio of the largest unbalanced force and the system load is greater than a tolerance value, the slope is considered in a non equilibrium situation and vice versa otherwise. For this study, the tolerance value is chosen as 10^{-4}. The location and shape of the slip surface can be determined by the plots of displacement vectors or shear strain increment contours.

UDEC is particularly well suited to problems involving jointed media and has been used extensively in the investigation of both landslides and surface mine slopes. Benko et al. (1998) used finite difference method (FLAC) and distinct element techniques (UDEC) to analysis the failure mechanism of the Frank Slide in 1903 on the east face of Turtle Mountain, southwestern Alberta, Canada. Eberhardt et al. (2004) applied UDEC to investigate the underlying mechanisms contributing to the episodic nature of the rockslide. Lei et al. (2006) have studied the feasibility of UDEC Strength Reduction Method in jointed rock slopes.

7.4. Procedure of the RS-DEM in rock slope stability analysis

On the occasion of the 35th Rankine Lecture, Goodman (1960) pointed out: "Charged with responsibility for design, an engineer hopes to have available tools appropriate to the applicable materials and conditions. When the materials are natural rock, the only thing known with certainty is that this material will never be known with certainty".

For example, Sakurai and Shimizu referred to this problem (1978): "Compared with materials such as steel and concrete, the determination of a probability density function for the mechanical constants of rock masses is extremely difficult. In other words, there is no reliable way to determine the input data for the probabilistic approach. This means that the probabilistic approach may be less applicable to practical engineering problems."

In rock slope engineering, because the discontinuous joints are involved, therefore, there are more influential parameters and the geometry is more complicated than a soil slope. The parameters are mostly obtained from the laboratory and in-situ investigations, and expert experience. Therefore, most of the parameters cannot be determined very accurately, and only a proximate interval is available. In this situation, it is senseless to conduct the deterministic analysis or probabilistic analysis. In this chapter, by combining the non-probabilistic analysis method random set theory with the distinct element method, the Random Set Distinct Element Method (RS-DEM) has been developed. The procedure of RS-DEM is shown in Fig. 7.2.
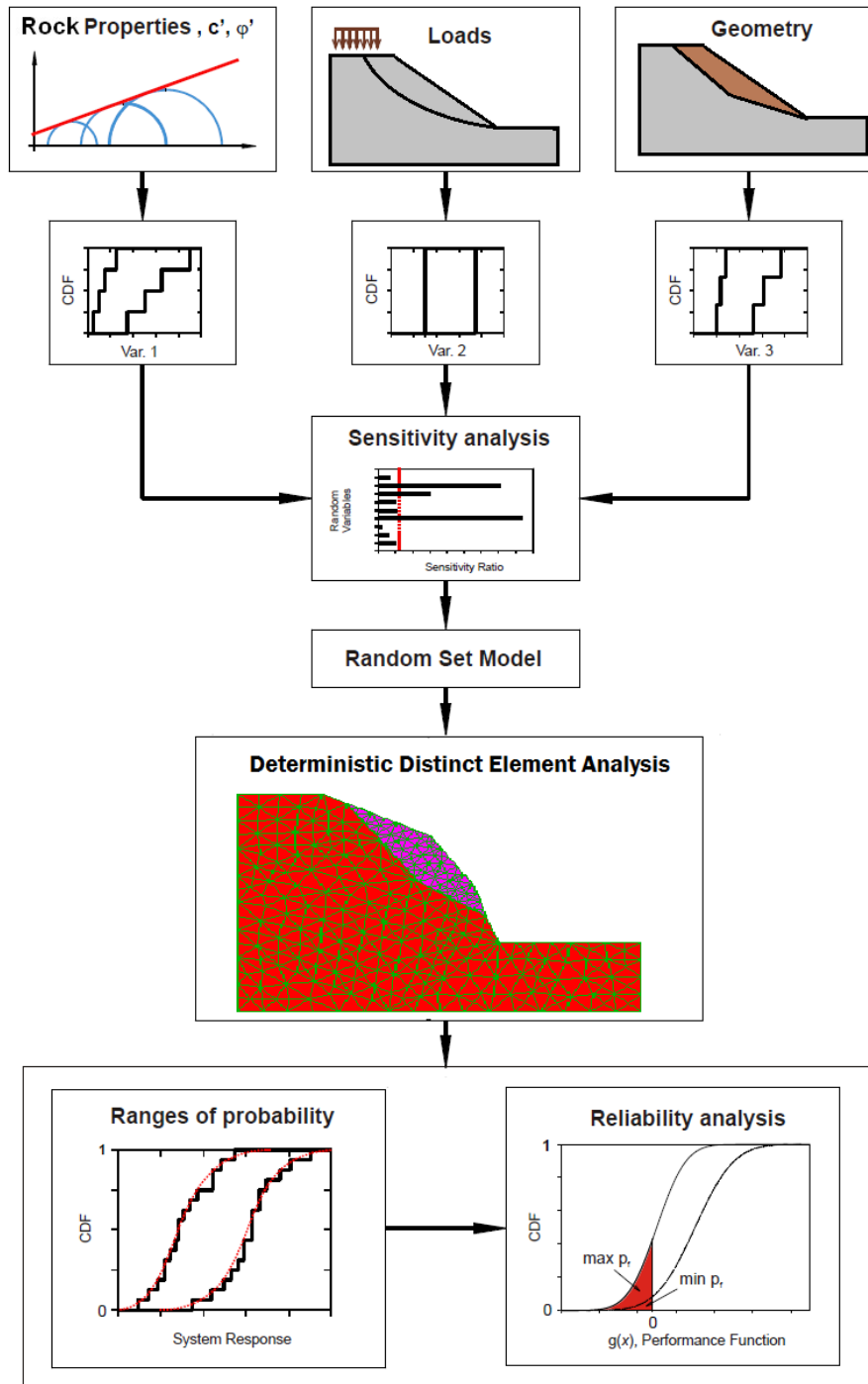
Fig. 7.2 RS-DEM procedure (modified from Peschl, 2004)

7.5. Application of RS-DEM to rock slope stability analysis

7.5.1 Slope overview

In this part, a real case study is conducted to demonstrate the feasibility and efficiency of RS-DEM in the rock slope stability analysis.

The slope is located in north of Zagunao town, Sichuan Province. It is an active rock collapse slope. After years' of weathering, denudnation and falling, the collapsed sediments have accumulated at the top of the fence of the residents' houses located at the foot of the slope. Especially in 2008 the Wenchuan Earthquake and its aftershocks loosened the rock block, and induced local collapse and falling resulting in three new collapse sediments. The falling rocks bashed the masonry fence with a length of 7.7 m, broke 3 telegraph poles (in Fig. 7.3) and made holes in the building wall; luckily no one was hurt. The collapse sediments are composed of gravel and rock blocks having a depth of 0.5-2.5 m. The diameter of collapsed rock is 10-40 cm; the biggest one reached to 0.8 m.

The full view of the slope is shown in Fig. 7.4. The slope has shape of a triangle. The maximum length of the slope is 330 m, and the height varies from 99 to 425 m. The total area of this slope is about 77,900 m^2. The orientation of the potential collapse is 255-265° N. Based on the in-site investigations, one of the potential dangerous areas has been selected as case study for detail analysis.

Fig. 7.3 Destroyed fence and telegraph poles

According to the field observation, the area of the potential dangerous zone is about 17.15 m^2 (3.5×4.9 m), and the average depth is 3.6 m. The volume of potential rockfall is about 61.74 m^3. The top elevation is 1969 m. The rock blocks in this zone are strongly weathered, and the rock is cracked by many joints and fissures. The bedding plane dips parallel to the surface of the slope, and some fissures cut the rock into blocks. The experts assessed that this rock zone has a low stability, and may slide along the bedding plane.

Fig. 7.4 Full view of the slope

7.5.2 Input geomechnical parameters

In rock slope models, there are many input parameters which can influence the safety factor, for example, the rock density, strength of the rock material as well as the joints strength, among these parameters, 5 most important parameters have been chosen as basic variables. They are density of rock (γ), normal stiffness (kn), shear stiffness (ks) of the joints, joint friction angle ($j\varphi$) and joint cohesion (jc). If necessary, other more parameters can be considered in this step, and the parameters with little influence on slope stability can be eliminated after the sensitivity analysis in the next section.

The random sets of basic variables can be collected from different sources, like geotechnical tests, expert experience, similar projects, and published literature. These are in the form of ranges, and at least two sets are needed in order to build the probability distributions. In this case, the ranges of basic variables are obtained from two sources, first from the geotechnical tests including laboratory test and in-situ tests, and second from the expert experience which accumulated from the previous and similar investigations in this area after the earthquake. The basic values are presented in Table 7.1. The probability assignments of both sources are

considered to be 0.5, so there is no preference and both sources have the same reliability. In Table 7.1, the reference values are the values adopted for the previous deterministic analysis. These are the mean value of the upper and lower limits of two sets.

Table 7.1 Basic variables of rock slope

Set No.	Probability assignment	γ (kN/m^3)	kn (GPa/m)	ks (GPa/m)	$j\varphi$ (°)	jc (MPa)
1	0.5	20-24	9-12	4-6	18-22	35-65
2	0.5	22-26	10-13	5-9	20-24	40-70
reference value		23	11	6	21	47.5

The basic variables are illustrated in Fig. 7.5~7.9 in the forms of p-box.
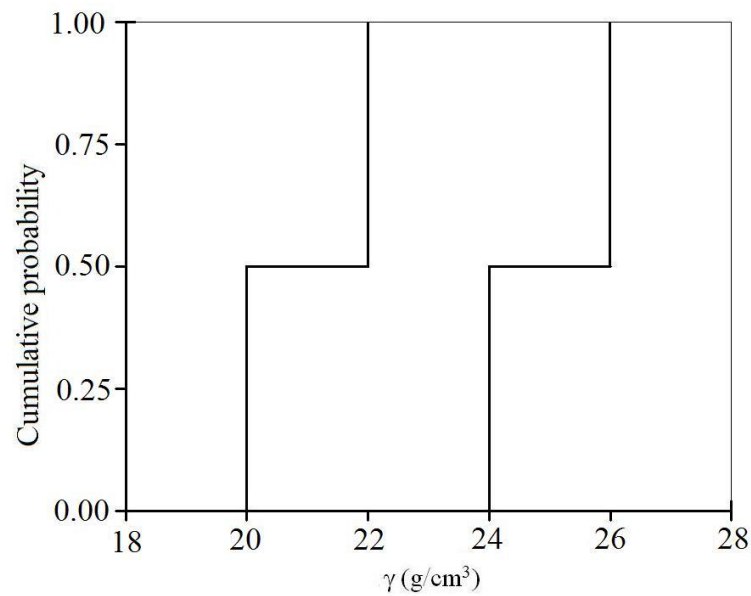
Fig. 7.5 Random sets of rock density
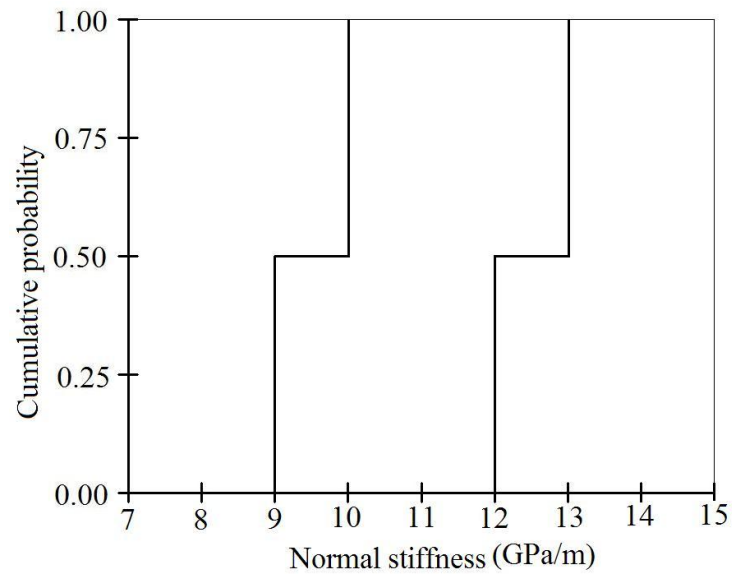
Fig. 7.6 Random sets of normal stiffness of joints
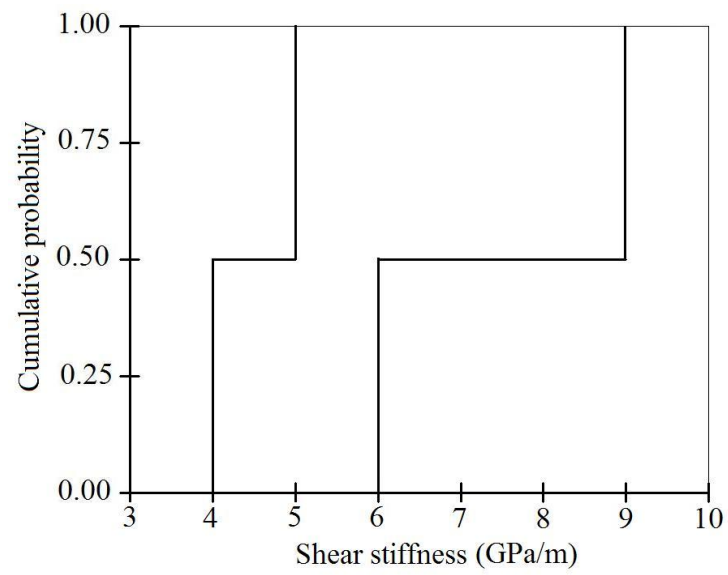
Fig. 7.7 Random sets of shear stiffness
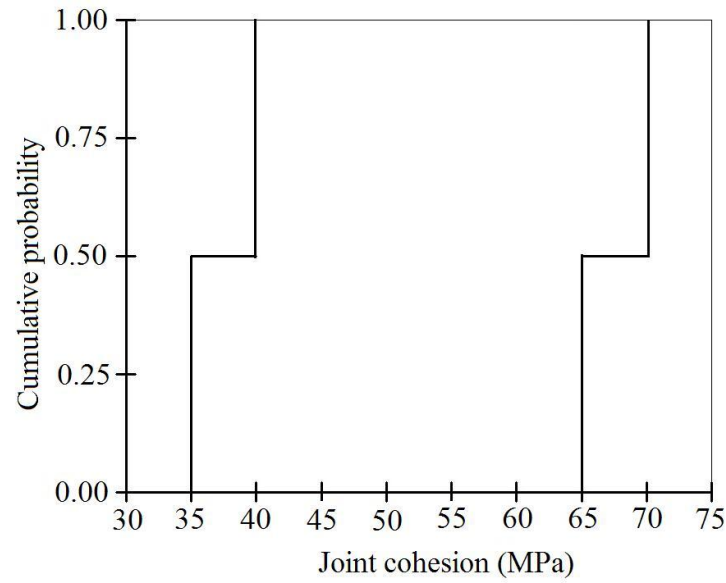
Fig. 7.8 Random sets of cohesion of joints
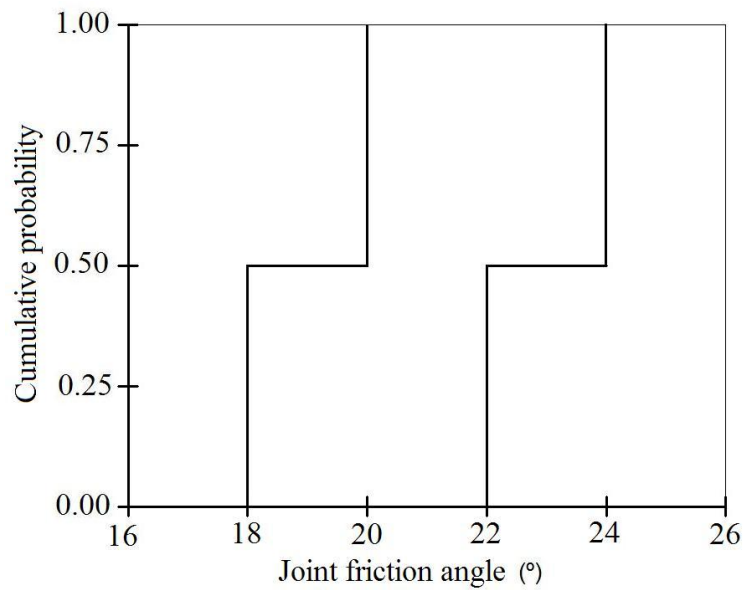
Fig. 7.9 Random sets of friction angle of joints

For UDEC, the rock blocks can be considered as rigid or deformable. In this case, the Mohr Coulomb model is applied for deformable rock blocks. The rock block has significantly higher strength than the joints, and the fluctuation of these parameters has almost no influence on the slope stability. Hence the strength parameters of rock, which are necessary input parameters for UDEC code running, are considered as single values, as shown in Table 7.2.

Bulk (Pa)	Shear (Pa)	Friction angle (ͦ)	Cohesion (Pa)	Tension (Pa)
1.5e9	6.25e8	39	1.2e6	1.5e7

Table 7.2 Parameters input in DEM model as single values

7.5.3 Deterministic analysis of rock slope based on the DEM

The Strength Reduction Method is applied in this part to perform the rock slope deterministic analysis. The model has a length of 105 m and a height of 123 m (Fig. 7.10). Distinct element code UDEC treat the problem domain as an assemblage of distinct, interacting bodies or blocks, and the other part of the slope is considered as a large intact deformable block. A force-displacement law is applied to specify the interaction between deformable intact rock blocks. Joints are viewed as interfaces between the blocks, but they are treated as a special element with strength parameters rather than boundary conditions. Movement is allowed vertically on both lateral boundaries, while the constraint is imposed in both directions on the base boundary.
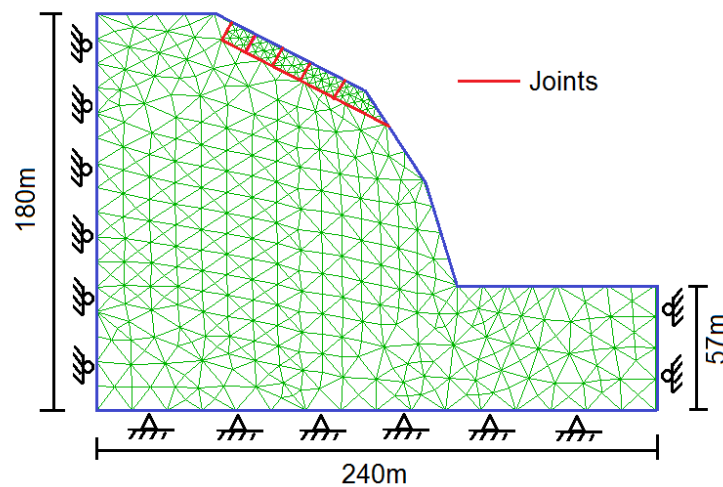
Fig. 7.10 Distinct element model of rock slope

The value of safety factor calculated by UDEC Strength Reduction Method is 1.15. Fig. 7.11 and 7.12 show the maximum shear strain rate contours and displacement vectors after the shear strength of rock blocks and discontinuity joints is reduced by a coefficient of 1.15. One can see that the slip face is located in the joint which is parallel to the surface of the slope. And the displacement concentrates in the rock blocks which are cut by joints.
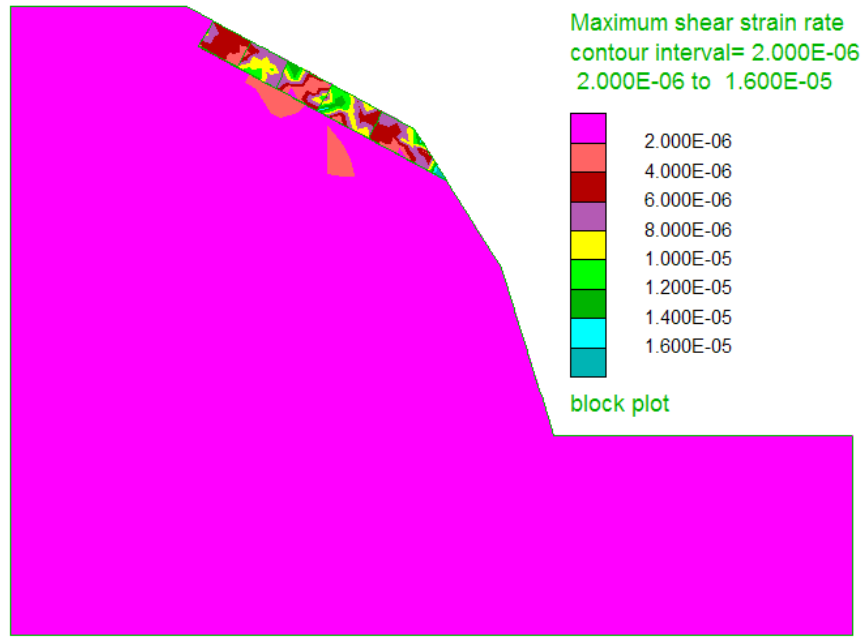
Fig. 7.11 Maximum shear strain rate contour after the shear strength reduced by coefficient of 1.15
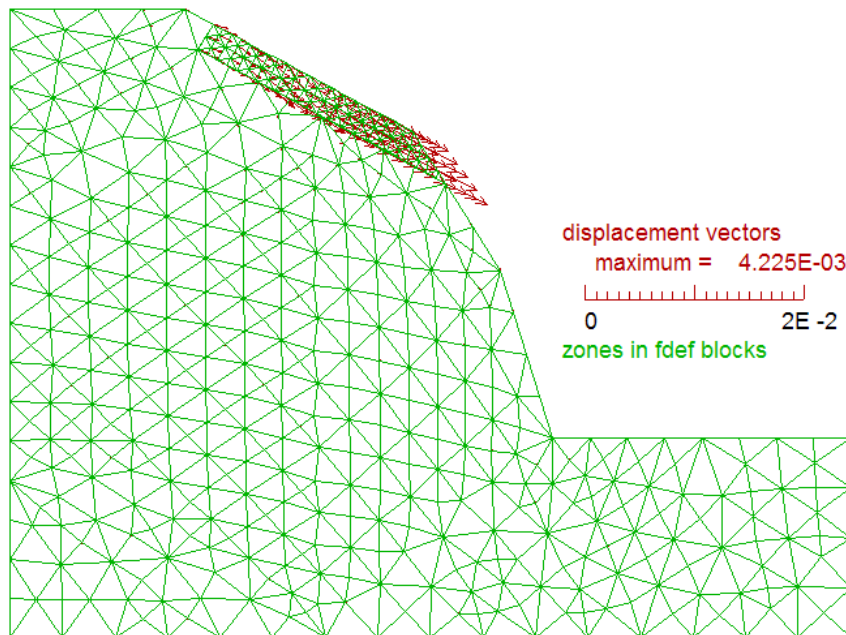
Fig. 7.12 Displacement vectors after the shear strength reduced by coefficient of 1.15

7.5.4 Sensitivity analysis

The sensitivity analysis is to identify the degree of influence of every input parameter on slope stability. The purpose of this step is to reduce the number of basic variables in RS-DEM analysis. The reduction of number of basic variables can increase the efficiency of RS-DEM

analysis significantly. For example, the slope reliability analysis with 4 basic variables and with two sets of each variable requires running deterministic distinct element analysis for 256 times, while this amount gets decreased to 81 times in case of 3 basic variables.

Here, a relatively simple sensitivity method is applied. This method was originally proposed by U.S. EPA: TRIM (1999) and extended by Peschl (2004) in order to make it compatible with the Random Set approach. In this method, there are basically three steps.

First, the change in model output per unit change of an input variable is calculated according to Eq. 7.3.

$$\eta_{SR} = \left| \frac{\left[\frac{f(x_{L,G}) - f(x_r)}{f(x_r)} \right]}{\left(\frac{x_{L,G} - x_r}{x_r} \right)} \right| \tag{7.3}$$

where, η_{SR} is called the sensitivity ratio of variable x, and it is independent of the units of the variable. In the process of random set analysis, each variable has four sensitivity ratios over both a small and a large amount of change in input variables which are called local and global intervals respectively (Fig. 7.13). Therefore, $x_{L,G}$ means the upper or lower limits of the local and global intervals of variable x. x_r is the reference value.

The results of this step can also be used to assess the monotonicity of the system response, which can help to reduce the number of combination of basic variables in following reliability analysis procedure.

Second, the error of the sensitivity ratio is reduced because of different intervals of variables using Eq. 7.4.

$$\eta_{SS} = \left(\eta_{SR}, x_L^{lo} + \eta_{SR}, x_L^{up} + \eta_{SR}, x_G^{lo} + \eta_{SR}, x_G^{up} \right) \cdot \left(\frac{x_G^{up} - x_G^{up}}{x_r} \right) \tag{7.4}$$

where η_{SS} is the sensitivity score of variable x.

At last, after the calculation of the sensitivity score of every variable, the relative sensitivity α of every variable is obtained as follows:

$$\alpha(x_i) = \frac{\eta_{SS,i}}{\sum_i^n \eta_{SS,i}} \tag{7.5}$$
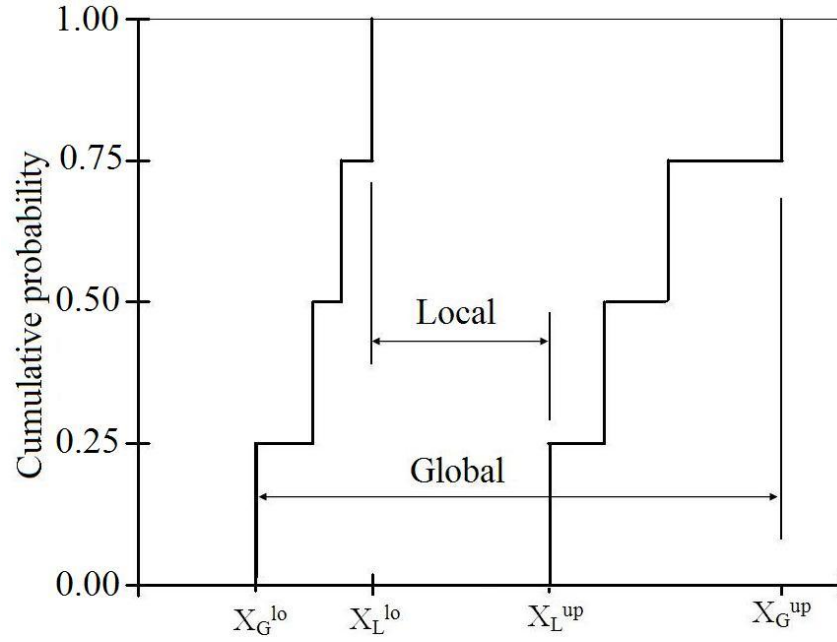
Fig. 7.13 Local and global intervals

Depending on the different performance function, the relative sensitivity of the same variable may be different. For instance, the relative sensitivity of joint cohesion on the safety factor of slope and the displacement may be different, which means it has a different degree of influence on the safety factor and displacement analyses. In this study, only the performance function of safety factor is taken into account.

The sensitivity analysis process described above is applied in the case study with 5 basic variables. A total number of $4 \times 5 + 1$ deterministic analyses are needed to accomplish the sensitivity analysis. In each deterministic analysis, lower or upper limit of the local and global interval of one variable is adopted, and other input parameters are keeping with reference value. The impact of each input parameters on safety factor is shown in Fig. 7.14 as a relative sensitivity.

A threshold value has to be introduced to determine which parameters have great impact on the safety factor. Usually a threshold value between 5 to 10 percent can be considered appropriate (Nasekhian 2011). Here, a threshold value of 8% was chosen. As depicted in Fig. 7.14 with the acceptance of the 8% threshold value, three parameters rock density γ, joint friction angle $j\varphi$ and joint cohesion jc were chosen as basic variables for the RS-DEM analysis. Experience shows that usually 3 to 4 basic variables are sufficient to obtain relatively smooth cumulative probability distribution functions of output variables.
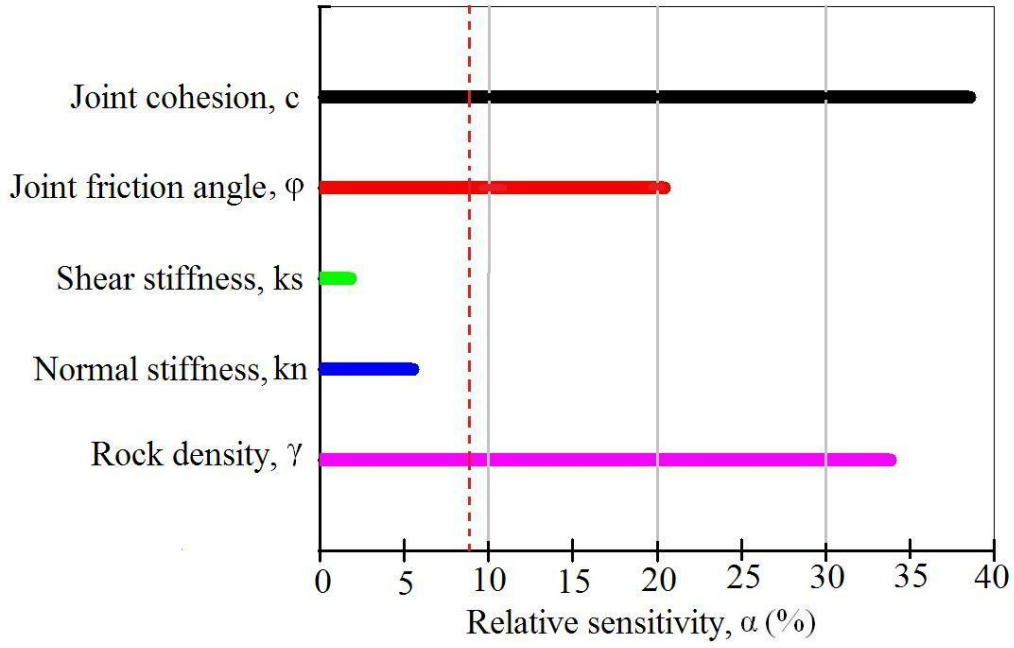
Fig. 7.14 Results of sensitivity analysis

7.5.5. Reliability analysis of rock slope by RS-DEM

After sensitivity analysis, the reliability analysis of rock slope can be conducted. Since the uncertainty of slope geometry has not been considered, the DEM model of the slope in Random Set approach is the same and the Mohr Coulomb criterion is adopted for the slope material. The three basic variables: rock density γ, joint cohesion jc and joint friction angle $j\varphi$, which are determined by sensitivity analysis in advance will be changed in every deterministic DEM analysis. For every basic variable, there are two random sets. Therefore, there are 8 different cases, which are given in the following vector:

$$\gamma \times jc \times j\varphi = \{(\gamma_1, jc_1, j\varphi_1)_1, (\gamma_2, jc_1, j\varphi_1)_2, (\gamma_1, jc_2, j\varphi_1)_3, \dots, (\gamma_2, jc_2, j\varphi_2)_8\} \quad (7.6)$$

here the index of parameters denotes the relevant set number and the index of pairs signifies one case of basic variables.

After that, the best (largest safety factor) and the worst (smallest safety factor) combinations of each case need to be calculated based on the input of upper and lower limits of each random set. For there are one upper and one lower limit of every random set, there are 8 possible combinations of each case. As an example, the deterministic input values of such analysis for the case of $(\gamma_1, jc_1, j\varphi_1)$ are presented in Table 7.3.

126

Table 7.3 Inputs variables of case 1 in the deterministic distinct element calculation

Var.	Prob.	Set No.	LLL*	LLU	LUL	ULL	LUU	ULU	UUL	UUU
γ†	0.5	1	20	20	20	24	20	24	24	24
jc	0.5	1	35	35	65	35	65	35	65	65
$j\varphi$	0.5	1	18	22	18	18	22	22	18	22
	Safety factor		1.15	1.19	1.41	0.96	1.49	1.12	1.25	1.34

† units: γ, g/cm^3; jc, MPa; $j\varphi$, degree.

 * L denotes the lower limit of a random set variable and U denotes the upper limit.

From Table 7.3, the best and the worst combinations are LUU and ULL, and the largest and smallest safety factors are 1.49 and 0.96 respectively. It means the rock density has a negative influence on the slope stability, the density is higher, the safety factor will be smaller; and the joint cohesion or the joint friction angle has a positive influence on the slope stability, the joint cohesion or friction angle is higher, the safety factor will be larger. These relations can also be improved by the monotonicity of system response. According to the results of the sensitivity analysis process, the influences of these three basic variables on the safety factor can be illustrated in Fig. 7.15~17.

Therefore, in every case, only two combinations, (1) lowest rock density and the highest joint cohesion and joint friction angle, and (2) highest rock density, and the lowest joint cohesion and joint friction angle are necessary to be realized in order to obtain the lower and upper limits of safety factor. This has reduced the computation effect significantly, and the total number of DEM runs has been decreased from 64 to 16.
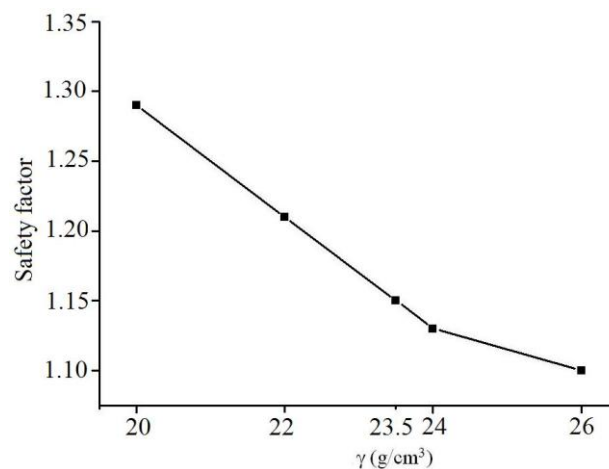
Fig. 7.15 Relation of safety factor and rock density
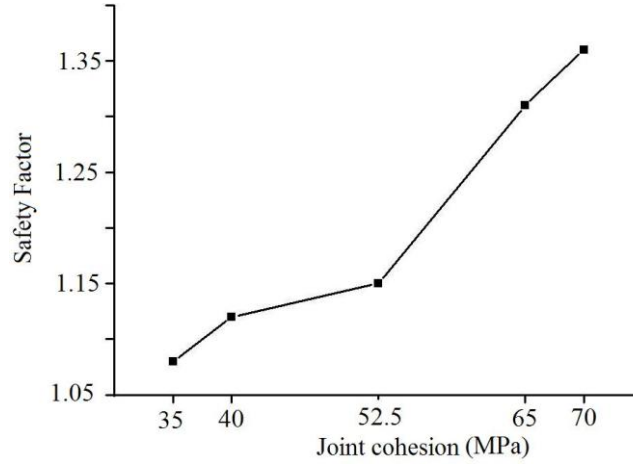
Fig. 7.16 Relation of safety factor and joint cohesion
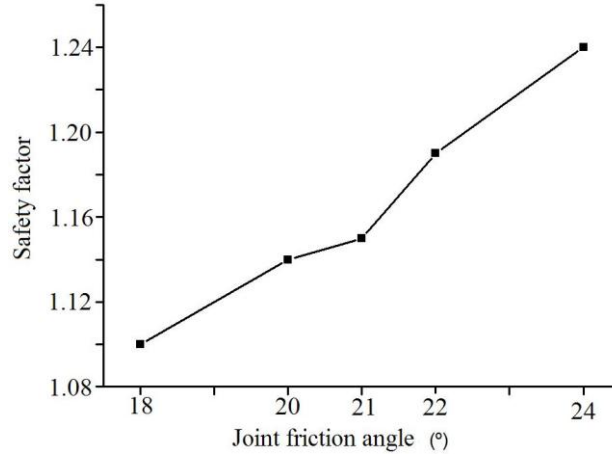
Fig. 7.17 Relation of safety factor and joint friction angle

The next step is to determine the probability of the assignment of each realization. In this case, the random variables are considered as independent from of one other; the joint probability of the response focal element obtained from the distinct element model is the product of the probability assignment m of input focal elements by each other. For the mass probability of each set equal to 0.5, the first realization can be obtained as follows:

$$m\big(f(\gamma_1, jc_1, j\varphi_1)\big) = m(\gamma_1) \cdot m(jc_1).m(j\varphi_1)$$

$$= 0.5 \times 0.5 \times 0.5$$

$$= 0.125 \tag{7.7}$$

The results of these 16 combinations are shown in Table 7.4.

Table 7.4 Results of 16 combinations and their probabilities

| No. | Cases | Probability | Safety factor | |
			Lower limit	Upper limit
1	$\gamma_1 \times jc_1 \times j\varphi_1$	0.125	0.96	1.43
2	$\gamma_2 \times jc_1 \times j\varphi_1$	0.125	0.93	1.37
3	$\gamma_1 \times jc_1 \times j\varphi_2$	0.125	1.01	1.51
4	$\gamma_1 \times jc_2 \times j\varphi_1$	0.125	1.00	1.48
5	$\gamma_2 \times jc_1 \times j\varphi_2$	0.125	0.97	1.44
6	$\gamma_2 \times jc_2 \times j\varphi_1$	0.125	0.97	1.43
7	$\gamma_1 \times jc_2 \times j\varphi_1$	0.125	1.00	1.48
8	$\gamma_2 \times jc_2 \times j\varphi_2$	0.125	1.00	1.49

At last, the random set results of safety factor can be constructed in the form of p-box as Fig. 7.18. Contrary to classical probability theory, the probability of failure computed by RS-DEM cannot be interpreted as a frequency of failure. The safety factor ranges with different credibility are presented in Fig. 7.18.

The practical purpose of the random set analysis of rock slope stability is to get the most likely safety factors. The most likely safety factor is the result which obtains most frequently when every possible parameters values input in the DEM model. For simplification, it is assumed that the most likely results are those values, whose measure of their belief degree are less than 50% and their corresponding plausible likelihood of occurrence are larger than 50% (Nasekhian, 2011) as shown in Fig. 7.18.

The mean value of the true system response obtained by random set bounds is within the following range given by Tonon et al. (2000a):

$$\mu = \left[\sum_i^n m_i \cdot inf(A_i) \, ; \sum_i^n m_i \cdot sup(A_i) \right] \tag{7.8}$$

where inf(A) and sup(A) denote lower and upper limits of focal element A, respectively. There is a good conformity between the intervals obtained from both the most likely range definition and those calculated from Eq. 7.8, and have been presented in Table 7.5.
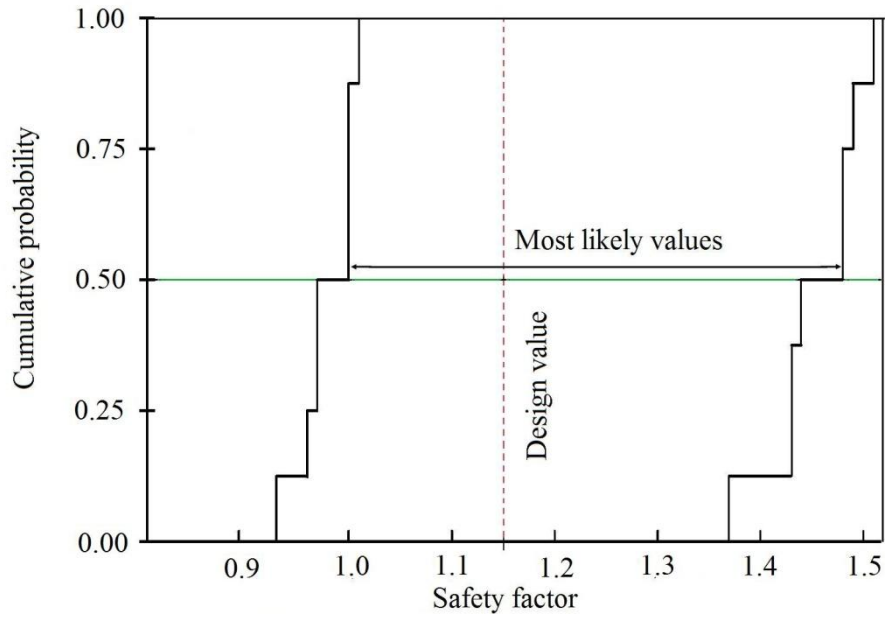
Fig. 7.18 Lower and upper bounds of safety factors of rock slope

Table 7.5 lower and upper mean values of true system response

	Interval of true mean values		Interval of most likely values	
	lower	upper	lower	upper
Safety factor	0.98	1.45	1.00	1.48

7.6 Conclusion

In this chapter, the RS-DEM analysis was applied to a real rock slope in China. Based on the previous researches, the rock slope stability is impacted by the strength of the discontinuity joints. Therefore, in this study, the discontinuous joints geomechanical parameters as well as rock block geomechanical parameters were considered in the distinct element model, and their influences on the results were assessed by the sensitivity analysis. After that, the basic variables which have the highest influence on the slope stability for the RS-DEM analysis were chosen. The RS-DEM results for the slope safety factor were presented in the form of lower and upper probability bounds.

From this study, we can see that RS-DEM is one of the most suitable methods to deal with the uncertainty in the rock slope stability analysis, considering the complexity of rock material and the difficulty of the geomechanical parameters determination.

8. Conclusions and Further Research

Introduction

The aim of this research was to give a further contribution to the application of well known non-deterministic methods with numerical simulation to the study of the reliability of slope, showing that a non-deterministic analysis does not require considerably more effort than that needed in a conventional deterministic study, but it provides a very useful mean of modeling uncertainties involved in the calculations.

In the next section the most important conclusions of the present thesis are given, followed by some recommendations for further research.

8.1 Conclusions with respect to the numerical modeling based on GIS

Strength Reduction Method is a kind of efficient numerical simulation method which always applied in finite element code or finite difference code. Compared with the conventional limit equilibrium methods, it is more competent for slope stability analysis. It not only can give the safety factor, but can also simulate the failure progress of slope considering the constitutive relationship of slope material. However, construction of models is always a complicated and time consuming work in numerical simulation. In chapter 4, for improving the method of numerical modeling, the excellent spatial function of GIS technique was adopted. The GIS data of the slope topography was transformed into ASCII data, and some programs were written to transform the GIS data into FLAC by means of FISH programming language. At last, both 2D and 3D slope models are constructed and their slope stability analyses are conducted. The case study has approved that the using of GIS can make the numerical modeling easier and more precise. Compared with the simulation results, one can see that the location and distribution of the failure zone by 2D and 3D are matched very well. However, the safety factor from 2D is a little conservative as compared to 3D, because the horizontal restrict in the vertical direction of the plane is ignored in 2D.

8.2 Conclusions with respect to the slope probabilistic analysis methods

In chapter 5, well-known probabilistic methods combined with Strength Reduction Method were applied to the study of two examples, one is a homogeneous slope, and the other is a non-homogeneous slope, considering different probability density functions and correlation coefficients between the soil parameters.

It has been shown that the Monte Carlo Simulation requires only fundamental knowledge of statistics and of probability theory to solve the slope stability problem. It is generally considered as the most accurate and reliable probabilistic method. Furthermore, the example proved that combination of MCS and Strength Reduction Method is more accurate than the combination of MCS and limit equilibrium methods, because Strength Reduction Method is more rigorous than the limit equilibrium methods and its results are more reasonable. The example also expounded that the probability distribution of safety factor is dependent on the distribution of input soil parameters, which will be the practical evidence of the assumption of probability density function of safety factor in the following studies.

However, MCS is the most time consuming method, and the Strength Reduction Method also need much time for iteration to get the safety factor. For solving this problem, the author developed a simplified MCS-RSM. This method omits the iteration process which is used to calculate the safety factor in strength reduction technique, but only judges the slope stability in every simulation to get the probability of slope failure, and calculates the mean safety factor by means of soil properties. After that, based on the probability statistics theory, the variance of safety factor and reliability of slope stability can be achieved. This treatment saves about 4/5 of time of traditional MCS-RSM, and retain almost the same accuracy. This development supplies a practical way to apply MCS in rigorous numerical simulation without reducing the accuracy.

The moment's method First Order Reliability Method was chosen as an alternative approach to replace the Monte Carlo Simulation, because it involved a limited amount of calculations. FORM uses Taylor's series expansion to estimate the local uncertainty of the factor of safety at a selected expansion point, and the closed form solution of the partial derivatives is used to calculate the mean and standard deviation of the performance function. For lack of explicit performance function in Strength Reduction Method, the derivative expressions is replaced with equivalent difference quotients to solve the differential quotients approximately. The accuracy of FORM is lower than MCS, because it does not provide the shape of the probability density function and the skewness coefficient of the performance function. The probability of failure by normal distributed random variables from FORM is a little smaller than MCS, but the probability of failure by log normal distributed random variables is a little greater.

It has been highlighted that the Point Estimate Method decreases the computational effort of

the probabilistic analysis of slope stability significantly. On one hand, the PEM did not involve the evaluation of partial derivatives of the safety factor formula, thus being more straightforward applied than FORM. On the other hand, when both soil cohesion and friction angle were considered as input variables, at least thousands of Monte Carlo simulations were necessary to get accurate statistical values of the slope stability, while only four calculations were required by the PEM to get results as accurate and reliable as those of the Monte Carlo method in terms of mean value and standard deviation.

In last decades, the PEM is finding increasing application in practical problems. However, there are many limits for its application in some conditions, like the correlation between soil properties are considered. In this study, the formula proposed by Christian et al. (1999) was adopted. Unfortunately this formula is valid only for symmetrical input variables. Thus one should normalize the unsymmetrical input variables first. All of these approximations decrease the accuracy of results.

Another important finding in this chapter refers to the correlation between the soil parameters cohesion and friction angle. Many researchers discovered negative correlation between cohesion and friction angle on the basis of experimental data. However, most literatures have often neglected this correlation for simplifying the calculations. In this study, different correlations between cohesion and friction angle was taken into account for the probabilistic analysis of the slope stability. By increasing the correlation coefficient of cohesion and friction angle from -1.0 to 0.0, the failure probability of slope increased about 13%.

At last, the probabilistic analysis of a two-layered slope with four input random variables has been studied. The results showed that the probability of failure by PEM is closer to MCS than FORM.

8.3 Conclusions with respect to the spatial variability

Spatial variability is one of the most important factors influencing the property of soil. Since Vanmarke leaded the random field model in the geotechnical engineering in 1977, spatial variability of soil properties has received more and more attention in the literature. However, all of the studies were only focused on the stationary random field, i.e. the mean of soil property is the same everywhere of the soil deposit. But most of the time, because of the earth stress and self weight, the property of sediment varies in depth, which is called non-stationary random field.

In this study, the author reviewed the random field modeling and local averaging technique in slope stability analysis, and applied them in numerical simulation. Furthermore, an example about a slope with random field of cohesion was studied. In this case, both stationary random field and non-stationary random field were investigated, and the probabilistic analysis of slope stability was carried out by using Monte Carlo Simulation. From the comparison study of probabilistic analysis about different correlation length of cohesion, we found that the influence of spatial variation on probability of failure is very strong. Based on the same average domain T, the probability of failure increased from about 1% to 70% as the correlation length of cohesion increased from 0.1 m to 10 m. after that, the same slope geometry with both cohesion and friction angle considered as random field was studied.

8.4 Conclusions with respect of RS-DEM

In this study, combing with the random set theory and the distinct element method, the non deterministic slope stability analysis method RS-DEM has been developed, and it has been applied in a rock slope from China.

It was illustrated that the RS-DEM is very practical to deal with the uncertainty in rock slope stability analysis. Based on the imprecise probabilities concepts, it can predict the system response within a range in the form of a p-box. RS-DEM provides user-friendly framework that can apply the advanced constitutive models available in DEM programs. The rock blocks and discontinuity joints can be simulated appropriately.

The relatively smooth bounds on the system responses were obtained after small number of simulations. In this case with 3 basic variables, after the monotonicity analysis, only 16 realizations were needed. The application of RS-DEM requires much less computational effort as compared to fully probabilistic methods like Monte Carlo Simulation.

8.5 Recommendations for further research

Many issues could be recommended, based on the outcomes of this research, and considering the stage of development of slope stability analysis research. In this section, a number of the main recommendations are presented.

As extend of this thesis, the non-deterministic slope stability analysis methods developed in this study should be applied in more real landslides to test their feasibility and efficiency. The non-deterministic analysis can be used not only in the natural soil or rock slopes, but also in the manmade slopes which has been reinforced by geotextile or vegetable (Wu,

2007, 2011). This process can make the slope design more reasonable and economic.

More research is needed in the area of application of geography information system (GIS) in slope stability analysis. GIS is very powerful in spatial analysis as explained in Chapter 4, so it should be applied in geohazard prediction and protection more extensively, from single slope stability analysis to landslide risk analysis for a region; from the slope deterministic analysis to the slope non-deterministic analysis. For example, by coupling limit equilibrium analysis and Monte Carlo analysis with GIS, Shou et al. in 2005 have tried to implement a method that can evaluate the risk (corresponding to probability of failure) of landslide with consideration of spatial uncertainties in Li-shan landslide in Central Taiwan.

The analysis of complex landslides, no matter the deterministic or non deterministic analysis, can be carried out using various user-friendly numerical codes on desktop computers. If the benefit of these methods is to be maximized then the advanced and more comprehensive field data collection techniques are very important. There is little change for most of current data collection methodology which is aimed towards limit equilibrium analysis. Data including slope mass, discontinuities and groundwater should be collected enough to describe the whole slope mechanisms. Anyway, if there is no adequate and reliable input data, any rigorous analysis model (like random field method) is just a numerical game. Therefore, it is necessary to improve some efficient and cheap lab and in-situ test methods. And the uncertainty levels of input variables or inter-dependency of the variables need to be further studied, which are essential issues for further development of the probabilistic analysis model (Shou, 2005).

Furthermore, other control factors, such as earthquake (Shou, 2001), heavy rain (Baum, 2003; Borja, 2011), and time effect are also important for practical risk estimation of a landslide. In future studies, the uncertainties of seismic loads or rainfall can be considered in slope probabilistic analysis model based on numerical simulation,

At last, the probabilistic analysis can not only be carried out in the slope stability analysis, but also in the whole landslide risk assessment, while vulnerability can be conveniently expressed as a conditional probability (Einstein, 2001). For example, a rock block crossing a road and hitting a car, it can be determined with straightforward models including block dynamics, traffic density, average traffic speed, road geometry, all the input parameters should not be single numbers, but some ranges.

As emphasized by the observation of Chen (2000), "In the early days, slope failure was always written off as an act of God. Today, attorneys can always find someone to blame and someone to pay for the damage - especially when the damage involves loss of life or property". Therefore, any uncertainty in slope stability analysis is deserved to be considered by all relevant available slope analysis techniques.

Appendix: Programs by FLAC

A1. Program of Strength Reduction Method of slope stability by FISH in FLAC

```
def calfos
; --- define the possible range of safety factor ---
fs=1.0
loop while fs<1.4
fs=fs+0.1
; --- calculate the safety factor of the slope with a friction of 0.675 and a cohesion of 20 kPa
---
refric=atan(0.675/fs)*180/3.14
recoh=20000/fs
    command
        ini sxx 0.0 syy 0.0
        ini xvel 0.0 yvel 0.0
        ini xdis 0.0 ydis 0.0
        pro fric refric cohesion recoh range group soil
        solve step 5000
        hist unblance
        hist fs
    end_command
aa=mec_ratio
    ; --- print results ---
    command
        print aa
        print fs
    endcommand
end_loop
end
```

A2. Program of Strength Reduction Method of slope stability by FISH in FLAC3D

```
def calfos
; --- define the possible range of safety factor ---
fs=1.0
```

```
loop while fs<1.4
fs=fs+0.1
; --- calculate the safety factor of the slope with a friction of 0.675 and a cohesion of 20 kPa
---
refric=atan(0.675/fs)*180/3.14
recoh=20000/fs
  command
     ini sxx 0.0 syy 0.0 szz=0.0
     ini xvel 0.0 yvel 0.0 zvel 0.0
     ini xdis 0.0 ydis 0.0 zdis 0.0
     pro fric refric cohesion recoh range group soil
     solve step 5000
     hist unblance
     hist fs
  end_command
aa=mec_ratio
; --- print results ---
  command
     print aa
     print fs
  endcommand
end_loop
end
```

A3. Monte Carlo Simulation considering normal distributed random variables

```
Config
; --- build slope model ---
grid 30,30
gen (0.0,0.0) (0.0,20.0) (20.0,20.0) (20.0,0.0) i 1 9 j 1 11
gen (20.0,0.0) (20.0,20.0) (90.0,20.0) (90.0,0.0) i 9 31 j 1 11
gen (20.0,20.0) (60.0,50.0) (90.0,50.0) (90.0,20.0) i 9 31 j 11 31
model mohr i=1,8 j=1,10
model mohr i=9,30 j=1,10
model mohr i=9,30 j=11,30
```

```
prop density 1950 bulk 1.8e9 shear 1.2e9
set gravity 10
fix x i 1
fix x i 31
fix x y j 1
; --- define initial soil parameters ---
def parm_mech
     u_c=20000; --- mean of cohesion ---
     a_c=5000; --- variance of cohesion ---
     u_f=25.0; --- mean of friction angle ---
     a_f=5.0; --- variance of friction angle ---
end
parm_mech
def monte
  ; --- generate normal distributed random variables ---
  array norm(2,1000)
  loop ii(1,1000)
     a1=urand
     b1=urand
     c1=sqrt((-2)*ln(a1))*cos(2*3.14*b1)
     d1=sqrt((-2)*ln(a1))*sin(2*3.14*b1)
     norm(1,ii)=abs(c1*a_c+u_c)
     norm(2,ii)=min(abs(d1*a_f+u_f),89)
  end_loop
  ; --- input generated random variables ---
  loop nn(1,1000)
     c_c=norm(1,nn)
     f_f=norm(2,nn)
     command
        ini sxx 0.0 syy 0.0 sxy 0.0
        ini xvel 0.0 yvel 0.0
        ini xdis 0.0 ydis 0.0
        prop friction f_f cohesion c_c notnull
        set sratio=1e-3
```

```
      solve step 5000
    end_command
  aa=mech_ratio
 ; --- calculate probability of failure ---
  command
    print aa
  endcommand
   if aa>1e-3 then
   fs=fs+1
   end_if
   command
      print fs
   endcommand
  end_loop
pf=fs/1000.0
; --- print result ---
command
print pf
endcommand
end
monte
```

A4. Monte Carlo Simulation considering log normal distributed random variables

```
config
; --- build slope model ---
grid 43,34
gen (0.0,0.0) (0.0,20.0) (20.0,20.0) (20.0,0.0) i 1 9 j 1 14
gen (20.0,0.0) (20.0,20.0) (90.0,20.0) (90.0,0.0) i 9 44 j 1 14
gen (20.0,20.0) (60.000004,50.0) (90.0,50.0) (90.0,20.0) i 9 44 j 14 35
model mohr i=1,8 j=1,10
model mohr i=9,30 j=1,10
model mohr i=9,30 j=11,30
prop density 1950 bulk 1.8e9 shear 1.2e9
set gravity 10
```

```
fix x i 1
fix x i 44
fix x y j 1
; --- define initial soil parameters ---
def parm_mech
    u_c=20000.0; --- mean of cohesion ---
    a_c=5000.0; --- variance of cohesion ---
    aln_c=sqrt(ln(1+(a_c/u_c)^2));
    uln_c=ln(u_c)-(aln_c^2)/2;
    u_f=25.0; ---mean of friction angle ---
    a_f=5.0; ---variance of friction angle ---
    aln_f=sqrt(ln(1+(a_f/u_f)^2));
    uln_f=ln(u_f)-(aln_f^2)/2;
  end
  parm_mech
  def monte
    ; ---generate random variables---
    array norm(2,1000)
loop ii(1,1000)
    ; --- generate standard normal distributed random variables ---
    a1=urand
    b1=urand
    c1=sqrt((-2)*ln(a1))*cos(2*3.14*b1)
    d1=sqrt((-2)*ln(a1))*sin(2*3.14*b1)
    ; --- transfer to log normal distributed random variables ---
    norm(1,ii)=exp(c1*aln_c+uln_c)
    norm(2,ii)=exp(d1*aln_f+uln_f)
  end_loop
    ; --- input random variables ---
loop nn(1,1000)
      c_c=norm(1,nn)
      f_f=norm(2,nn)
      command
          ini sxx 0.0 syy 0.0 sxy 0.0
```

```
                    ini xvel 0.0 yvel 0.0
                    ini xdis 0.0 ydis 0.0
                    prop friction f_f cohesion c_c notnull
                    set sratio=1e-3
                    solve step 5000
            end_command
aa=mech_ratio
; --- calculate probability of failure ---
command
    print aa
    endcommand
if aa>1e-3 then
    fs=fs+1
end_if
    command
    print fs
    endcommand
    end_loop
pf=fs/1000.0
; --- print result ---
command
print pf
endcommand
end
monte
```

A5. Monte Carlo Simulation considering correlated random variables

```
config
; --- build slope model ---
grid 30,30
gen (0.0,0.0) (0.0,20.0) (20.0,20.0) (20.0,0.0) i 1 9 j 1 11
gen (20.0,0.0) (20.0,20.0) (90.0,20.0) (90.0,0.0) i 9 31 j 1 11
gen (20.0,20.0) (60.0,50.0) (90.0,50.0) (90.0,20.0) i 9 31 j 11 31
model mohr i=1,8 j=1,10
```

```
model mohr i=9,30 j=1,10
model mohr i=9,30 j=11,30
prop density 1950 bulk 1.8e9 shear 1.2e9
set gravity 10
fix x i 1
fix x i 31
fix x y j 1
; --- define initial soil parameters ---
def parm_mech
     u_f=25.0; --- mean of friction angle ---
     a_f=5.0; --- variance of friction angle ---
     u_c=20000.0; --- mean of cohesion ---
     a_c=5000.0; --- variance of cohesion ---
end
parm_mech
  def monte
  ; --- generate random variables with a correlation coefficient of -0.6 ---
  array norm(2,1000)
  loop ii(1,1000)
    a=urand
    b=urand
    c=sqrt((-2)*ln(a))*cos(2*3.14*b)
    e=sqrt((-2)*ln(a))*sin(2*3.14*b)
    d=(-0.1)*c+sqrt(1-0.6^2)*e
    norm(1,ii)=abs(c*a_c+u_c)
    norm(2,ii)=abs(min(d*a_f+u_f,89))
  end_loop
    ; --- input random variables ---
  loop nn(1,1000)
      f_f=norm(2,nn)
      c_c=norm(1,nn)
      command
          ini sxx 0.0 syy 0.0 sxy 0.0
          ini xvel 0.0 yvel 0.0
```

```
        ini xdis 0.0 ydis 0.0
        prop cohesion c_c friction f_f notnull
        set sratio=1e-3
        solve step 5000
    end_command
aa=mech_ratio
; --- calculate probability of failure ---
command
    print aa
    endcommand
if aa>1e-3 then
    fs=fs+1
end_if
    end_loop
pf=fs/1000.0
; --- print results ---
command
print pf
endcommand
end
monte
```

A6. Failure probability of slope with stationary random field

```
config
; --- build slope model with two layers ---
grid 60,30
gen (0.0,0.0) (0.0,10.0) (20.0,10.0) (20.0,0.0) i 1 21 j 1 21
gen (20.0,0.0) (20.0,10.0) (40.0,30.0) (40.0,0.0) i 21 41 j 1 21
gen (40.0,0.0) (40.0,30.0) (60.0,30.0) (60.0,0.0) i 41 61 j 1 21
group rock j 1 21
gen (0 10) (0 20) (20 20) (20 10) i 1 21 j 21 31
gen (20 10) (20 20) (40 40) (40 30) i 21 41 j 21 31
gen (40 30) (40 40) (60 40) (60 30) i 41 61 j 21 31
group soil j 21 31
```

```
model mohr i=1,60 j=1,30
prop density 2000 bulk 2e9 shear 1.5e9 cohesion 4e4 fric 25 j 1 21
prop density 1950 bulk 1.8e9 shear 1.2e9 friction 22 j 21 31
set gravity 10
fix x i 1
fix x i 61
fix x y j 1
def monte
fs=0
loop iii(1,800)
command
    ini sxx 0.0 syy 0.0 sxy 0.0
    ini xvel 0.0 yvel 0.0
    ini xdis 0.0 ydis 0.0
endcommand
; --- define initial parameters ---
    loop m_m(21,30)
        p_p=m_m+1
        y_y=m_m
    a_c=4000; --- variance of cohesion ---
    u_c=21000; --- mean of cohesion ---
    r_a=0.0138; --- variance-reduction coefficient ---
    ; --- generate reduced normal distributed random variables ---
    array norm(1,60)
  loop ii(1,60)
    a=urand
    b=urand
    c=sqrt((-2)*ln(a))*cos(2*3.14*b)*sqrt(r_a)
    d=sqrt((-2)*ln(a))*sin(2*3.14*b)*sqrt(r_a)
    norm(1,ii)=abs(c*a_c+u_c)
  end_loop
  ; --- build random field ---
  nn=0
  loop x_d(1,60)
```

```
        q_q=x_d+1
         nn=nn+1
        c_c=norm(1,nn)
        command
           prop coh c_c i x_d q_q j m_m p_p
       end_command
     end_loop
   end_loop
; --- calculate probability of failure ---
command
set sratio=1e-3
    solve step 5000
    end_command
    aa=mech_ratio
    command
    print aa
    endcommand
if aa>1e-3 then
    fs=fs+1
end_if
command
print fs
endcommand
end_loop
pf=fs/800.0
; --- print result ---
command
print pf
endcommand
end
monte
```

A7. Failure probability of slope with non stationary random field

```
config
```

```
; --- build slope model with two layers ---
grid 60,30
gen (0.0,0.0) (0.0,10.0) (20.0,10.0) (20.0,0.0) i 1 21 j 1 21
gen (20.0,0.0) (20.0,10.0) (40.0,30.0) (40.0,0.0) i 21 41 j 1 21
gen (40.0,0.0) (40.0,30.0) (60.0,30.0) (60.0,0.0) i 41 61 j 1 21
group rock j 1 21
gen (0 10) (0 20) (20 20) (20 10) i 1 21 j 21 31
gen (20 10) (20 20) (40 40) (40 30) i 21 41 j 21 31
gen (40 30) (40 40) (60 40) (60 30) i 41 61 j 21 31
group soil j 21 31
model mohr i=1,60 j=1,30
prop density 2000 bulk 2e9 shear 1.5e9 cohesion 4e4 fric 25 j 1 21
prop density 1950 bulk 1.8e9 shear 1.2e9 friction 22 j 21 31
set gravity 10
fix x i 1
fix x i 61
fix x y j 1
def monte
fs=0
loop iii(1,800)
command
    ini sxx 0.0 syy 0.0 sxy 0.0
    ini xvel 0.0 yvel 0.0
    ini xdis 0.0 ydis 0.0
endcommand
    ; --- define initial parameters ---
    loop m_m(21,30)
        p_p=m_m+1
        y_y=m_m
    a_c=4000; variance of cohesion
    u_c=72000-2000*y_y; --- mean of cohesion ---
    r_a=0.0138; ---variance reduction coefficient ---
    ; --- generate reduced normal distributed random variables ---
    array norm(1,60)
```

```
    loop ii(1,60)
       a=urand
       b=urand
       c=sqrt((-2)*ln(a))*cos(2*3.14*b)*sqrt(r_a)
       d=sqrt((-2)*ln(a))*cos(2*3.14*b)*sqrt(r_a)
       norm(1,ii)=abs(c*a_c+u_c)
    end_loop
    ; --- build random field ---
    nn=0
    loop x_d(1,60)
        q_q=x_d+1
         nn=nn+1
       c_c=norm(1,nn)
       command
          prop coh c_c i x_d q_q j m_m p_p
      end_command
      end_loop
    end_loop
; --- calculate probability of failure ---
command
set sratio=1e-3
    solve step 5000
    end_command
    aa=mech_ratio
    command
    print aa
    endcommand
if aa>1e-3 then
    fs=fs+1
end_if
command
print fs
endcommand
end_loop
```

148

```
pf=fs/800.0
; --- print result ---
command
print pf
endcommand
end
monte
```

A8. Failure probability of slope with double random fields

```
config
; --- build slope model with two layers ---
grid 60,30
gen (0.0,0.0) (0.0,10.0) (20.0,10.0) (20.0,0.0) i 1 21 j 1 21
gen (20.0,0.0) (20.0,10.0) (40.0,30.0) (40.0,0.0) i 21 41 j 1 21
gen (40.0,0.0) (40.0,30.0) (60.0,30.0) (60.0,0.0) i 41 61 j 1 21
group rock j 1 21
gen (0 10) (0 20) (20 20) (20 10) i 1 21 j 21 31
gen (20 10) (20 20) (40 40) (40 30) i 21 41 j 21 31
gen (40 30) (40 40) (60 40) (60 30) i 41 61 j 21 31
group soil j 21 31
model mohr i=1,60 j=1,30
prop density 2000 bulk 2e9 shear 1.5e9 cohesion 4e4 fric 25 j 1 21
prop density 1950 bulk 1.8e9 shear 1.2e9 j 21 31
set gravity 10
fix x i 1
fix x i 61
fix x y j 1
def monte
fs=0
loop iii(1,500)
command
    ini sxx 0.0 syy 0.0    sxy 0.0
    ini xvel 0.0 yvel 0.0
    ini xdis 0.0 ydis 0.0
```

```
endcommand
    ; --- define initial parameters ---
    loop m_m(21,30)
        p_p=m_m+1
        y_y=m_m
    a_c=4000; --- variance of cohesion ---
    u_c=72000-2000*y_y; --- mean of cohesion ---
    a_f=5; --- variance of friction angle ---
    u_f=76-2*y_y; --- mean of friction angle ---
    r_a=0.6120; --- variance reduction coefficient
    ; --- generate reduced random variables ---
    array norm(2,60)
  loop ii(1,60)
    a=urand
    b=urand
    c=sqrt((-2)*ln(a))*cos(2*3.14*b)*sqrt(r_a)
    d=sqrt((-2)*ln(a))*sin(2*3.14*b)*sqrt(r_a)
    norm(1,ii)=abs(c*a_c+u_c)
    norm(2,ii)=abs(d*a_f+u_f)
  end_loop
; --- build random fields ---
    nn=0
  loop x_d(1,60)
      q_q=x_d+1
       nn=nn+1
      c_c=norm(1,nn)
      f_f=norm(2,nn)
      command
        prop coh c_c friction f_f i x_d q_q j m_m p_p
      end_command
    end_loop
  end_loop
; --- calculate random fields ---
command
```

150

```
set sratio=1e-3
    solve step 5000
    end_command
    aa=mech_ratio
    command
    print aa
    endcommand
if aa>1e-3 then
    fs=fs+1
end_if
command
print fs
endcommand
end_loop
pf=fs/500.0
; --- print result ---
command
print pf
endcommand
end
monte
```

Reference

Adhikari, S. (2004) Reliability analysis using parabolic failure surface approximation [J]. Journal of Engineering Mechanics, 12(1): 1407-1427.

Alkasawneh, W., Malkawi, A. I. H., Nusairat, J. H. and Albataineh, N. (2008) A comparative study of various commercially available programs in slope stability analysis [J]. Computers and Geotechnics. 35(3): 428-435

Alonso, E. E. (1976) Risk analysis of slopes and its application to slopes in Canadian sensitive clays [J]. Geotechnique, 26(3): 453-472.

Anbalagan, D. (1992) Landslide hazard evaluation and zonation mapping in mountainous terrain [J]. Engineering Geology 32(4): 269-277.

Ang, A. H. S., Tang, W. H. (1975) Probability concepts in engineering planning and design [M]. Vol. 1. Basic principles. John Wiley, New York.

Ang, A. H. S., Tang, W. H. (1984) Probability concepts in engineering planning and design [M]. Vol. 2. Basic principles. John Wiley, New York.

Auvinet, G., Gonzalez, J. L. (2000) Three dimensional reliability analyses of earth slopes [J]. Computers and Geotechnics. 26(3-4): 247-261.

Azzam, R., Fernandez-Steeger, T. M., Arnhardt, C., Klapperich, H., Shou, K. -J. (2011) Monitoring of landslides and infrastructures with wireless sensor networks in an earthquake environment , *In: 5th International Conference on Earthquake Geotechnical Engineering (5ICEGE), Paper: MOLAZ* . Read online

Baker, R. (1980) Determination of critical slip surface in slope stability computations [J]. International Journal of Numerical and Analytical Methods in Geomechanics. 4(4): 333-359.

Baum, R.L., Savage, W.Z., Godt, J.W. (2003) TRIGRS—a Fortran program for transient rainfall infiltration and grid-based regional slope-stability analysis. U.S. Geological Survey Open-File Report 02-424.

Ben-Haim, Y., Elishakoff, I. (1990) Convex Models of Uncertainty in Applied Mechanics. Amsterdam: Elsevier.

Benko, B., Stead, D. (1998) The Frank slide: A reexamination of the failure mechanism [J]. Can.

Geotech. J., 35(2): 299-311.

Bennett, R. M., and Ang, A. H. S. (1986) Formulations of Structural System Reliability [J]. Journal of Engineering Mechanics. ASCE, 112(11), 1135-1151.

Bhasin, R., Grimstad, E., Larsen, J. O., Dhawan, A. K., Singh, R., Verma, S. K., Venkatachalam, K. (2002) Landslide hazards and mitigation measures at Gangtok, Sikkim Himalaya [J]. Engineering Geology 64(4):351-368.

Bhattacharya, G., Jana, D., Ojha, S., Chakraborty, S. (2003) Direct search for reliability index of earth slopes [J]. Computers and Geotechnics. 30(6): 452-462.

Bishop, A.W. (1959) The principle of effective stress. Teknisk Ukeblad 39:859-863.

Bishop, Aw (1955) The Use of the Slip Circle in the Stability Analysis of the slopes [J]. Geotechnique 5(1):7-17.

Borja, I. R., White, A. J., Liu, X., Wu, W. (2011) Factor of safety in a partially saturated slope inferred from hydro-mechanical continuum modeling [J]. International Journal for Numerical and Analytical Methods in Geomechanics 36(2): 111-248.

Box, G.E.P. and Muller, M.E. (1958). A note on the generation of random normal deviates. Annals of Mathematical Statistics, 29(2): 610-611.

Box, G. E. P., Wilson, K. B. (1954) The exploration and exploitation of response surfaces: some general considerations and examples [M]. Biometrics 10: 16-60.

Breitung, K. (1984) Asymptotic approximation for multi-normal integrals [J]. Journal of Engineering Mechanics, 110(3): 357-366.

Brown, C. B., and King, I. P. (1966) Automatic Embankment Analysis: Equilibrium and Instability Conditions [J]. Geotechnique, 16(3): 209-219.

Bucher, C. G., Bourgund, U. (1990) A fast and efficient response surface approach for structural reliability problems [J]. Structural Safety, 7(1): 57-66.

Cambou, B. (1971) Application of first order uncertainty analysis in the finite element method in linear elasticity [A]. Proc. Second Int. Conf. on Applications of Statistic and Probability in Soil and Structural Engineering [C]. London, England, 117-122.

Catane, S. G., Cabria, H. B., Tomarong, C. P., Saturay, R. M., Zarco, M. A. H., Pioquinto, W. C. (2007)

Catastrophic rockslide–debris avalanche at St. Bernard, Southern Leyte, Philippines [J]. Landslides, 4(1): 91-94

Cellestino, Y. B., Duncan, J. M. (1981) Simplified search for noncircular slip surface [A]. 10th Int. Conf. on Soil Mech. and Found. Engr. 391-394.

Chen, F. H. (2000) Soil Engineering: Testing, Design, and Remediation. CRC Press: Boca Raton, F. L.

Chen, C. Y., Martin, G. R. (2002) Soil-Structure interaction for landslide stabilizing piles [J]. Computers and Geotechnics, 29(5): 363-386.

Chen, Z. Y., Morgenstern, N. R. (1983) Extensions to the generalized method of slices for stability analysis [J]. Canadian Geotechnical Journal, 20(1): 104-119.

Chen, Z. Y., Shao, C. M. (1988) Application of optimization method in determine the minimum safety factor of slope [J]. Chinese Journal of Geotechnical Engineering, 10(4): 1-13.

Cheng, Y. M., Lansivaara, T., Wei, W. B. (2007) Two-dimensional slope stability analysis by limit equilibrium and Strength Reduction Methods [J]. Computers and Geotechnics. 34(3): 137-150.

Cherubini, C. (2000) Reliability of shallow foundation bearing capacity on c´, φ´ soils [J]. Canadian Geotechnical Journal, 37: 264-269.

Chowdhury, R. N. (1978) Slope analysis [M]. New York: Elsevier scientific publishing company.

Chowdhury, R. N. (1984) Recent developments in landslide studies: probabilistic methods [A]. In proceedings of the 4th International Symposium on Landslides [C], Toronto, Ont., September 16-21. Canadian Geotechnical Society, 1: 209-228.

Chowdhury, R. N., (1992) Recent developments in landslide studies: probability in stability analysis, in stability and performance of Slopes and Embankments Ⅱ. ASCE Geotechnical Special Publications, 12: 1071-1111.

Chowdhury, R. N., Tang, W. H. (1987) Comparison of risk models for slopes [A]. In Proceedings of the 5th International Conference on Applications of Statistics and Probability in Soil and Structural Engineering [C], Vancouver, 2: 863-869.

Chowdhury, R. N., Xu, D. W. (1993) Rational Polynomial Technique in Slope Reliability Analysis [J]. Journal of Geotechnical Engineering, 119(12): 1910-1927.

Christian, J., and Baecher, G. (1999) The point estimate method as numerical quadrature [J]. Journal of

Geotechnical and Geoenvironmental Engineering, 125(9): 779-786.

Christian, J. T. (1996) Reliability methods for stability of existing slopes [A]. In Proceedings of Uncertainty [C]. Geotechnical Special Publication, 2: 409-419.

Christian, J. T., Ladd, C. C., Baecher, G. B. (1994) Reliability and probability in stability analysis [J]. Journal of Geotechnical Engineering, ASCE, 120(12): 1071-1111.

Christian, J. T., Urzua, A. (1998) Probabilistic evaluation of earthquake-induced slope failure [J]. Journal of Geotechnical and Geoenvironmental Engineering, 124(11): 1140-1143.

Close, U., McCormick, E. (1922) Where the Mountains Walked [J]. National Geographic Magazine 41(5):445-464.

Collison, A., Wade, S., Griffiths, J., Dehn, M. (2000) Modelling the impact of predicted climate change on landslide frequency and magnitude in SE England [J]. Engineering Geololy 55(3):205-218.

Cornell , J. A. (1990) How to apply response surface methodology. The ASQC Basic References in Quality Control: Statistical Techniques, Vol. 8, ASQC, Wisconsin.

Cornell, C. A. (1969) A probabilistic based structural code [J]. Journal of the American Concrete Institute, 66(12): 974-985.

Cornell, C. A. (1971) First-order uncertainty analysis of soils deformation and stability [A]. In: Proc. 1st Int. Conf. On Application of Probability and Statistics in Soil and Structural Engineering (ICAPI) [C], Hong Kong, 129-144.

Cruden, D. M. and Varnes, D. J. (1996) Landslide types and processes. In: Turner, A.K. and Schuster, R.L. (eds.) Landslides, Investigation and Mitigation, Transportation Research Board Special Report 247, Washington D.C., 36-75.

Dampster, A. P. (1967) Upper and lower probabilities induced by a multivalued mapping. Annals of Mathematical Statistics, Vol.38, 325-339.

Dawson, E. M., Roth, W. H., Drescher, A. (1999) Slope stability analysis by strength reduction [J]. Geotechnique, 49(6): 835-840.

DeGroot, D. J, Baecher, G. B. (1993) Estimating autocovariance of in-situ soil properties [J]. Journal of Geotechnical Engineering, ASCE, 119(1): 147-166.

Dodagoudar, G. R., Venkatachalam, G. (2000) Reliability analysis of slopes using fuzzy set theory.

Computers and Geotechnics, Vol. 27, No. 2, 101-115.

Duan, Y. H. (1999) Basic characters of geo-hazards and its development trend in china. Quaternary Sciences, 19(3):208-216. (in Chinese)

Dubois, D., Prade, H. (1991) Random sets and fuzzy interval analysis. Fuzzy Sets and Systems, Vol. 42, 87-101.

Duncan, J. M. (1996) State of the Art: Limit Equilibrium and Finite Element Analysis of Slopes [J]. Journal of Geotechnical Engineering, ASCE, 122(7): 577-596.

Duncan, J. M. (2000) Factors of safety and reliability in geotechnical engineering [J]. Journal of Geotechnical and Geoenvironmental Engineering, ASCE, 126(6): 307-316.

Eberhardt, E., Kaiser, P. K., Stead, D. (2004) Numerical analysis of initiation and progressive failure in natural rock slopes-the 1991 Randa rockslide [J]. International Journal of Rock Mechanics & Mining Sciences, 41: 69-87.

Einstein, H. H., Karam, S. K. (2011) Risk assessment and uncertainties. In Pro. International Conference on Landslides: Causes, Impacts and Coutermeasures, 457-488.

Elkateb, T., Chalaturnyk, R., Robertson, P. K. (2002) An overview of soil heterogeneity: quantification and implications on geotechnical field problems [J]. Canadian Geotechnical Journal, 40: 1-15.

Evans, M., Hastings, N., Peacock, B. (1993) Statistical distributions. Wiley, New York.

Faheem, H., Cai, F., Ugai, K. (2004) Three dimensional base stability of rectangular excavations in soft soil using FEM [J]. Computers and Geotechnics, 31(2): 67-74.

Faravelli, L. (1989) Response surface approach for reliability analysis [J]. Journal of Engineering Mechanics, 115(12): 2763-2781.

Faravelli, L. (1992) Structural reliability via response surface [A]. In: Bellomo N, Casciati F, editors. Proc of IUTAM symposiumon nonlinear stochastic mechanics [C]. Springer Verlag; 213-223.

Fell, R., Mostyn, G. R., Maguire, P., and O'Keeffe, L. (1988) Assessment of the probability of rain induced landsliding. Proc. Fifth Australia-New Zealand Conference on Geomechanics. 73-77.

Fellenius, W. (1936) Calculation of the stability of earth dams. Transactions, 2nd international congress on large dams. Int Commiss Large Dams: 445-449.

Fenton, G. A. and Griffiths, D. V. (1993) Statistics of flow through a simple bounded stochastic

medium   [J]. Water Resource Research, 29(6): 1825-1830.

Fenton, G. A. and Vanmarcke, E. H. (1990) Simulation of random fields via local average subdivision [J]. Journal of Engineering Mechanics, ASCE, 116(8): 1733-1749.

Fenton, G. A., Griffiths, D. V. (1997) A mesh deformation algorithm for free surface problems [J]. International Journal for Numerical and Analytical methods in Geomechanics, 21(12): 817-824.

Fenton, G. A., Griffiths, D. V., and Williams, M.B. (2005) Reliability of traditional retaining wall design [J]. Geotechnique, 55(1): 55-62.

Fernandez-Steeger, T.M., Arnhardt, C., Walter, K., Haß, S., Niemeyer, F., Nakaten, B., Homfeld, S.D., Asch, K., Azzam, R., Bill, R., Ritter, H. (2009) SLEWS-A Prototype System for Flexible Real Time Monitoring of Landslides Using an Open Spatial Data Infrastructure and Wireless Sensor Networks. GEOTECHNOLOGIEN Science Report 13, 3-15.

Fiessler, B, Neumann, H. J, Rackwitz, R. (1979) Quadratic limit states in structural reliability [J]. Journal of Engineering Mechanics, ASCE, 105(4): 661-676.

Freudenthal, A. M. (1947) The safety of structures. Transaction of ASCE, 112: 125-159.

Fu, H. L. (2000) Theoretical analysis model for block crack rockmass slope stability and its application. Central South University, Dissertation. (in Chinese)

Ge, X. R., Ren, J. X., Li, C. G., et al. (2003) 3D-FEM analysis of deep sliding stability of 3# dam foundation of left power house of the Three Gorges Project [J]. Chinese Journal of Geotechnical Engineering, 25(4): 389-394. (in Chinese)

Giam, S. K., Donald, I. B. (1988) Determination of critical slip surfaces for slopes via stress-strain calculations [A]. 5th A. N. Z. Conference on Geomechanics [C], Sydney, 461-464.

Goodman, I. R., Nguyen, H. T. (1985) Uncertainty models for Knowledge-based Systems; A Unified Approach to the Measurement of Uncertainty. New York, Elsevier Science Inc.

Goodman, R. E. (1995) Block theory and its application [J]. Geotecnique, Vol. 45, No. 3, 383-423.

Greco, Y. R. (1997) Efficient Monte-Carlo technique for locating critical slip surface [J]. Journal of Geotechnical Engineering, 122(7): 517-525.

Griffiths, D. V, Fenton, G. A. (2004) Probabilistic slope stability analysis by finite elements [J]. Journal of Geotechnical and Geoenvironmental Engineering, 130(5): 507-518.

Griffiths, D. V. and Fenton, G. A. (2000) Influence of soil strength spatial variability on the stability of an undrained clay slope by finite elements. In Slope Stability 2000, Proceeding of GeoDenver ASCE, 184-193.

Griffiths, D. V. and Fenton, G. A. (2001) Bearing capacity of spatially random soil: the undrained clay Prandtl problem revisited [J]. Geotechnique, 51(4): 351-359.

Griffiths, D. V., Lane, P. A. (1999) Slope stability analysis by finite element [J]. Geotechnique, 49(3): 387-403.

Harr, M. E. (1977) Mechanics of particular media [M]. New York: McGraw-Hill.

Harr, M. E. (1989) Probabilistic estimates for multivariate analyses [J]. Applied Mathematical Modelling, 13(5): 313-318.

Hart, R. D. (1993) An introduction to distinct element modeling for rock engineering. In Comprehensive Rock Engineering: Principles, Practice & Projects. Pergamon Press: Oxford, 245-261.

Hasofar, A. M., Lind, N. C. (1974) An exact and invariant first order reliability format [J]. Journal of Engineering Mechnics, ASCE, 100(EM1): 111-121.

Hassan, A. M., Wolff, T. F. (1999) Search algorithm for minimum reliability index of earth slopes [J]. Journal of Geotechnical and Geoenvironmental Engineering, ASCE, 125(4): 301-308.

Hatami, K., Bathurst, R. J. (2006) Numerical model for reinforced soil segmental walls under surcharge loading [J]. Journal of Geotechnical and Geoenvironmental Engineering. 132(6): 673-684.

Hong, H. P. (1998) An efficient point estimate method for probabilistic analysis [J]. Reliability Engineering & System Safety, 59(3): 261-267.

Huang, R. Q. (2009) Some catastrophic landslides since the twentieth century in the southwest of China [J]. Landslides, 6(1): 69-81.

Huang, R. Q., Zhao, S. J., Song, X. B. (2005) The formation and mechanism analysis of Tiantai landslide, Xuanhan County, Sichuan Province [J]. Hydrogeology Engineering Geology, 32(1):13-15.

Hutchinson, J. N. (1988) General report: Morphological and geotechnical parameters of landslides in relation to geology and hydrology. In: Proc. 5th International Symposium on Landslides, Lausanne, 1: 3-35.

ITASCA, 2005a. FLAC2D (Fast Lagrangian Analysis of Continua) version 5.0 user's manual. Itasca

Consulting Group, Minneapolis, MN, USA.

ITASCA, 2005b. FLAC3D (Fast Lagrangian Analysis of Continua) version 3.1 user's manual. Itasca Consulting Group, Minneapolis, MN, USA.

Itasca. UDEC—universal distinct element code, version 3.1.Minneapolis: Itasca Consulting Group, Inc.; 2000.

Janbu, N. (1954) Application of composite slip surface for stability analysis [A]. Proc. European Conf. on stability of earth slope [C], Sweden, 3: 43-49.

Janbu, N. (1973) Slope Stability Computations, Embankment-Dam Engineering, Casagrande Volume, Hirschfeld, R.C. and Poulos, S.J. (ed.), John Wiley and Sons, New York, USA, 47-86.

Jiang, C. S. (2000) Present state and prevention of China's geological disasters [J]. Geology in China, 4:3-5.

Jiang, Y. S. (1990) Slope analysis using boundary elements. New York: Springer-Verlag Publishers.

Kaufman, A., Gupta, M. M. (1991) Introduction to fuzzy arithmetic: theory and applications. New York, Van Nostrand Reinhold Company.

Kendall, D. G. (1974) Foundations of a theory of random sets. In stochastic Geometry, Harding & Kendall (eds.). New York, Wiley.

Kim, J. Y., Li, S. R. (1997) An improved search strategy for the critical slip surface using finite element stress fields [J]. Computers and Geotechnics, 21(4): 295-313.

Kim, S. H., Na, S. W. (1997) Response surface method using vector projected sampling points [J]. Structural Safety, 19 (1): 3-19.

Kiureghian A. D., et al. (1988) The stochastic finite element in structural reliability. Proc. of Reliability and Optimization of Structural Systems. 3(2): 83-91.

Kiureghian, A. D. Ke, J. B. (1988) The stochastic finite element method in structural reliability [J]. Probabilistic Engineering Mechanics, 3(2): 83-91.

Kiureghian, A. D., et al. (1991) Recent developments in stochastic finite element [A], Proc. of Reliability and Optimization of Structural Systems [C].

Kiureghian, A. D., Ke, J. (1985) Finite element based reliability analysis of frame structures [A]. Proc 4th. Conf. on Struct. Safety and Reliability [C], Kobe, Japan, 395-404.

Kiureghian, A. D., Lin, H. Z., Hwang, S. J. (1987) Second-order reliability approximations [J]. Journal of Engineering Mechanics, 113(8): 1208-1225.

Kiureghian, A. D., Liu, P. L. (1986) Structural reliability under incomplete probability information [J]. Journal of Engineering Mechanics, 112(1): 85-104.

Kiureghian, A. D., Stefano, M. D. (1991) Efficient algorithm for second-order reliability analysis [J]. Journal of Engineering Mechanics, 117(12): 2904-2923.

Klapperich, H., Azzam, R., Fernandez-Steeger, T.M. und Shen, H. (2011) Erdebeninduzierte Massenbewegungen-Neue Ansätze für das Monitoring und die Modellierung mit Echtzeitdaten von Sensornetzwerken, In Proc. 12. D-A-CH Tagung-Erdbeben und Baudynamik, Hannover.

Kottegoda and Rosso, R. (1997) Statistics, probability and reliability methods for civil and environmental engineers, McGraw-Hill, New York

Koyluoglu, H. U., Nielsen, S. R. K. (1994) New approximations for SORM integrals [J]. Structural Safety, 13(4): 235-246.

Lane, P. A., Griffiths, D. V. (2000) Assessment of stability of slopes under drawdown conditions [J]. Journal of Geotechnical and Geoenvironmental Engineering, 126(5): 443-450.

Latha, G. M., Garaga, A. (2010) Stability analysis of a rock slope in Himalayas [J]. Geomechanics and Engineering, 2(2): 125-140.

Lechman, J. B., Griffiths, D. V. (2000) Analysis of the progression of failure of earth slopes by finite elements [A]. In: Geotechnical Special Publication: Slope Stability 2000 [C]. U.S.A: ASCE, 250-265.

Lei, Y. J., Wang S. L. (2006) Stability analysis of jointed rock slope by Strength Reduction Method based on UDEC [J]. Rock and Soil Mechanics. 27(10): 1693-1698. (in Chinese)

Li, K. S. (1992) Point-Estimate Method for Calculating statistical Moments [J]. Engineering Mechanics, 118(7):1506-1511.

Li, K. S., Lumb, P. (1987) Probabilistic design of slopes [J]. Canadian Geotechnical Journal, 24(4): 520-535.

Li, K. S., White, W. (1987) Rapid evaluation of the critical slip surface in slope stability problems [J]. International Journal of Numerical and Analytical Methods in Geomechanics, 11(5): 449-473.

Li, N. (1992) Landfall-landslide blocking river disasters and its prevention measures in Yunnan

Province[C]. Commission of Proceedings of Landslides ed. Proceedings of Landslides (No. 9). China Railway, Beijing, 50-55, (in Chinese)

Li, T. B., Chen, M. D., Wang, L. S. (1999) Real-time following prediction of the landslides. Chengdu University of Technology, Chengdu, (in Chinese)

Liang, R. Y., Nusier, O. K., Malkawi, A. H. (1999) A reliability based approach for evaluating the slope stability of embankment dams [J]. Engineering Geology, 54(3-4): 271-285.

Lin, P. S., Lin, J. Y., Hung, J. C., Yang M. D. (2002) Assessing debris-flow hazard in a watershed in Taiwan [J]. Engineering Geology, 66(3-4):295-313.

Lind, N. C. (1983) Modeling uncertainty in discrete dynamical systems [J]. Applied Mathematical Modelling, 7(3): 146-152.

Liu, Y. W., Moses, F. (1994) A sequential response surface method and its application in the reliability analysis of aircraft structural systems [J]. Structural Safety, 16(1-2): 39-46.

Low, B. K. (1997) Reliability analysis of rock wedges [J]. Journal of Geotechnical and Geo nvironmental Engineering, 123(6): 498-505.

Low, B. K., Gilbert, R. B., Wright, S. G. (1998) Slope reliability analysis using generalized method of slices [J]. Journal of Geotechnical and Geoenvironmental Engineering, 124(4): 350-362.

Lumb, P. (1969) Safety factors and the probability distribution of soil strength [J]. Canadian Geotechnical Journal, 7(3): 225-242.

Madsen, P. A. and Larsen, J. (1987) An efficient finite difference approach to the mild slope equation [J]. Coastal Engineering, 11(4): 329-351.

Malkawi, A. I. H., Hassan, W. F., Abdulla, F. A. (2000) Uncertainty and reliability analysis applied to slope stability [J]. Structural Safety, 22(2): 161-187.

Mankelow, M. J., Murphy, W. (1998) Using GIS in probabilistic assessment of earthquake triggered landslide hazard [J]. Journal of Earthquake Engineering, 2(4): 593-623.

Marinilli, A., Cerrolaza, M. (1999) Computational stochastic analysis of earth structure settlements [J]. Computers and Geotechnics, 25(2): 107-121.

Matheron, G. (1975) Random Sets and Integral Geometry. New York, John Wiley & Sons.

Matsui, T., San, K. C. (1990) A hybrid slope stability analysis method with its application to reinforced

slope cutting [J]. Soils and Foundations, 30(2): 79-82.

Matsui, T., San, K. C. (1992) Finite element slope stability analysis by shear strength reduction technique [J]. Soils and Foundation, 32: 59-70.

Matsuo, M. (1976) Reliability in embankment design [R]. M.I.T. Dept. of Civil Engineering Research Report R 76-33. Cambridge, MA: Massachusetts Institute of Technology.

Matsuo, M., Kuroda, K. (1974) Probabilistic approach to design of embankments [J]. Soils and Foundations, 14(2): 1-17.

Mauritsch, H. J., Seiberl, W., Arndt, R., Römer, A., Schneiderbauer K., Sendlhofer G. P. (2000) Geophysical investigations of large landslides in the Carnic Region of southern Austria [J]. Engineering Geology 56(3-4): 373-388.

Moore, R. E. (1996) Interval analysis. Printice-Hall, Englewood Cliffs, NJ.

Morgenstern, N. R. (1995) Management risk in geotechnical engineering. The 3rd Casagrande lecture. Proc. 10th Pan American Conference on Soil mechanics and Foundation Engineering. 4: 102-126.

Morgenstern, N. R., and Price, V. E. (1965) The Analysis of the Stability of General Slip Surfaces [J]. Geotechnique, 15(1):79-93.

Mostyn, G. R. and Soo, S. (1992) The effect of autocorrelation on the probability of failure of slopes. In 6th Australia, New Zealand Conference on Geomechanics: Geotechnical Risk, 542-546.

Muhanna, R. L., Zhang, H., Mullen, R. L. (2007) Interval Finite Elements as a Basis for Generalized Models of Uncertainty in Engineering Mechanics. Reliable Computing, Vol. 13, 173-194.

Nasekhian, A. (2011) Application of N0n-probabilistic and Probabilistic Concepts in Finite Element Analysis of Tunnelling. Graz University of Technology, Dissertation.

Nemčok, A., Pašek, J. and Rybář, J. (1972) Classification of landslides and other mass movements [J]. Rock Mechanics, 4: 71-78.

Nguyen, V. U. (1985) Determination of critical slope failure surfaces [J]. Journal of Geotechnical Engineering, 111(2): 238-250.

Nguyen, V. U., Chowdhury, R. N. (1985) Simulation for risk analysis with correlated variables [J]. Geotechnique, 35(1): 47-58.

Nour, A., Slimani, A., Laouami, N. (2002) Foundation settlement statistics via finite element analysis

[J]. Computers and Geotechnics, 29(8): 641-672.

Oberguggenberger, M., Fellin, W. (2002) From probability to fuzzy sets: The struggle for meaning in geotechnial risk assessment. Proc. Of Int. Conf. on Probabilistics in Geotechnics-Technical and Economical Risk Estimation, Pöttler, Klapperich & Schweiger (eds.), Graz, Austria. Essen: VGE; 215-221.

Oka, Y., Wu, T. H. (1990) System reliability of slope stability [J]. Journal of Geotechnical Engineering, ASCE, 116(8): 1185-1189.

Paice, G. M. (1997) Finite element analysis of stochastic soils. PhD thesis, University of Manchester. U.K.

Parise, M., Wasowski, J. (1999) Landslide Activity Maps For Landslide Hazard Evaluation: three case studies from Southern Italy [J]. Natural Hazards, 20(2-3):159-183.

Peschl, G. M. (2004) Reliability Analysis in Geotechnics with the Random Set Finite Element Method. Graz University of Technology, Dissertation.

Peschl, G. M., Schweiger, H. F. (2003) Reliability Analysis in Geotechnics with Finite Elements-Comparison of Probabilistic Stochastic and Fuzzy Set Methods. Proc. Of the Third Int. Symp. On Imprecise Probabilities and Their Applications (ISIPTA '03), Bernard, Seidenfeld & Zaffalon (eds.), Lugano, Switzerland. Canada: Carleton Scientific, 437-451.

Price, G. M., Griffiths, D. V., Fenton, G. A. (1996) Finite element modeling of settlements on spatially random soil [J]. Journal of Geotechnical Engineering ASCE, 122(9): 777-779.

Rackwitz, R., Fiessler, B. (1978) Structural reliability under combined random load sequences [J]. Computers and Structures, 9(5): 489-494.

Radbruch-Hall, D. H., Colton, R. B., Davies, W. E., Lucchitta I., Skipp B. A., Varnes D. J. (1983) Landslide Overview Map of the Conterminous United States. U.S. Geol Surv Prof Pap 1183.

Rajashekhar, M. R., Ellingwood, B. R. (1993) A new look at the response surface approach for reliability analysis [J]. Structural Safety, 12: 205-220.

Ramly, H. E., Morgenstern, N. R., Cruden, D. M. (2002) Probabilistic slope stability analysis for practice [J]. Canadian Geotechnical Journal, 39: 665-683.

Rosenblueth, E. (1975) Point estimate for probability moment [J]. Proceedings of the National Academy of Sciences, 72(10): 3812-3814.

Rosenblueth, E. (1981) Two-point estimates in probability [J]. Applied Mathematical Modelling, 5(2): 329-335.

Sakurai, S., Shimizu, N. (1987) Assessment of rock slope stability by Fuzzy Set Theory. Proc. 6th Int. Cong. Rock Mechs., Montreal, 503-506.

Sarma, S. K. (1973) Stability analysis of embankments and slopes [J]. Geotechnical, 23(3): 423-433.

Schad, H., Wallrauch, E. (1985) Rutschungen im Keuper. Otto-Graf Institut (MPA), Universität Stuttgart.

Schafer, G. (1976) A Mathematical Theory of Evidence. Princeton: Princeton University Press.

Schuster, R. L. (1996) The 25 most catastrophic landslides of the 20th century. In: Chacon, J., Irigaray, C., Fernandez, T. (eds) Landslides, Proc. 8th Intel Conf. Field Trip on Landslides, Granada, Spain, 27-28 Sept. Balkema, Rotterdam.

Schuster, R. L., Highland, L. (2001) Socioeconomic and environmental impacts of landslides in the Western Hemisphere. U.S. Geological Survey Open-file Report 01-9276.

Schweiger, H. F., Peschl, G. M., Pöttler, R. (2007）Application of the random set finite element method for analysing tunnel excavation [J]. Georisk 1, S. 43-56.

Shinozuka, M., Lenoe, E. (1976) A probabilistic model for spatial distribution of material properties [J]. Fracture Mechanics, 8(1): 217-227.

Shou, K. J., Su, M. B., Wang, C. F. (2001) On the Chiufengershan Landslide triggered by Chi-Chi earthquake in Taiwan, In: Proc. of International Conference on Landslides Causes, Impacts and Countermeasures. 319-328.

Shou, K. J. (2003) Analysis of the Chiufengershan Landslide Triggered by the 1999 Chi-Chi Earthquake in Taiwan, *Engineering Geology*, Vol. 68, pp.237-250.

Shou, K. J., Chen, Y. L. (2005) Spatial risk analysis of Li-shan landslide in Taiwan [J].Engineering Geology, 80, 199-213.

Shrestha, B., Duckstein, L. (1998) A fuzzy reliability measure for engineering applications. In: Uncertainty Modeling And Analysis in Civil Engineering, Ayyub (ed.), CRC Press LLC, Boca Raton, 121-135.

Song, E. X. (1997) Finite element analysis of safety factor for soil structures [J]. Chinese Journal of

Geotechnical Engineering, 19(1):1-7. (In Chinese)

Song, E. X., Gao, X., Qiu, Y. (2005) Finite element calculation for safety factor of soil nailing through reduction of strength parameters [J]. Chinese Journal of Geotechnical Engineering, 27(3): 258-263. (In Chinese)

Speedie, M. G. (1956) Selection of Design Value from Shear Test Results, Proceedings of the 2nd Australia-New Zealand Conference on Soil Mechanics and Foundation Engineering, Wellington, pp. 107-109.

Spencer, E. (1967) A Method of Analysis of the Stability of Embankments Assuming Parallel Interslice Forces [J]. Geotechnique, 17(1):11-26.

Stead, D., Eberhardt, E., Coggan J., Benko, B. (2001) Advanced numerical techniques in rock slope stability analysis-application and limitations. In: Proc. of International Conference on Landslides Causes, Impacts and Countermeasures. 615-624.

Sun, D. Y. (2000) Project regulation of Badu Landslide in Nan-Kun Railway. Chinese Railway, Beijing.

Surfer 8 (2003) Contouring and 3D Surface Mapping. Golden Software Inc., Colorado, USA.

Swan, C. C., Seo, Y. K. (1999) Limit state analysis of earthen slopes using dual continuum/FEM approaches [J]. International Journal for Numerical and Analytical Methods in Geomechanics, 23: 1359-1371.

Tabba, M. M. (1984) Deterministic versus risk analysis of slope stability. 4th International Symposium on Landslides, Toronto. 2: 491-498.

Tamaskovices, N., Klapperich, H. (2001) Prediction, prevention and protection against the risk related to granular flows: explosions for groundimprovement. In: International Conference on landslides causes, impacts and countermeasures. 421-431.

Tobutt, D. C. (1982) Monte Carlo simulation methods for slope stability [J]. Computer & Geosciences, 8(2):199-208.

Tonon, F., Bernardini, A., Mammino, A. (2000) Determination of parameter range in rock engineering by means of random set theory [J]. Reliability Engineering & System Safety, 70(3): 241-261.

Tvedt, L. (1990) Distribution of Quadratic forms in normal space-application to structural reliability [J]. Journal of Engineering Mechanics, 116(6): 1183-1197.

U.S. Geological Survey (2000) Landslide hazards. USGS Fact Sheet Fs-071-00.

U.S. EPA: TRIM (1999） TRIM, Total Risk Integrated Methodology. TRIM FATE Technical Support Document Volume I: Description of Module. EPA/43/D-99/002A, Office of Air Quality Planning and Standards.

US Army Corps of Engineers (1997) Introduction to probability and reliability methods for use in geotechnical engineering. Engineering Technical Letter No. 1110-2-547.

Vammarcke, E. H. (1977) Reliability of earth slopes [J]. Journal of Geotechnical Engineering, ASCE, 103(11): 1247-1265.

Van Westen, C. J. (1998) GIS in landslide hazard zonation: a view, with cases from the Andes of Colombia. In: Martin FP, Heywood DI, editors. Mountain environment and geographic information systems. Taylor & Francis, 35-165.

Van Westen, C. J., Terlien, M. T. J. (1996) Deterministic landslide hazard analysis in GIS: a case study from Manizales (Colombia). Earth Surface Processes Landforms, 21: 853-868.

Vanmarke, E. H. (1977) Probabilistic modeling of soil profiles [J]. Journal of Geotechnical Engineering, ASCE, 103(11): 1227-1246.

Vanmarke, E. H. (1983) Random Fields: Analysis and Synthesis. The MIT Press, Cambridge, MA.

Varnes, D. J. (1978) Slope movements: types and processes. In: Schuster, R.L. and Krizek, R.J. (eds.) Landslide analysis and control, National Academy of Sciences, Transportation Research Board Special Report 176, Washington, 11-33.

Voight, B., Faust, C. (1992) Frictional heat and strength loss in some rapid landslides: error correction and affirmation ofmechanism for the Vaiont landslide [J]. Géotechnique 42(4):641-643

Wally, P. (1991) Statistical Reasoning with Imprecise Probabilities. Chapman and Hall, London.

Wang, S. J. (1999) Tasks and future of engineering geology [J]. Journal of Engineering Geology 7(3):195-199 (in Chinese)

Wolff, T. F. (1985) Analysis and design of embankment dam slopes: a probabilistic approach. Ph.D. thesis, Purdue University, West Lafayette,

Wong, F. S. (1984) Uncertainties in dynamic soil-structure interaction [J]. Journal of Engineering Mechanics, 110(2): 308-324.

Wong, F. S. (1984) Uncertainties in FE Modeling of Slope Stability [J]. Computers and Structures, 19(5):777-791.

Wong, F. S. (1985) Slope reliability and response surface method [J]. Journal of Geotechnical Engineering, ASCE, 111(1): 32-53.

Woodward, P. K. (1999) Stability of slopes with beams on rigid foundations [J]. Geotechnical and Geological Engineering, 16: 309-320.

WP/WLI - International Geotechnical societies' UNESCO Working Party on World Landslide Inventory (1990) A suggested method for reporting a landslide. International Association Engineering Geology Bulletin, 41: 5-12.

Wright, S. G., Kulhawy, F. H., Duncan, J. M. (1973) Accuracy of equilibrium slope stability analysis [J]. Journal of Soil Mechanics and Foundation Engineering, 99(10): 783-791.

Wu, W., Tensay, B. G., Webb, S., Doanh, T., Ritzkowski, M., Muhidinov, Z., Anarbaev, M. (2008) Investigation on stability of landfill slopes in seismically active regions in Central Asia. In: 10th International Symposium on Landslides and Engineered Slopes, 1475-1480.

Wu, W. J., Wang, S. Y. (1989) The mechanism of Saleshan Landslide. In Proc. of National landslide conference on landslides, Chengdu, 1989. Sichuan Science and Technology, Chengdu, 184-189.

Wu, W., Ferstl, F., Aschauer, F. (2007) Model testing of biotechnically reinforced slopes in geotechnical centrifuge. In: Geophysical Research Abstracts Ed., , European Union Geosciences Assembly , 15.04.2007 - 19.04.2007, Vienna, 9.

Wu, W. (2011) Zur Wechselwirkung zwischen Boden und Pflanzenwurzel. In: Institut für Geotechnik der TU Bergakademie Freiberg, Geotechnik-Kolloquium "Moderne Bodenmechanik in der Geotechnik" im Rahmen des 62. Berg- und Hüttenmännischen Tages der TU Bergakademie Freiberg; ISBN: 1611-1605.

Yamagami, T., Ueta, Y. (1988) Search for critical slip lines in finite element stress fields by dynamic programming [A]. Proc. 6th International Conference on Numerical Methods in Geomechanics [C]. Innsbruck, Australia, 1335-1339.

Yamagishi, H. (2000) Recent Landslides in Western Hokkaido, Japan [J]. Pure and Applied Geophysics, 157(6-8):1115-1134.

Yang, S. L., Nadim F. and Forsberg C. F. (2007) Probability Study on Submarine Slope Stability

International centre for Geohazards, Norwegian Geotechnical Institute, Oslo, Norway.

Yin, G. L., Han, Z. S., Li, Z. Z. (2000) Progress of landslide researches in the world [J]. Hydrogeology and Engineering Geology, 27(5):1-4, (in Chinese)

Yin, Y. P. (2000) The research on characteristics of rapid huge landslide in Yigong River in the Bomi, Tibet and disaster relief [J]. Hydrogeology and Engineering Geology, 27(4):8-11, (in Chinese)

Yin, Y. P. (2001) A review and vision of geological hazards in China [J]. Management Geological Science and Technology, 18(3):26-29

Zadeh, L. A. (1965) "Fuzzy sets". Information and Control, 8, 338-353.

Zadeh, L. A. (1978) Fuzzy sets as a Basis for a Theory of Possibility. Fuzzy Sets and Systems, Vol. 1, 3-28.

Zhangeneh, N., Azizian, A., Lye, L., Popescu, R. (2002) Application of response surface methodology in numerical geotechnical analysis. In: Proc. of the 55th Canadian geotechnical conference, Hamilton, Ontario, 321-329.

Zhao Y. Y., Ono, T. (1999) New approximations for SORM: Part 1 [J]. Journal of Engineering Mechanics, 125(1): 79-85.

Zhao Y. Y., Ono, T. (1999) New approximations for SORM: Part 2 [J]. Journal of Engineering Mechanics, 125(1): 86-93.

Zhen, Y. R., Zhao, S. Y., Shi, W. M., Lin, L. (2001) The progress of slope stability analysis [J]. Underground Space, 21(4): 262-271.

Zheng, H., Tham, L. G. and Liu D. F. (2006) On two definitions of the factor of safety commonly used in the finite element slope stability analysis [J]. Computers and Geotechnics, 33(3): 188-195

Zheng, Y., Das, P. K. (2000) Improved response surface method and its application to stiffened plate reliability analysis [J]. Engineering structures, 22(5): 544-551.

Zhong, L. X. (1999) Case study on significant geohazards in China [J]. The Chinese Journal of Geological Hazard and Control 10(3):1-10, (in Chinese)

Zhou, J. and Nowak, A. S. (1988) Integration Formulas to Evaluate Functions of Random Variables [J]. International Journal of Structural Safety, 5(4): 267-284.

Zhu, D. Y., Lee, C. F., Jiang, H. D. (2003) Generalized framework of limit equilibrium methods for

slope stability analysis [J]. Geotechnique, 53(4): 377-395.

Zou, J. Z., Williams, D. J. (1995) Search for critical slip surface based on finite element method [J]. Canadian Geotechnical Journal, 32(1): 233-246.